OUTCROP ANALOG FOR LOWER PALEOZOIC HYDROTHERMAL DOLOMITE RESERVOIRS, MOHAWK VALLEY, NY

Final Report

Prepared for

THE NEW YORK STATE ENERGY RESEARCH AND DEVELOPMENT AUTHORITY

Albany, NY

John Martin
Project Manager

Prepared by

THE RESERVOIR CHARACTERIZATION GROUP AT THE NEW YORK STATE MUSEUM

Albany, NY

Brian Slater
Langhorne Smith

NYSERDA
Agreement# 8162

November 2008

NOTICE

This report was prepared by the Reservoir Characterization Group at the New York State Museum in the course of performing work contracted for and sponsored by the New York State Energy Research and Development Authority (hereafter the "Sponsors"). The opinions expressed in this report do not necessarily reflect those of the Sponsors or the State of New York, and reference to any specific product, service, process, or method does not constitute an implied or expressed recommendation or endorsement of it. Further, the Sponsors and the State of New York make no warranties or representations, expressed or implied, as to the fitness for particular purpose or merchantability of any product, apparatus, or service, or the usefulness, completeness, or accuracy of any processes, methods, or other information contained, described, disclosed, or referred to in this report. The Sponsors, the State of New York, and the contractor make no representation that the use of any product, apparatus, process, method, or other information will not infringe privately owned rights and will assume no liability for any loss, injury, or damage resulting from, or occurring in connection with, the use of information contained, described, disclosed, or referred to in this report.

ABSRACT

Geochemical analysis and field relations of linear dolomite bodies occurring in outcrop in the Mohawk Valley of New York suggest that they have undergone significant fault-related hydrothermal alteration. The dolomite occurs in the Lower Ordovician Tribes Hill Formation, which is regionally an early Ordovician shaley limestone with patchy dolomitization. The outcrop has an en echelon fault, fracture, and fold pattern. A 3D ground penetrating radar survey of the quarry floor has helped to map out faults, fractures, anticlines, synclines and the extent of dolomitization. Most of the dolomitization occurs in fault-bounded synclines or “sags” flanked by anticlines. The dolomite structures are highly localized, occurring around faults and are absent away from the faults and fractures. Trenches cut across the outcrop help relate offset along faults to the overall geometry of the dolomitized bodies. Geochemical analysis, though helpful in characterizing the conditions of dolomitization, does not define its origin absolutely. This study uses fluid inclusions, stable isotopes, 3D-ground penetrating radar, core analysis, and surficial observation which all show a link between faulting, dolomitization, and other hydrothermal alteration. Although the outcrop is much too small and shallow to act as a producing gas field, it serves as a scaled analog for Trenton – Black River hydrothermal dolomite reservoirs of the eastern United States. It may therefore be studied to help petroleum geologists characterize existing gas plays and prospect future areas of exploration.

Key words: hydrothermal dolomite, outcrop analog, Mohawk Valley, natural gas, Trenton – Black River

AKNOWLEDGMENTS

We express our gratitude to NYSERDA, Fortuna Energy Inc., Ansbro Petroleum Co., and Triana Energy for their financial support. We'd also like to thank everyone in the Reservoir Characterization Group at the New York State Museum for their countless hours of hard work in excavating the outcrop, Fluid Inclusion Technologies for their fluid inclusion analyses, Steve Howe at the University of Albany and Mihai Ducea at the University of Arizona for their isotope analyses, the Department of Transportation for drilling the cores, and Eagle Associates for cutting the trenches.

TABLE OF CONTENTS

Section Page

TABLE OF CONTENTS (continued)

FIGURES

FIGURES (continued)

FIGURES (continued)

TABLES

PLATES

Plates 1-6 are included in a separate poster sized insert.

SUMMARY

New York State is currently experiencing a gas boom. Large amounts of natural gas are being produced from dolomite bodies found in the south central region of the state. Unlike most of the bedrock in New York, these dolomite bodies are not sedimentary deposits. They occur where pre-existing rock units have been altered by hydrothermal fluid flow. The process of hydrothermal alteration, as described by Davies and Smith (2007), begins when fluids become trapped and buried to depths where they experience high temperatures and pressures. These fluids will remain trapped until faulting releases the pressure causing the fluids to travel upwards along the fault plane. As these fluids reach shallower, cooler, layers of rock such as limestone they tend to dissolve the limestone and precipitate dolomite crystals. This process literally changes the rock surrounding the fault from a limestone to a dolomite and is known as hydrothermal dolomitization. Many of these dolomite bodies make excellent oil and gas reservoirs because the process of dissolving the limestone increases pore space. Some of that porosity is filled back in with the precipitation of dolomite, but even the dolomitized bodies commonly have more porosity than the original limestone.

The hydrothermal dolomite reservoirs in NY are difficult to study because they occur between 7 and 10 thousand feet below the surface. Techniques such as seismic profiling allow geologists to digitally image the bodies, and rock cores taken from wells supply samples of the dolomite for chemical analysis, but the reservoir itself can never been seen directly. This problem is solved through the use of analogs such as the study site of this project. An outcrop of hydrothermal dolomite (180’ long, 3 – 5’ wide) was discovered in the floor of an abandoned quarry in Palatine Bridge, NY. It is much smaller than the reservoirs of south central part of the state, but every other physical and chemical characteristic of the outcrop matches that of the producing fields.

The Palatine Bridge outcrop took over two years to uncover. More than 90% of the feature was covered by two to three feet of rubble and debris. A skid-steer bucket loader was used to remove the majority of the overburden, then high-pressure water hoses were used to spray down the outcrop. A ground penetrating radar survey was run over the area to produce a digital image the body and a series of six cores were drilled in and around the dolomite. Six trenches, each measuring approximately 2.5’w x 18’l x 1.5’d, were cut across the dolomite bodies. The walls of these trenches act as a series of 12 profiles which allow the outcrop to be viewed in cross-section. Samples for geochemical analysis were collected along the length of the outcrop as well as from the cores.

Structural analysis reveals that the outcrop consists of three sections of dolomite. These sections are all long, linear features that can be discerned from the surrounding limestone by their orange color. In profile view, the dolomite bodies are characterized by a central sag in which the rock layers dip downward toward the middle of the body. This sag is flanked on either side by a small “hill” called an anticline. The cores show mineralization along faults and fractures which indicates that fluid flow took place along these

pathways. The dolomite bodies are also characterized by the breccias and vugs that can be seen on the surface, in the cores, and in the trench walls. Chemically speaking, the dolomites in the quarry are enriched in radiogenic strontium. They have a relatively light oxygen isotope signature, and fluid inclusion analysis indicate that they formed at temperatures of at least 130 – 150ºC. All of these features lead to the conclusion that the Palatine Bridge outcrop is indeed hydrothermal in origin.

NY gas reservoirs, such as the Quakenbush field in Steuben County, also occur as long linear features. Studies have shown that they are enriched in radiogenic strontium, have light oxygen isotope ratios, and fluid inclusions from the reservoirs yield temperatures between 130 and 150ºC. Seismic profiles reveal that these fields have a sag in the middle that is often flanked by anticlines and cores commonly contain breccias, vugs, and mineralized fractures. These similarities between the quarry outcrop and producing fields show that the outcrop has correlative value and can be used to aid in future exploration and development of New York's natural gas resources.

The following report provides a more detailed description of the accomplishments of this research effort, and is divided into six sections:

1. Introduction
2. Background
3. Methods
4. Data
5. Discussion
6. Conclusions

Section 1

INTRODUCTION

1.1 Aims and objectives of the investigation

The goal of this investigation was to test the hypothesis that dolomitization and associated mineralization of the Tribes Hill Limestone in Palatine Bridge, New York was caused by hydrothermal[1] fluid flow upward along faults and fractures. If this hypothesis is supported, then the outcrop may be used as an analog for the Trenton - Black River dolomite gas fields on the basis of their similar origin and comparable features. This study addresses three objectives:

1. Demonstrate the hydrothermal alteration of the Palatine Bridge outcrop
2. Constrain the timing of dolomitization
3. Confirm the value of the outcrop as an analog for Trenton - Black River fields

1.2 Association of Hydrothermal Dolomite with Gas Production

Although detailed research of its formation is relatively recent, hydrothermal dolomite has long been associated with the production of natural gas. In 1884 North America experienced its first real drilling boom along the Indiana-Lima trend of Indiana and Ohio (Hurley and Budros, 1990). Large amounts of both oil and gas were produced from the Ordovician-aged Trenton-Black River units. According to Keith (1986) half of the area's production came from the Bowling Green fault zone, a highly dolomitized linear feature.

In 1957-58 the Albion-Scipio fields were discovered along a similar Trenton-Black River dolomitized fault trend in Michigan (Fig. 1). With over 400 producing wells by 1961, this system was among the first to achieve the status of giant oil field. The fields' linear geometry and synclinal sags led to the interpretation that these features were created by hydrothermal fluid flow along riedel shears in a strike-slip pull-apart system (Fig. 2) (Hurley and Budros, 1990).

Since the discovery of these early fields, hydrothermally dolomitized sections of the Trenton-Black River in New York State have been proven to host some of the largest natural gas wells in recent years (Smith, 2006). Fields of this type are characterized by their long, linear shape, close proximity to fault zones, breccias, vugs, and structural depressions or sags (Smith, 2006).

---

[1] For the purposes of this paper hydrothermal fluids are defined as "aqueous solutions that are warm or hot relative to the surrounding environment" whereby temperature differences greater than 10°C are considered significant (White, 1957).

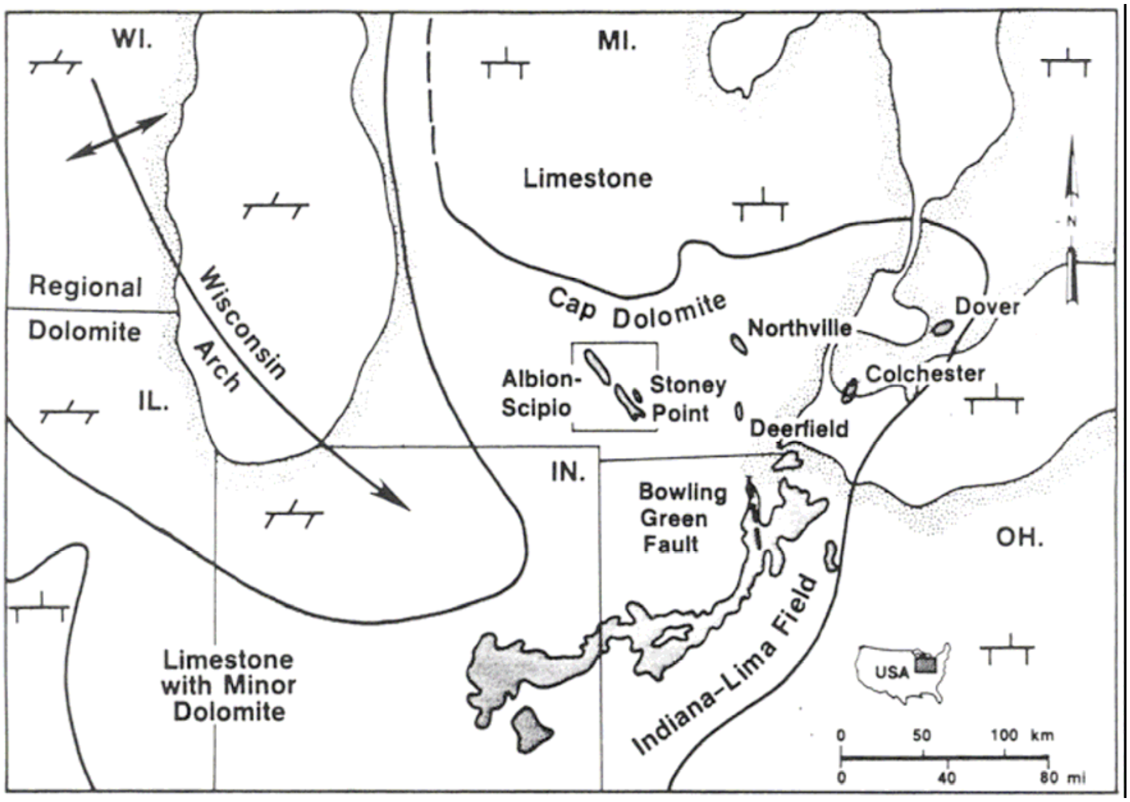

Figure 1 – Map outlining early oil and gas fields of the Great Lakes Region (Hurley and Budros, 1990)

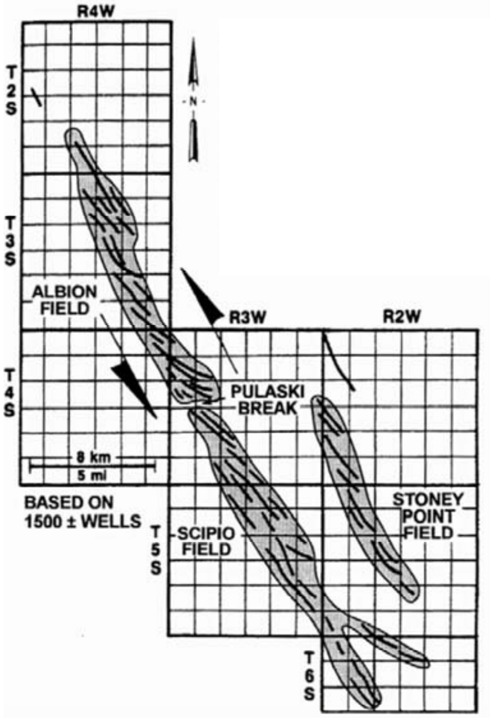

Figure 2 - Interpreted strike-slip motion of the Albion-Scipio fields (Hurley and Budros, 1990)

1.3 Fault-related Hydrothermal Alteration Model

The current model for fault-related hydrothermal alteration is based on the research done by Davies and Smith (2006). The process begins with the activation of basement-rooted faults. This most likely involves the reactivation of appropriately oriented preexisting faults but may also occur around entirely new ones (Sibson, 1994). Movement along strike-slip and transtensional faults can create a relatively low-resistance flow path for high-pressure, high-temperature fluids trapped at greater depths. The release of this pressure causes the fluids to travel upward along fault zones where they interact with the units above. This faulting is commonly transtensional in nature creating negative flower structures which are characterized by sagging. In the case of interaction with limestone, as the fluids cool they become under-saturated with respect to calcite and begin to leach the host rock creating secondary porosity in the form of vugs. Increased permeability created by the leaching process allows fluids to migrate farther away from the fault zone. The pressure and temperature change associated with these fluids traveling to shallower depths can also cause them to become super-saturated with dolomite, leading to precipitation of the mineral as both matrix replacement and vug and fracture fill. The evolution of these fluids can lead to the precipitation of a range of other minerals as well. Quartz, bitumen, sulfides, secondary calcite, and other minerals are all associated with hydrothermal alteration. Mineralization along faults and fractures may choke the flow path and cause fluid travel to cease (Sibson, 1994). However, continued tectonic activity and the build-up of pressure may reactivate these passageways and initiate another dolomitization event.

1.4 Brief Description of Palatine Bridge Outcrop

The Palatine Bridge study site is located in the Frye Estate quarry along the Mohawk River, approximately 50 miles west of Albany, New York (Fig. 3). Although at least three areas of the quarry have been dolomitized, this study focuses on the most easily accessible region (Fig 4). The study area consists of two dolomite bodies. The easternmost body (Body 1) is a long, linear feature approximately 55 feet long, 5 feet wide, and has a strike of 305°. The second body (Body 2) is located immediately west of the first, and is also a linear feature with similar strike, however this body is substantially longer than the first, measuring 110 feet long. Body 2 is broken into two parts which are separated by a southerly bend, referred to as the “jog” (Fig. 5).

The dolomite is easily distinguished from the surrounding limestone by its distinct tan color and massive texture. The bodies are characterized by their central sag, brecciation, and vuggy porosity (Fig. 5). A zone of enhanced fracturing surrounds the entire dolomite body outcrop increasing the width of the anomalous area to approximately 15 feet. Although it is orders of magnitude smaller than producing hydrothermal reservoirs, the quarry outcrop bears a striking resemblance to them in many other ways. This suggests that the outcrop may be studied as a small-scale analog of the larger, deeply buried Trenton-Black River fields.

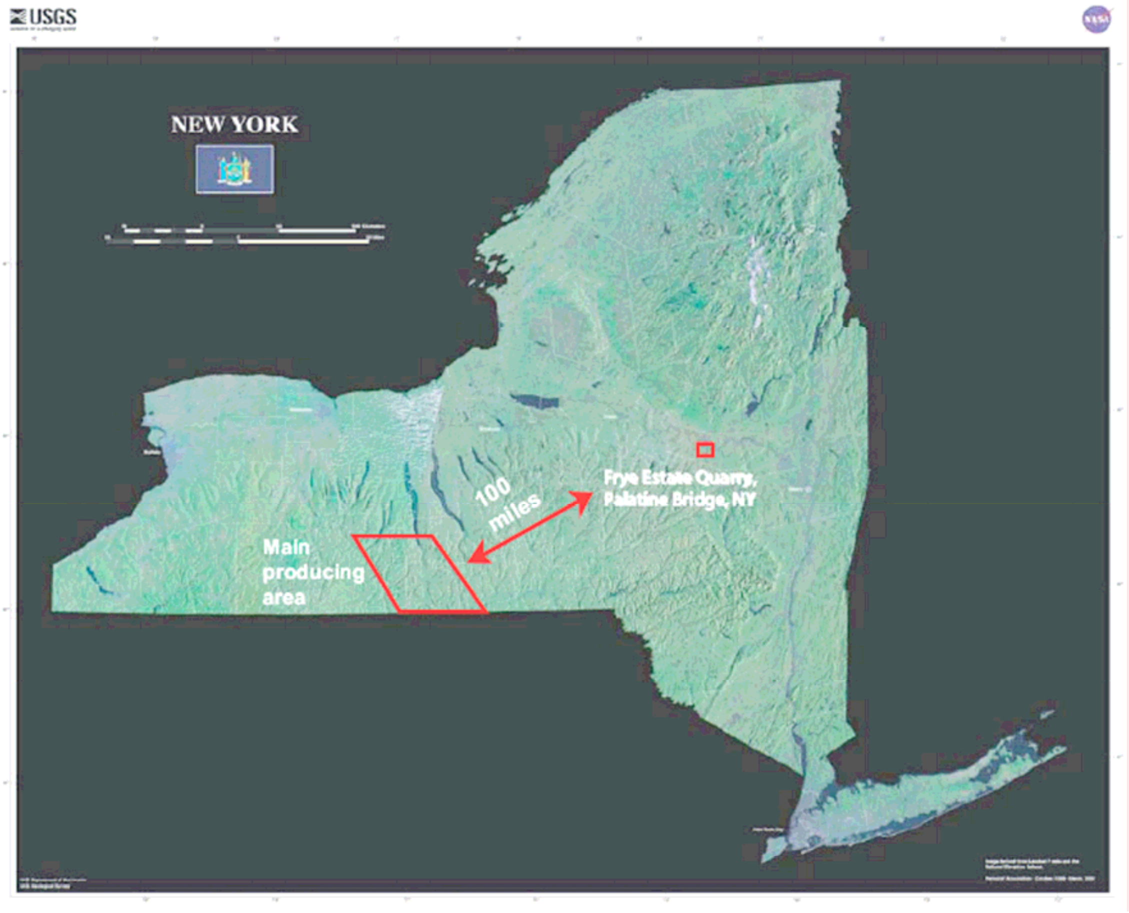

Figure 3 - Satellite image of New York State with Palatine Bridge Quarry location marked

Figure 4 - Panoramic view of Palatine Bridge Quarry outcrop (taken from the south looking north)

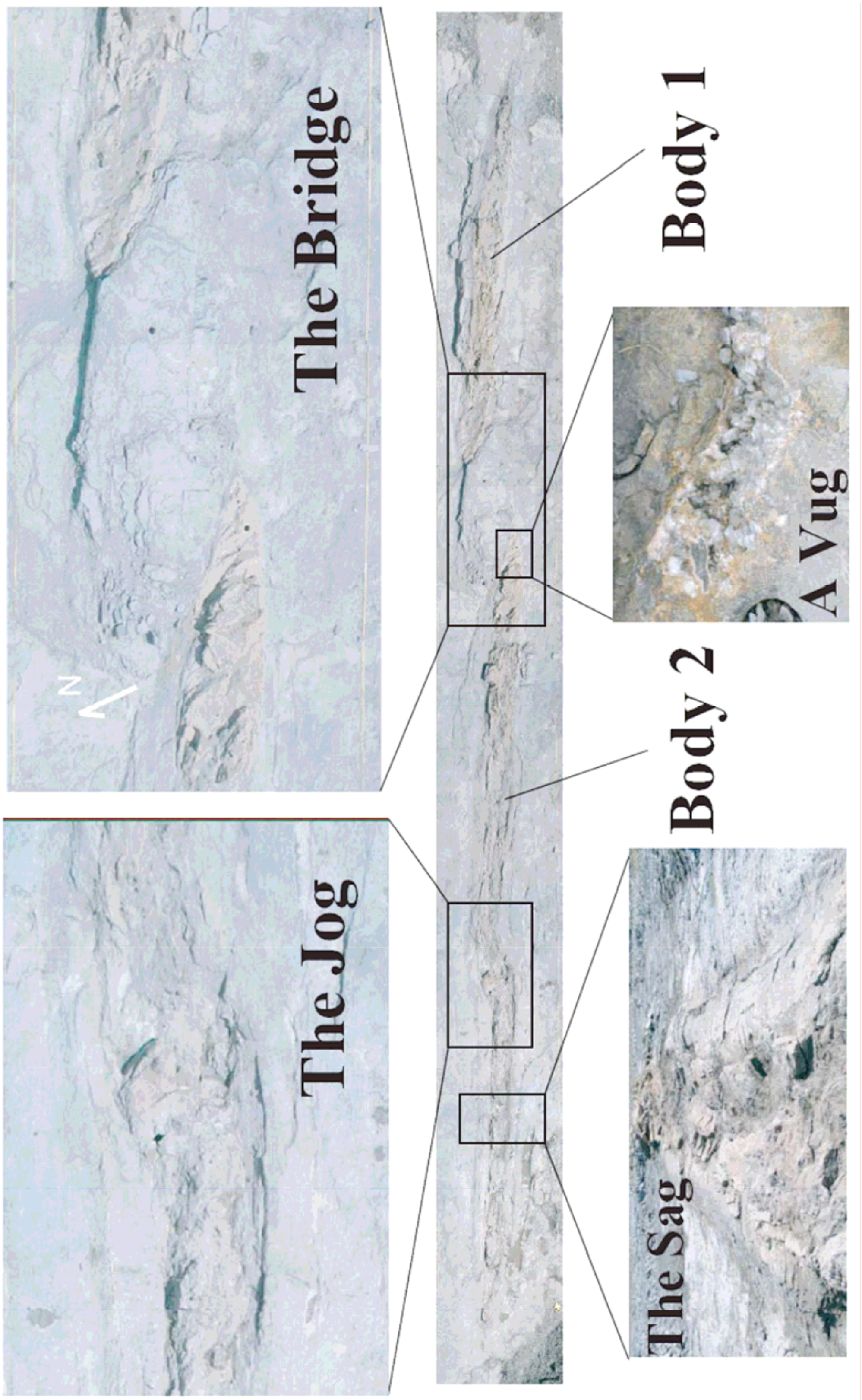

Figure 5 – Aerial view of the outcrop with labeled blow-ups of important features

Section 2

BACKGROUND

2.1 Site Location

The Palatine Bridge Outcrop is located in Central New York, along the Mohawk River Valley. It lies on the floor of the Frye Estate Quarry which is situated on the western edge of town just south of Route 5. The Mohawk River runs along the strike of the bodies only a few hundred feet south of the quarry's edge. Access to the quarry is limited as it has been inactive since the 1950's, when it was a source of aggregate for the construction of Interstate 90.

2.2 Stratigraphic Setting

The Palatine Bridge quarry is in the Lower Ordovician Tribes Hill Formation of the Beekmantown Group (Fig. 6 and 7). Fisher (1954), Zenger (1981), and Landing (1996) describe the Tribes Hill as a thin to medium-bedded argillaceous limestone with patchy dolomitization. It was deposited in a shallow, peritidal to subtidal environment. It is characterized by blackish laminae and shaley interbeddings. The formation has a regional thickness of about 130 feet. It is fossiliferous, containing abundant trilobite, brachiopod, and mollusk faunas (Landing, 1996). The Tribes Hill unconformably overlies the Upper Cambrian Little Falls Formation which is described as a thick-bedded dolomite and is also believed to have formed by deposition in a shallow, peritidal to subtidal environment (Zenger, 1981). According to Zenger, the Little Falls is approximately 400 feet thick in this portion of the Mohawk Valley. The Little Falls overlies the Potsdam sandstone which may or may not be present below the quarry as it thins to the east and the nearest outcrops are a significant distance away.

The Tribes Hill Limestone is capped by the Knox Unconformity which accounts for approximately 30 million years in this area. Above this unconformity lies the Upper Ordovician Black River Group and the Utica Shale. The Trenton and Black River units are known to host major oil and gas reservoirs in the eastern U.S. and southern Ontario. The majority of these plays are contained in hydrothermal dolomite reservoirs (Smith, 2006).

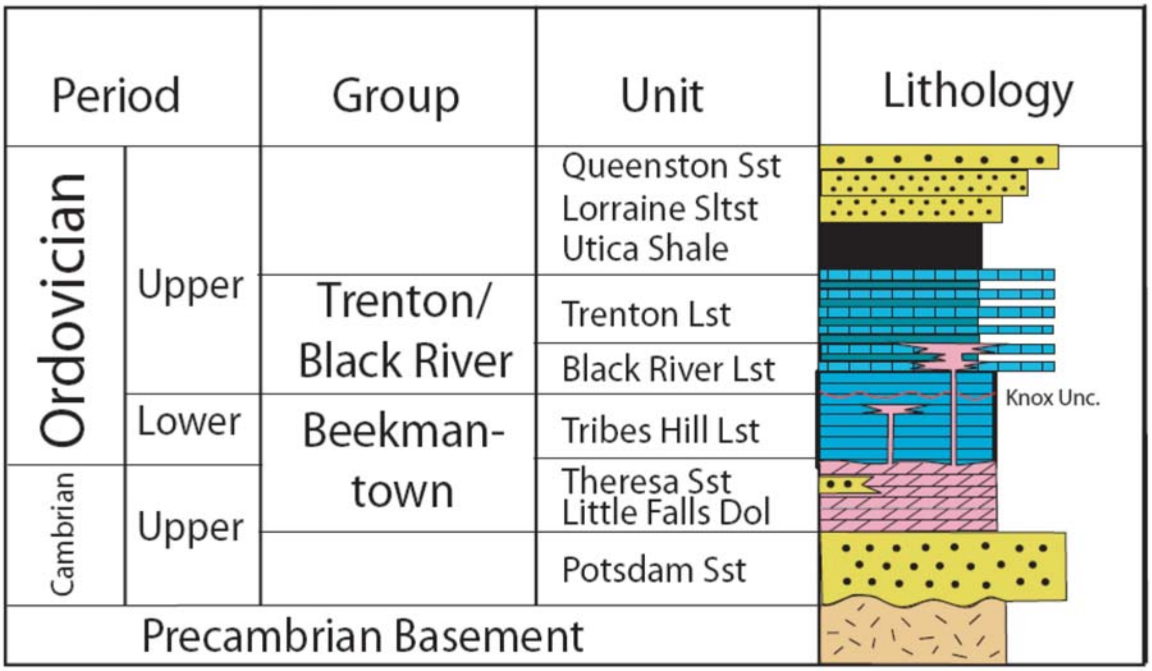

Figure 6 - Stratigraphic column of the Precambrian through Ordovician (Smith, 2006)

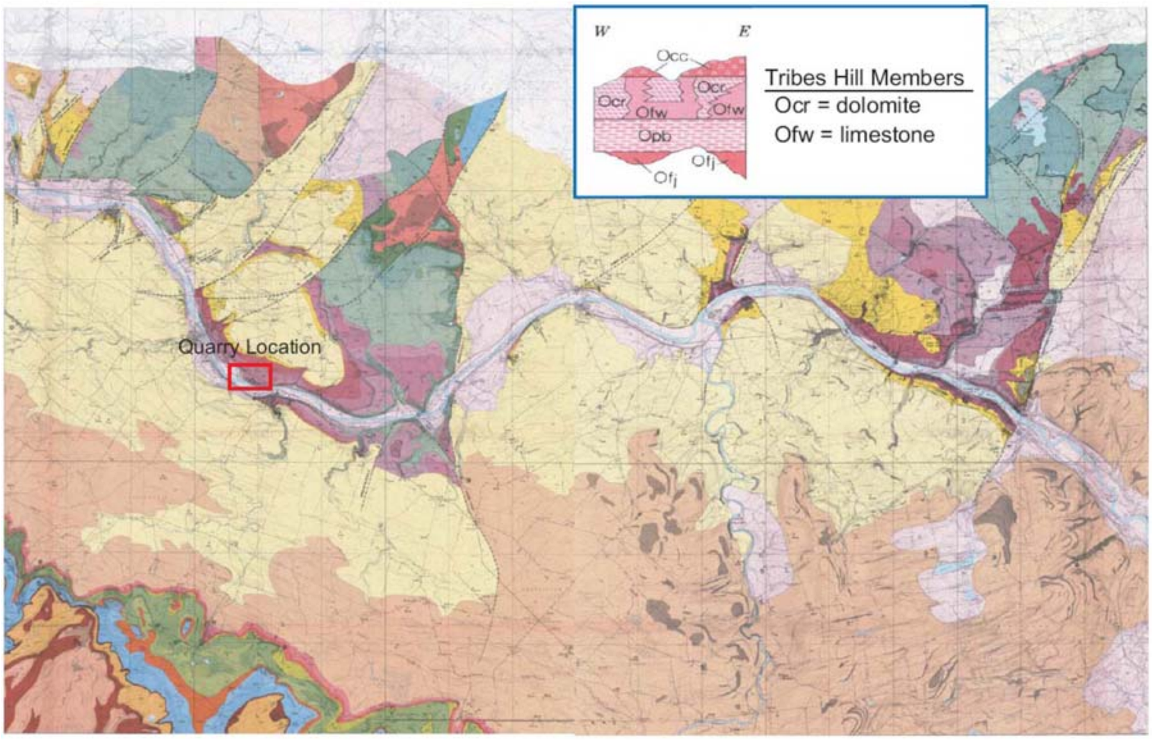

Figure 7 - Quarry Location plotted on geologic map of the Mohawk Valley (Fisher, 1980)

2.3 Tectonic Setting

The basement rock of New York State consists mainly of granitic gneiss. It is part of the Grenville Province which formed approximately 1.1 billion years ago during the Grenville Orogeny. These rocks were already exhumed to the surface by about the end of the Precambrian (543 Ma) when rifting led to the opening of the Iapetus Ocean and may have reactivated preexisting faults in the basement (Bird and Dewey, 1970; Jacobi and Fountain, 2002). Deposition of the Potsdam Sandstone, Beekmantown Group, and Black River Limestone during the Late Cambrian and Early Ordovician is thought to have occurred along a passive margin following the opening the Iapetus Ocean. Deposition of the Middle Ordovician Trenton Group has been demonstrated to have been fault controlled (Bradley and Kusky, 1986; Joy, 2000). Active tectonism during the Middle-Late Ordovician is associated with the Taconic Orogeny in which Proto-North America collided with the Taconic Island Arc terrane. Flexure of the North American plate during its attempt to be subducted under the island arc led to extensional faulting and produced a series of northeast-southwest striking normal faults, some with offsets of over 1000 feet (Jacobi, 1981; Bradley and Kidd, 1991). Closing of the Iapetus Ocean during the Devonian (410 – 380 Ma) caused by another mountain building event known as the Acadian Orogeny. The last orogeny recorded in New York took place during the Late Carboniferous and Early Permian (330 – 250 Ma). This collision involved a portion of proto-Africa colliding with eastern proto-North America. This event is known as the Alleghanian Orogeny.

Section 3

FIELDWORK AND METHODS

3.1 Site Preparation

The Palatine Bridge outcrop was initially discovered by Gareth Cross, a masters student from the University of Buffalo. While mapping fractures in the Mohawk Valley, he noted the orange-colored rubble on the floor of the quarry. Very few pieces of in-situ dolomite could be seen initially (Fig. 8).

The quarry floor was initially covered in most places by up to 3 feet of overburden. Excavation for this project began with the use of pick-axes and shovels, but it was soon realized that more effective machinery would be needed to expose the outcrop efficiently. A Dingo (walk behind bucket-loader) and a Caterpillar (skid-steer bucket loader) were rented from local tool stores and used to push aside the overburden and expose the dolomite bodies.

High-pressure hoses were then used to pump water from a nearby pond and spray off the outcrop. This served to remove the remaining debris and wash the in-situ rock surface. The excavation was followed by extensive photography both on the ground and from a 60 foot boom (Plate 1).

Figure 8 - Dolomite exposure prior to excavation

3.2 3-D Ground Penetrating Radar

During the excavation process, while much of the outcrop was still covered by overburden, a three dimensional ground penetrating radar (GPR) survey was run over the area. Mark Grasmueck and his student David Viggiano, from the University of Miami, conducted the survey. Data were collected using a shielded bistatic 250 MHz antenna, then processed using Promax 3DTM and GeoprobeTM software. Two survey sites were selected based on surficial observations. The first site was located in the area being excavated and only covered Body 2 since Body 1 had already been exposed (Fig. 9). The second site was located in a different part of the quarry approximately 50 feet higher in elevation. This second site was chosen based on the presence of dolomite rubble and because a preliminary 2-D run showed structure in the area. Results from the survey of the first site are presented in Chapter 4.

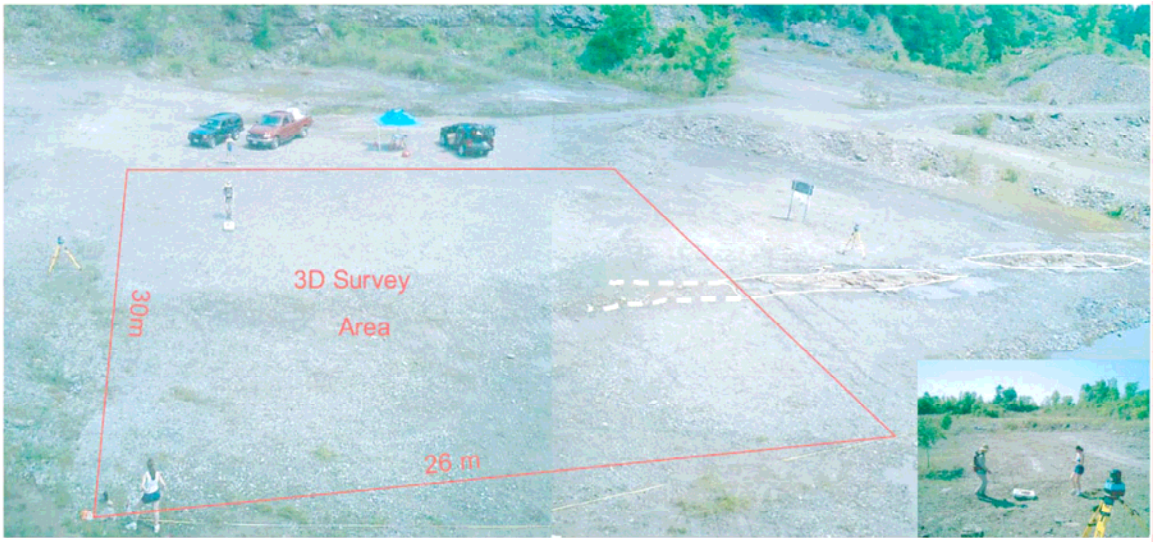

Figure 9 - Outline of 3-D survey area

3.3 Drill Cores

In January of 2005 the Department of Transportation agreed to drill a series of six cores in the study area. These holes ranged in depth from 38 to 73 feet. Figure 10 shows a map of the hole locations and total depths of all the holes are given in Table 3-1. Hole 1 was drilled approximately halfway between the jog and the eastern tip of Body 2. Holes 2 and 6 are located 5 and 15 feet outside Body 2 along a line drawn perpendicular to strike from Hole 1. Hole 5 was drilled inside the jog of Body 2. Hole 3 was located at the eastern tip of Body 2 while Hole 4 was drilled in the limestone gap between bodies 1 and 2. All six cores were slabbed and boxed for storage before analysis.

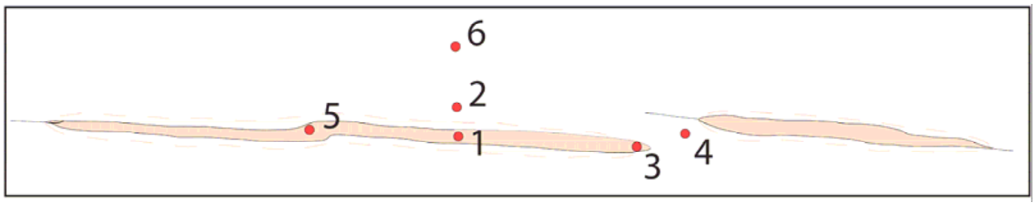

Figure 10 - Map of core drilling locations

Table 3-1 – Core holes and their corresponding total depths

Hole #	Total Depth (ft.)
1	38.8
2	54.0
3	55.0
4	55.0
5	73.0
6	45.0

3.4 Fracture Mapping

A fracture map covering the entire exposure was constructed using a 2 foot x 10 foot grid divided into five 2-foot squares with durable string. The grid was weighted on both ends and placed over the eastern end of the first body from north to south. The fracture content of each square was then drawn to scale on a sheet of graph paper. Once the row of squares were completely copied, the eastern end of the string grid was “flipped” over to cover the adjacent row of outcrop. The new row of squares was then copied and this flipping process was repeated. The entire outcrop was mapped in this fashion, then scanned and digitized. A copy of the finished map is presented in Plate 2.

3.5 Trenches

During the summer of 2005 Eagle Associates Concrete Cutting Company was contracted to cut six trenches across the dolomite bodies (Fig. 11). The location of each trench is given in Figure 12. These trenches each measure approximately 3 feet wide, 15 feet long, and 18 inches deep. The perimeter cuts for each trench were made using a 36- inch rail-mounted circular wet saw. Once the cuts had been made, a jackhammer was used to break apart the interior for removal. A series of digital photographs were taken of each trench wall and seamed together to make mosaic cross-sections of each trench. A full description of these cross-sections is given in Chapter 4.

Figure 11 - One of the six trenches cut across the dolomite bodies (trench 4 looking west)

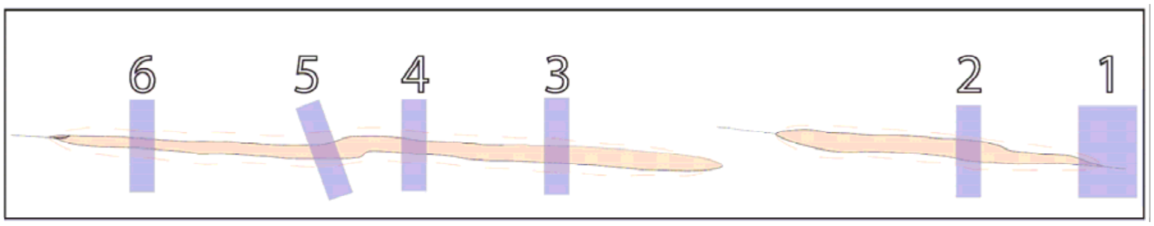

Figure 12 - Map of trench locations

3.6 Sample Collection and Geochemical Analysis

Samples of the outcrop were collected at various times throughout its excavation. The initial set consisted of 18 samples in and around the dolomite bodies. These samples were removed using a rock hammer and therefore have no consistent size or shape. Later, two additional series of samples were collected using a Pomeroy EZ core plugger. Each plug is a cylinder with a 1-inch diameter and a length varying from 1 to 3 inches. A set of plugs was taken along the bodies every two feet. Another set of plugs were taken as a transect cutting across the eastern portion of Body 2. A fourth set was collected from the cores using a drill press mounted with the same type bit as the plugger. Samples were taken from the cores every two feet starting from the surface and ending at the Tribes Hill / Little Falls contact. A portion of each sample was sent to Spectrum Petrographics in Vancouver, Washington to be made into thin sections. The remainder of some samples were crushed to a fine powder, then divided and sent to Stephen Howe at the University at Albany for stable isotope analysis and to Mihai Ducea at the University of Arizona for strontium isotope analysis.

Stable isotopes of carbon and oxygen were measured at the University at Albany and the University of Miami. For the samples analyzed at Albany, approximately 200 µg of powdered sample was dissolved in 100% phosphoric acid at 90°C in individual reaction vessels in a MultiPrep sample preparation device. The evolved CO_2 gas was then analyzed using a Micromass Optima gas-source triple-collector isotope ratio mass spectrometer. Samples of international standard NBS-19 were interspersed among the quarry-derived samples in analytical runs. The average isotopic compositions of ITS analyses of NBS-19 over a 5-month period during which the Palatine Bridge surface samples were analyzed were $\delta^{13}C$ = 1.950 ‰ and $\delta^{18}O$ = -2.201 ‰, with a standard deviation of 0.012 ‰ and 0.032 ‰, respectively. The Miami samples were reacted for 10 minutes using the common acid bath method at 90ºC and the CO_2 produced was analyzed using a Finnigan-MAT 251 mass spectrometer. Reaction was carried out for a period of 10 minutes at 90ºC. Standard isobaric corrections were applied, but no correction was applied for the differences in fractionation of $\delta^{18}O$ as a result of the dissolution of dolomite and calcite by phosphoric acid (Swart, et al., 2005). All carbon and oxygen isotopic compositions are reported as per mil deviations relative to Vienna Peedee belemnite (VPDB).

Strontium isotope ratios were acquired at the University of Arizona using a VG Sector 54 multi-collector TIMS instrument fitted with adjustable 1011 O Faraday collectors and Daly photomultipliers. Multiple analyses of standard SRM 987 were used for calibration and $\delta^{87}Sr$ values are reported as the actual ratio of ^{87}Sr to ^{86}Sr.

3.7. Fluid Inclusions

Two sets of fluid inclusion analyses were performed on various samples taken from the quarry. The first set consisted of two samples taken from the floor of the quarry. They were sent to Fluid Inclusion Technologies, Inc. where doubly polished thick sections were prepared and then analyzed using a Fluid Inc.-adopted USGS-type heating-freezing stage. Samples were heated by passing air through a heating element and then over the sample, located in a special chamber designed to minimize lateral and vertical thermal gradients. Similarly, for freezing the samples, nitrogen gas cooled by liquid nitrogen was passed through an unheated element before entering the sample chamber. Both homogenization temperatures (T_H) and freezing temperatures (T_m) were recorded to the nearest degree Celsius and inferred salinities are reported to the nearest 0.1 weight percent. Primary and secondary and pseudo-secondary inclusions were studied.

A second set of samples was collected and analyzed at the University of Albany using a similar USGS-type heating-freezing stage. Ten samples were taken from various locations. Three sections were made from mineralization occurring in dolomite/calcite veins in the fracture zone surrounding the outcrop. Two samples of the outcrop were collected from the dolomite bodies on the quarry floor and two samples were taken from the interior of vugs lined with saddle dolomite crystals. Three matrix dolomite sections were made from core plugs at intervals where grain-texture was most coarse. A total of 41 fluid inclusions were located and analyzed in this second set. Results from both studies are presented in Chapter 4.

DATA

4.1 3-D Ground Penetrating Radar

Because the GPR survey was done before the outcrop was fully exposed, its main purpose was to aid in directing the excavation process. However, not only did the radar results help pinpoint the dolomite bodies beneath the talus, they also gave an excellent cross-section of the bodies' structure at depth. Figure 13 shows a horizontal slice from the 3-D survey (map view). This image clearly shows Body 2 including the jog. Notice the sharp contact between the structure of the body and the relatively flat-lying unaltered limestone of the Tribes Hill. Figure 14 shows a vertical slice of the survey (profile view) taken across the eastern portion of Body 2. Here the body appears as a sag which is flanked by anticlines on either side. This image shows that the feature is not just a surface expression but extends down to the maximum depth of the survey. Due to uncontrollable circumstances such as wet soil and clay-rich inter-beddings, the radar signal was dampened and only penetrated to a depth of about five feet.

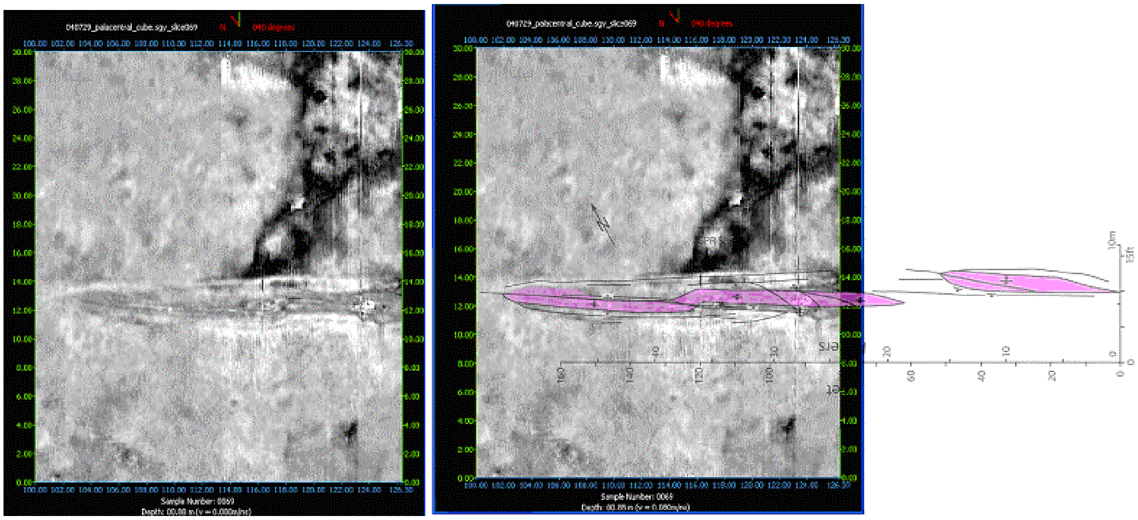

Figure 13 - Horizontal slice from ground penetrating radar survey, and same image with fracture map overlay

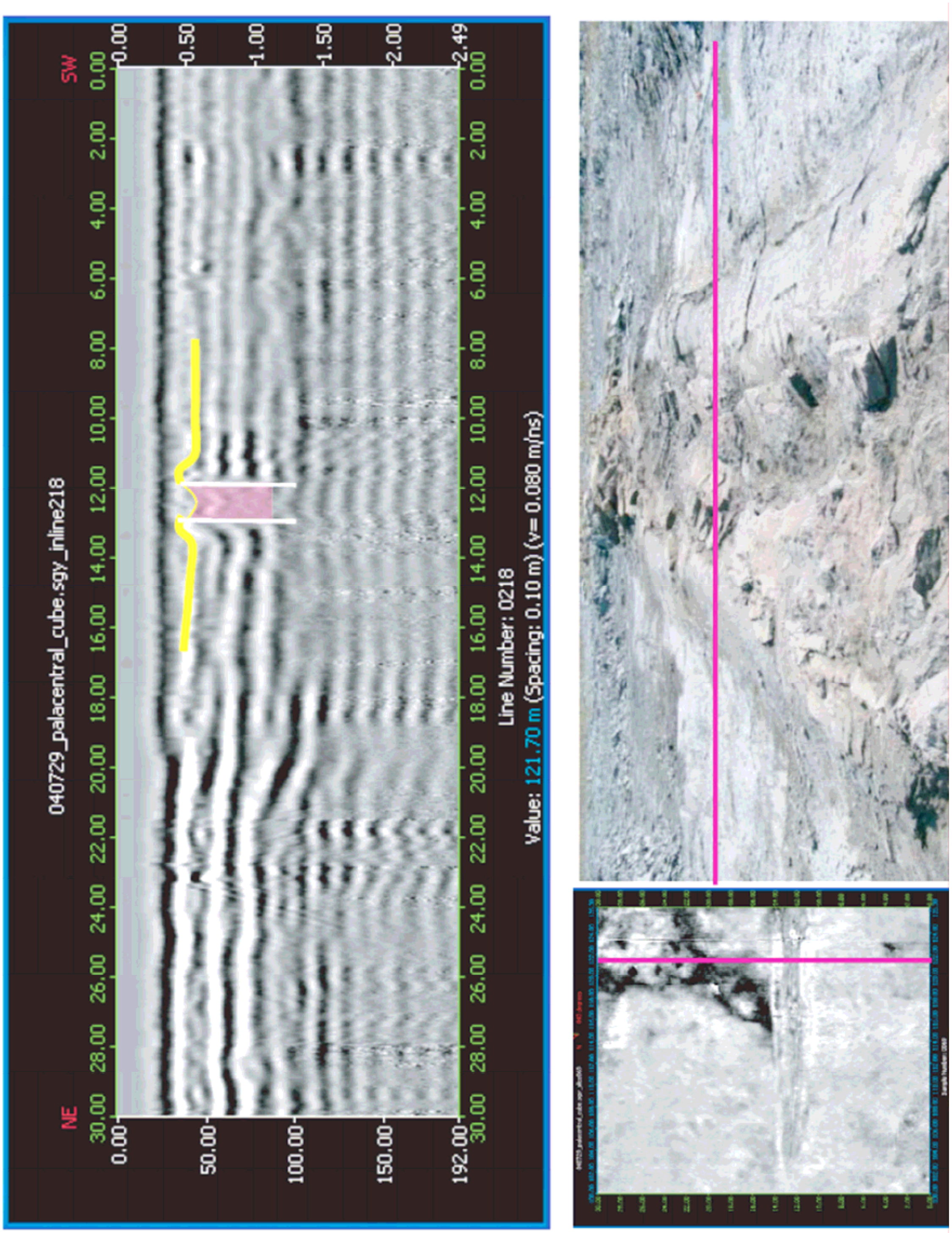

Figure 14 - Vertical slice from ground penetrating radar survey with reference lines drawn on horizontal slice and outcrop photo

4.2 Drill Cores

The six cores taken from the quarry were described by Richard D. Bray at the New York State Museum. A summary of his findings follows and the complete descriptions are available in Appendix 1. Figures 15 through 20 show stratigraphic columns for each of these core descriptions.

Hole 1 is located inside the eastern portion of Body 2 and the rock is dolomitized throughout its entire length. The upper 12 feet of the core has well-developed intercrystalline and vuggy porosity and contains a section 3-foot long of a fracture zone with well-defined breccia clasts. The next 11 feet of core contain less porosity, but have an increased pyrite and bitumen content (Figure 21). The Tribes Hill / Little Falls contact occurs at a depth of 22.5 feet. The remaining 15 feet of core contain pyrite and bitumen-filled fractures as well as a mottled red marker bed at 35 feet.

Hole 2 is located in the fracture zone approximately five feet north of Hole 1. The uppermost 12.6 feet of core are described as a dolomitic limestone. This zone contains three saddle dolomite-filled fractures at three, six, and seven feet. Between 12 and 16 feet the core grades into a slightly calcitic dolomite taking on the characteristics of the cores drilled within the dolomite bodies. The upper four feet of this zone has well-developed intercrystalline, intergranular, and vuggy porosity. The lower three feet of the Tribes Hill contains sparse vuggy porosity (Fig. 22), rare pyrite, and a high-angle bitumen-filled fracture which continues into the Little Falls Formation. A mottled red marker bed occurs at 35 feet.

Hole 3 is located at the eastern tip of Body 2 and is dolomitized throughout its entire length. The upper seven feet of the core are characterized by numerous breccia clasts, but rare porosity. Below this interval the remaining section of Tribes Hill contains zones of densely concentrated microstylolites, abundant intercrystalline and vuggy porosity, rare pyrite, and some bitumen. The contact between the Tribes Hill and Little Falls formations occurs at approximately 25 feet down below which bitumen and dolospar-filled fractures can still be observed. A mottled red marker bed occurs at 35 feet.

Hole 4 is located in the limestone gap or “bridge” between Bodies 1 and 2. The upper three feet of this core are a slightly dolomitic limestone in which the characteristics of unaltered Tribes Hill strata are preserved. However, the core then grades into a dolomite and displays the same characteristics as the other core in the dolomite bodies. From 3 to 23 feet vuggy and intercrystalline porosity increase and brecciation occurs throughout (Fig. 23). The Tribes Hill / Little Falls contact is at approximately 24 feet. A mottled red marker bed occurs at 35 feet.

Hole 5 is located in the “jog” at the center of Body 2 and is dolomitized throughout its entire length. The upper three feet of core does not show any porosity, however the remainder of the Tribes Hill section consists of zones ranging from sparse to abundant vuggy and intercrystalline porosity occurring near faults and in areas of brecciation. Beds often appear distorted by soft sediment deformation. The Tribes Hill / Little Falls contact is at approximately 24 feet. A mottled red marker bed occurs at 35 feet.

Hole 6 is located outside the fracture zone approximately 15 feet north of Hole 1. The Tribes Hill section of the core spans 25 feet from the surface to the Little Falls contact and is a slightly dolomitic limestone throughout. There is rare pyrite and no faults, brecciation, or visible porosity. Bedding near the bottom of the section appears to have been affected by soft sediment deformation. Within the Little Falls Formation a mottled red marker bed occurs at 35 feet.

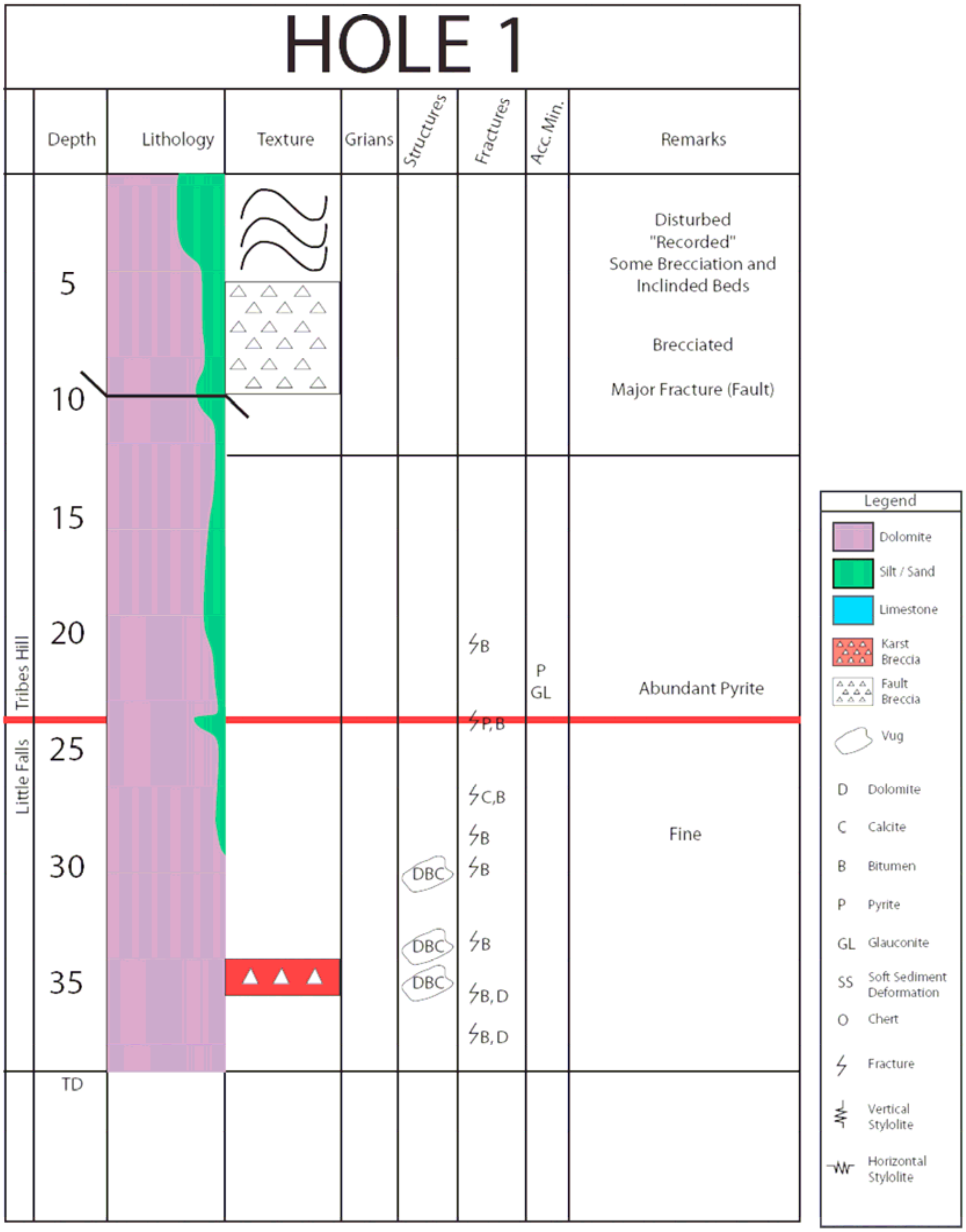

Figure 15 - Hole 1 stratigraphic column with description (digitized from Bray)

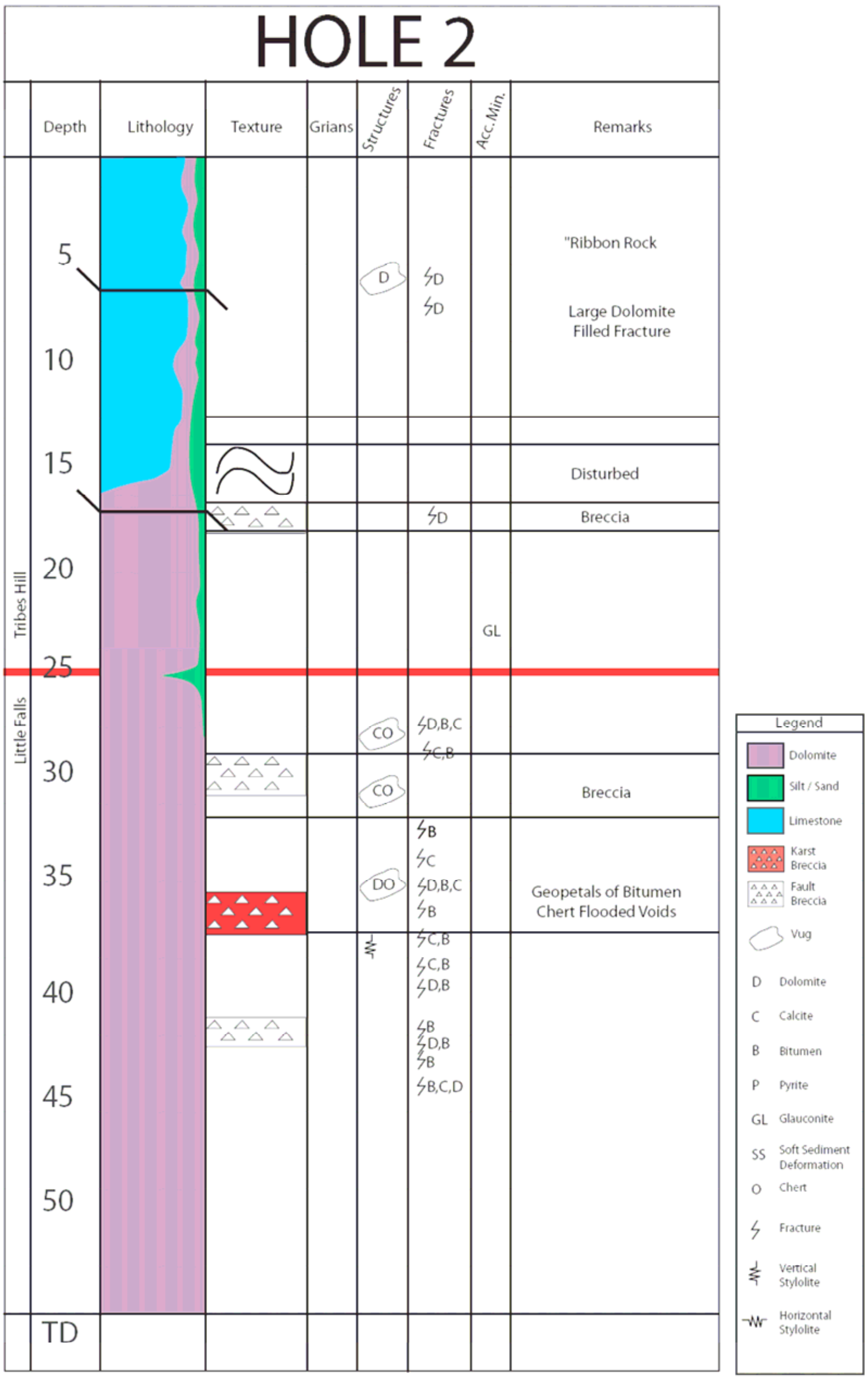

Figure 16 - Hole 2 stratigraphic column with description (digitized from Bray)

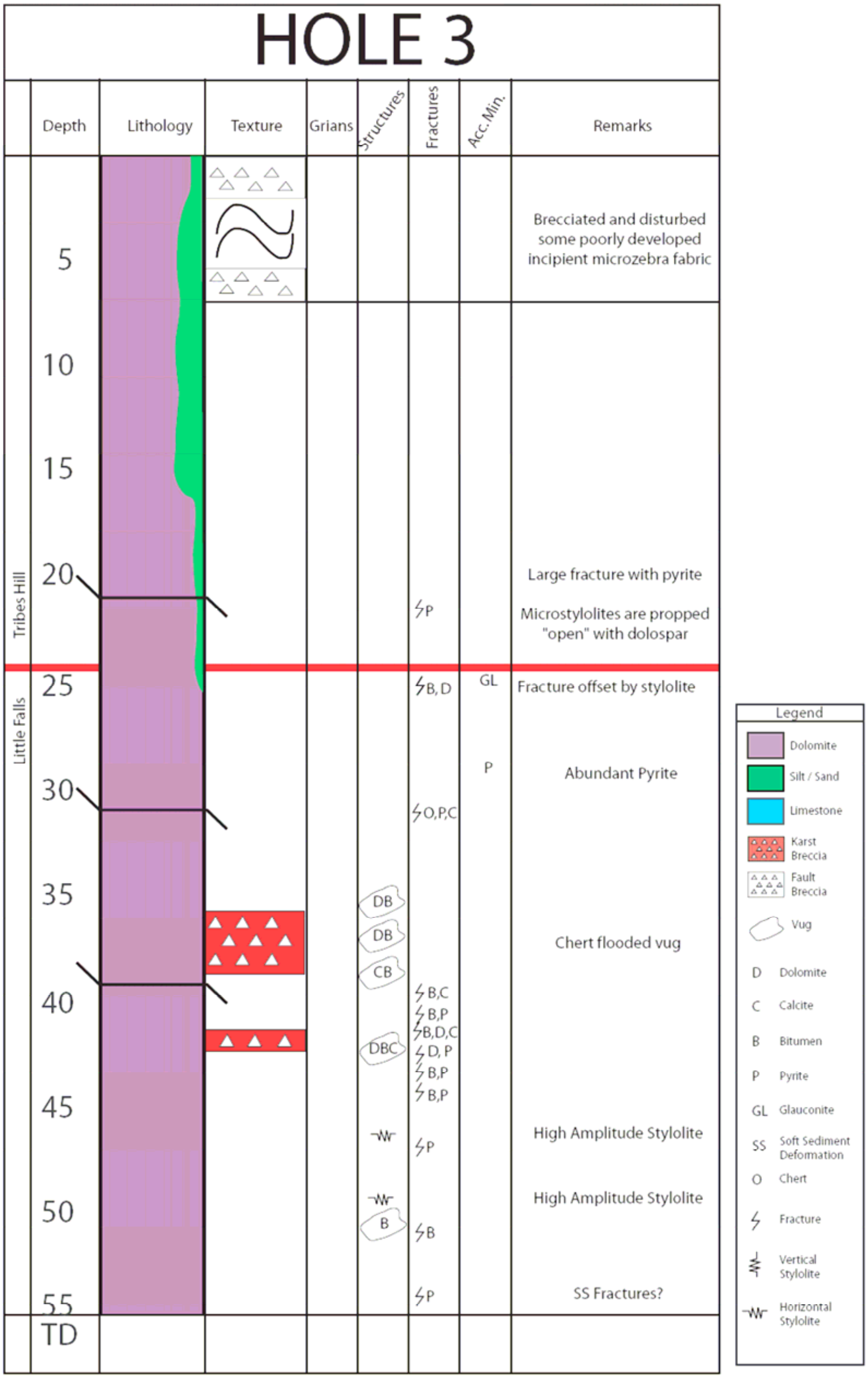

Figure 17 - Hole 3 stratigraphic column with description (digitized from Bray)

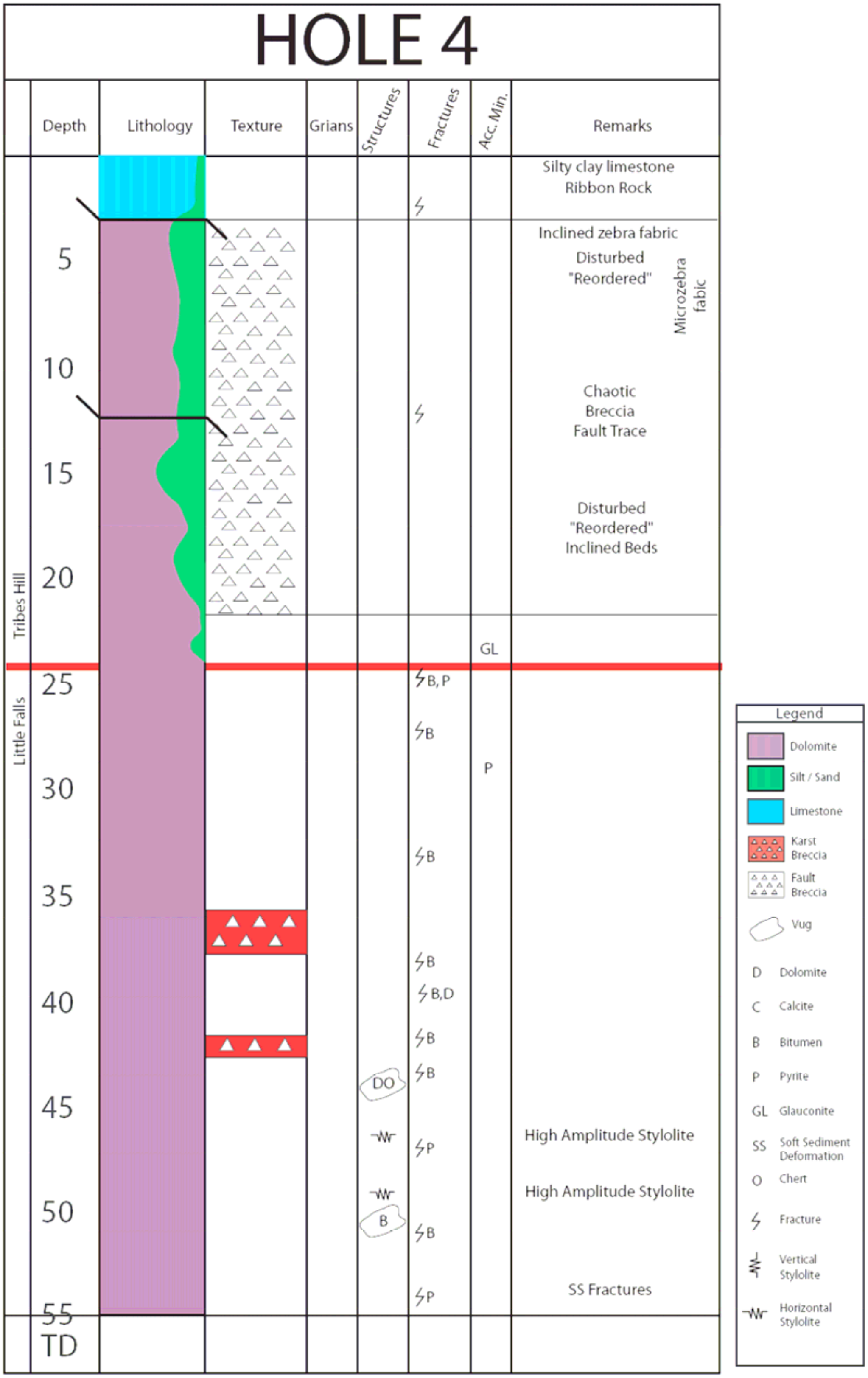

Figure 18 - Hole 4 stratigraphic column with description (digitized from Bray)

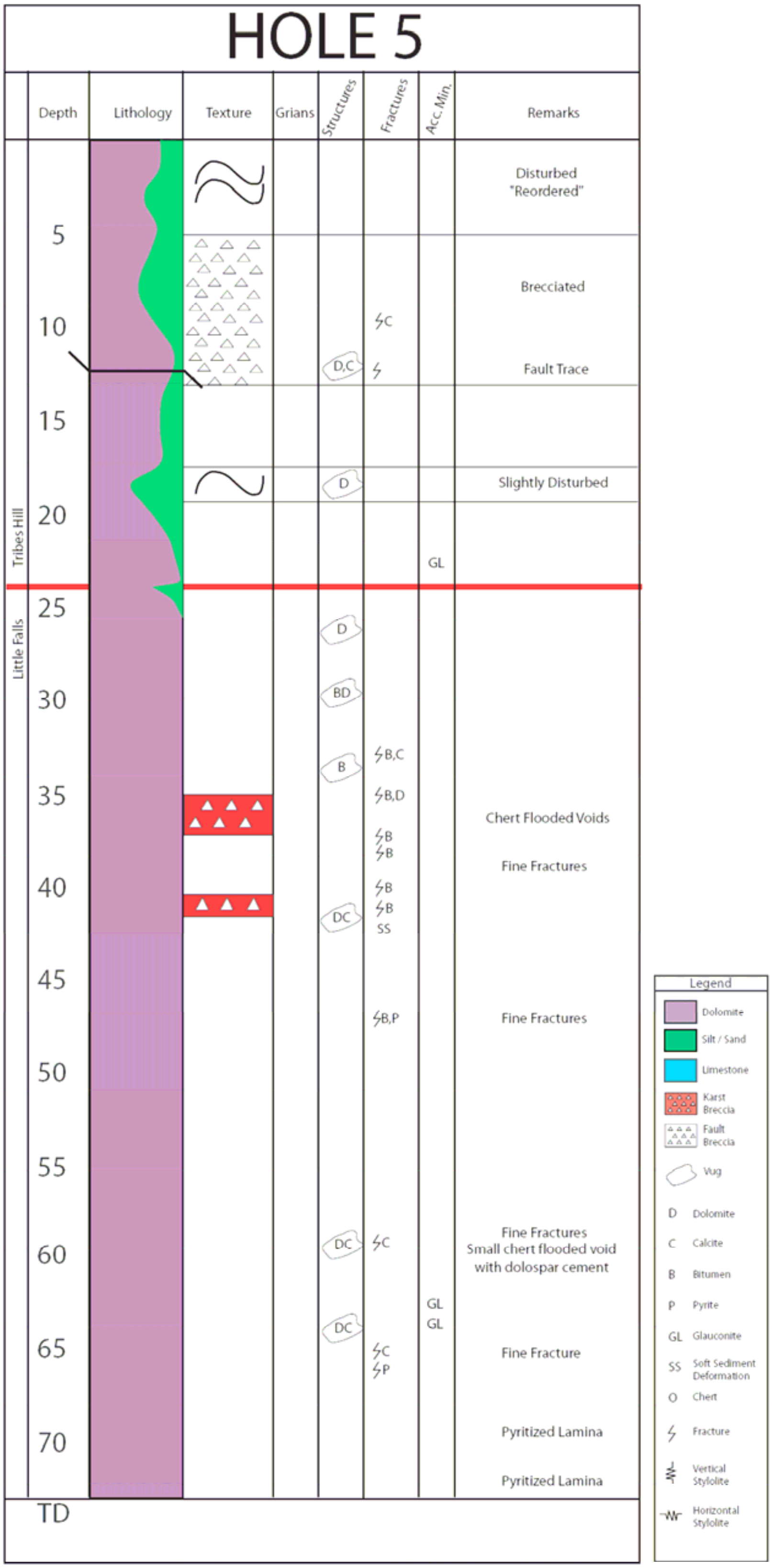

Figure 19 - Hole 5 stratigraphic column with description (digitized from Bray)

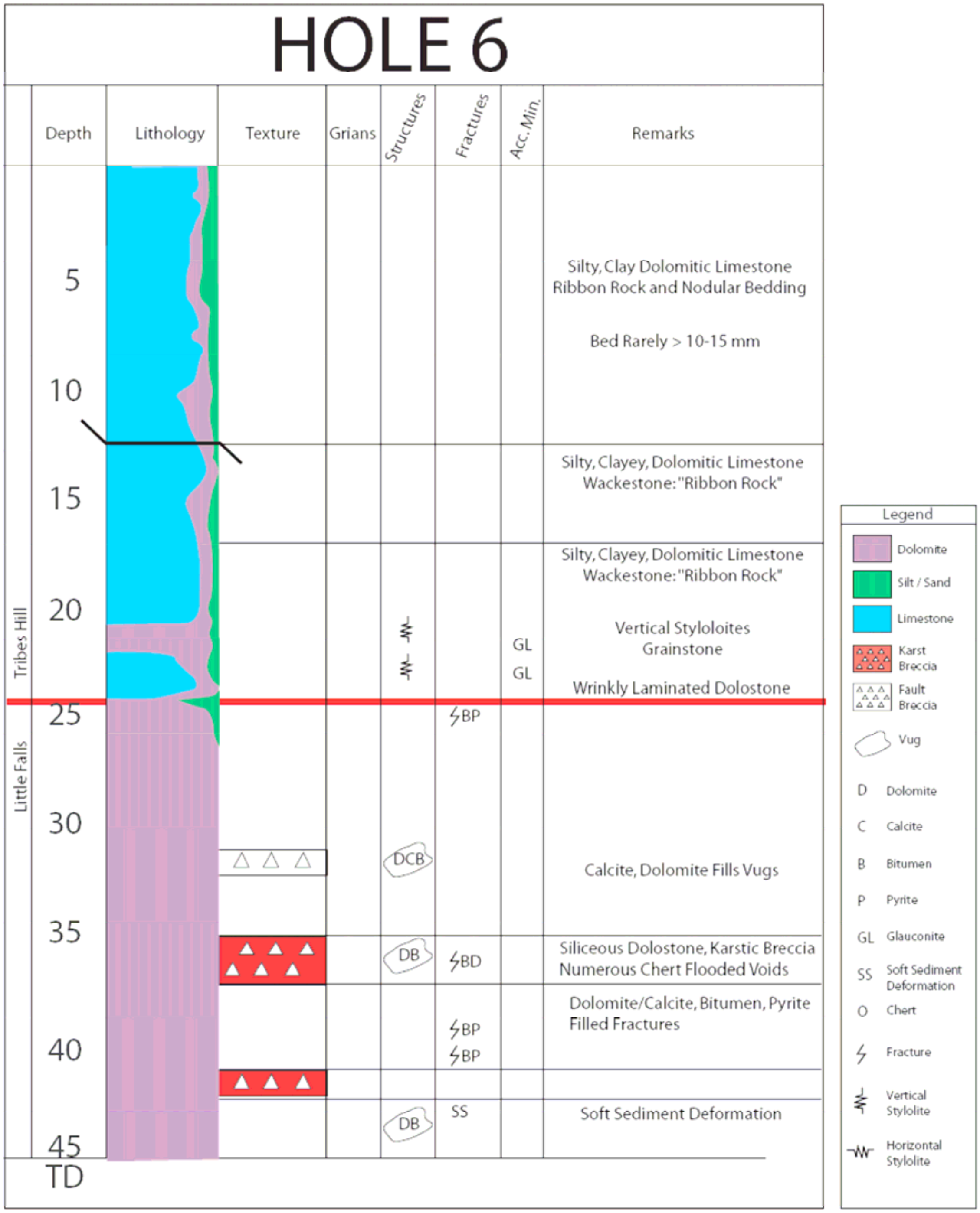

Figure 20 - Hole 6 stratigraphic column with description (digitized from Bray)

Figure 21 – Fracture filled with pyrite and bitumen
(from Hole 1: 23 ft.)

Figure 22 – Vugs lined with saddle dolomite (from Hole 2: 16.5 ft.)

Figure 23 – Fault breccia
(from Hole 4: 14 ft.)

Figure 24 shows cross-section 1 which connects Holes 1, 2, and 6. This serves as a stratigraphic profile from the center of Body 2 (Hole 1) across the fracture zone (Hole 2) and into the unaltered limestone (Hole 6). Hole 1 consists of dolomitized Tribes Hill from the surface to a depth of 24 feet where it reaches the Little Falls contact. Hole 2, located in the fracture zone, approximately five feet north of Hole 1, begins as unaltered limestone, but becomes dolomitized after crossing a fracture at 16 feet. Hole 6 was drilled outside of the fractured zone, about 15 feet north of Hole 1, and consists of undolomitized Tribes Hill for the entire thickness, with the exception of a one-foot interval of dolomite occurring at a depth of 20 feet.

Figure 25 shows cross-section 2 which connects Holes 1, 3, 4, and 5. Holes 1, 3, and 5 are all located inside the dolomite structure and are, as one would expect, dolomitized throughout their entire length. Hole 4, however, was drilled in the limestone bridge, or gap, between the first and second bodies. The core from this hole reveals that although the bridge is composed of unaltered Tribes Hill at the surface, it crosses a fault and the rock becomes dolomitized only 3 feet below the quarry floor.

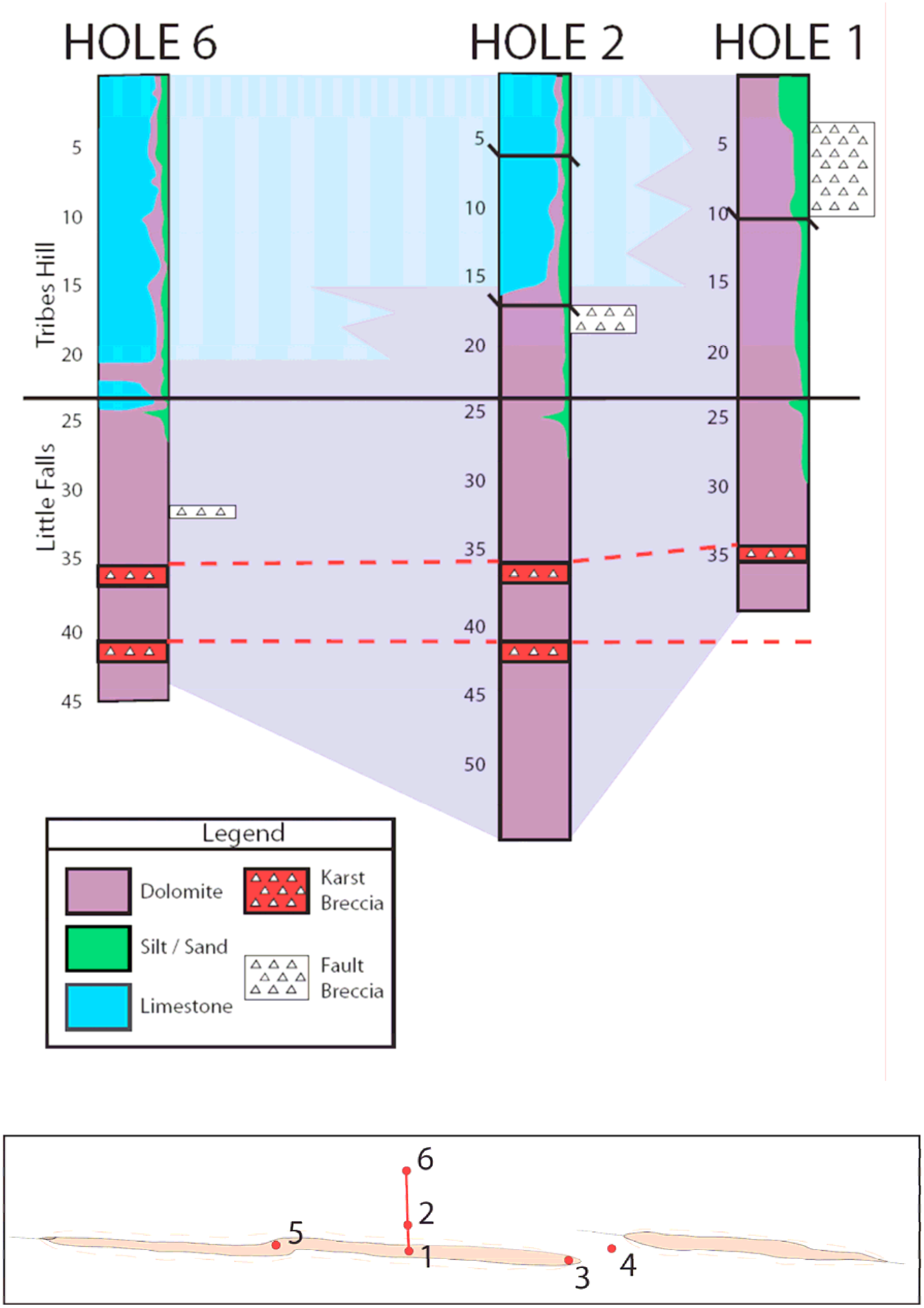

Figure 24 - Cross-section 1, connecting Holes 1, 2, and 6

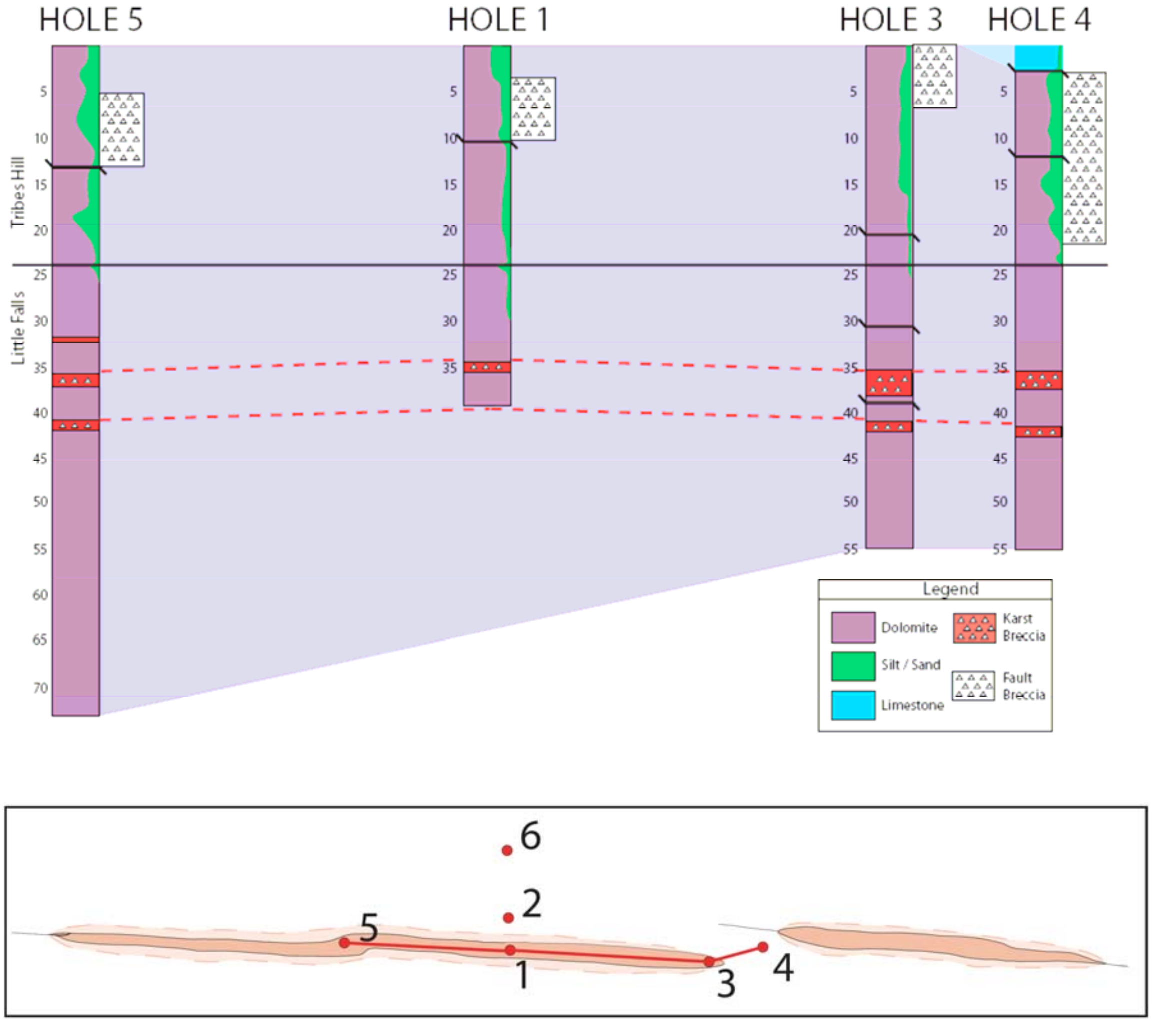

Figure 25 - Cross-section 2, connecting Holes 1, 3, 4, and 5

4.3. Fracture Mapping

The fracture map made in Chapter 3.4 reveals several structures and patterns that may act as clues to determining the orientation of stresses acting on the region during formation of the bodies. There are calcite veins running from the tips of each body (Fig. 26). These veins range in width from 0.3 to 0.8 inches. The vein associated with the eastern tip of Body 1 runs for roughly 10 feet and then bifurcates, forming two smaller veins, which run into a covered interval. Four smaller veins emerge from this covered interval leading to the interpretation that both veins split a second time. These four veins die out within a few feet of their origin. The western tip/vein of Body 1 and the eastern tip/vein of Body 2 overlap and form the northern and southern boundaries of the bridge (Fig. 27). Both of these veins die out within ten feet of the bodies.

Figure 26 - Calcite vein running from eastern tip of dolomite body 1

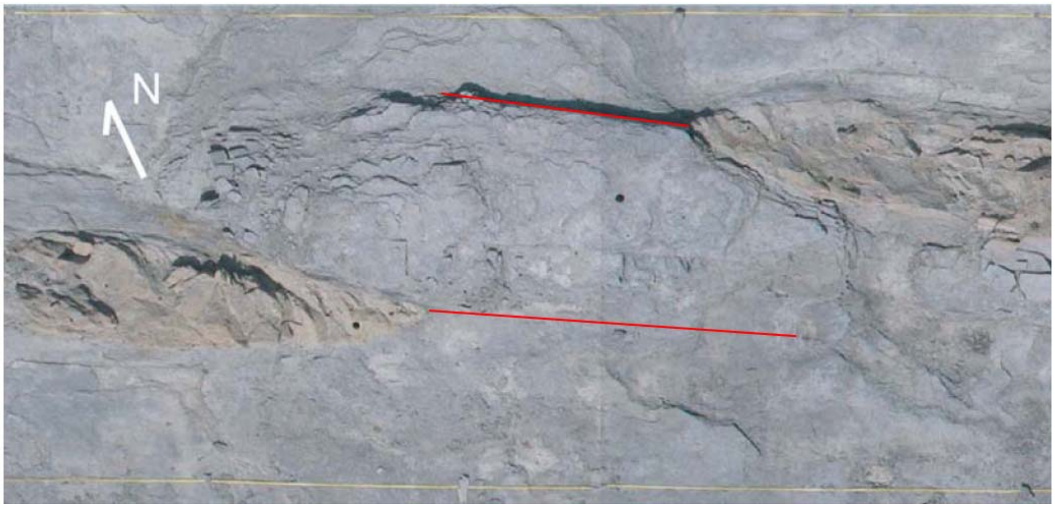

Figure 27 - Aerial view the bridge (calcite veins highlighted in red)

Another feature illustrated by the map is the scissor fault that cuts across Body 2 at the jog. This fault begins southeast of the jog and runs sub-parallel to the dolomite body dipping to the north. As the fault approaches the jog it bends toward the body and its dip steepens. The fault is nearly vertical as it intersects and cuts through the jog. After exiting the north side of the body the fault bends back to sub-parallel with the body and dips to the south. In this way the fault changes dip as it crosses the dolomite body. Figure 28 shows a series of pictures taken from Trenches 4 and 5 illustrating this change in dip. The significance of the structure is discussed in Chapter 5.3.

The fracture map also shows a relay ramp fault pattern located in the fracture zone along the northern edge of Body 2 (Fig. 29). A relay ramp, as defined by Peacock et al. (2000), is an area of reoriented bedding between two normal faults that overstep in map view and have the same dip direction. The structure begins as a single fault at the eastern tip of Body 2 and runs along the northern edge of the body. It splays to the north at three separate points within 20 feet of the tip, forming separate relay ramps. Note that, as a relay ramp, a single fault block may act as the footwall of one fault and the hanging wall of another.

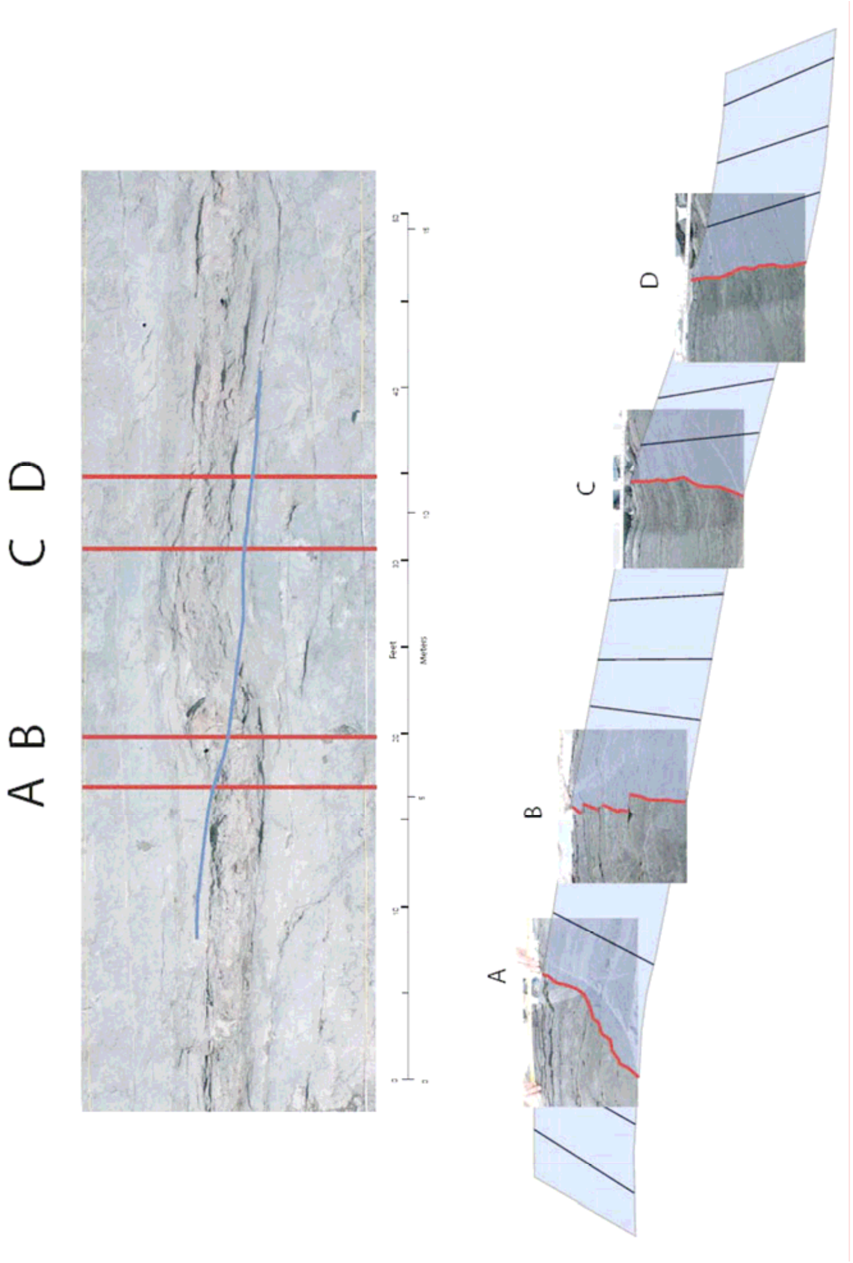

Figure 28 – Illustration of scissor-fault across four trench walls

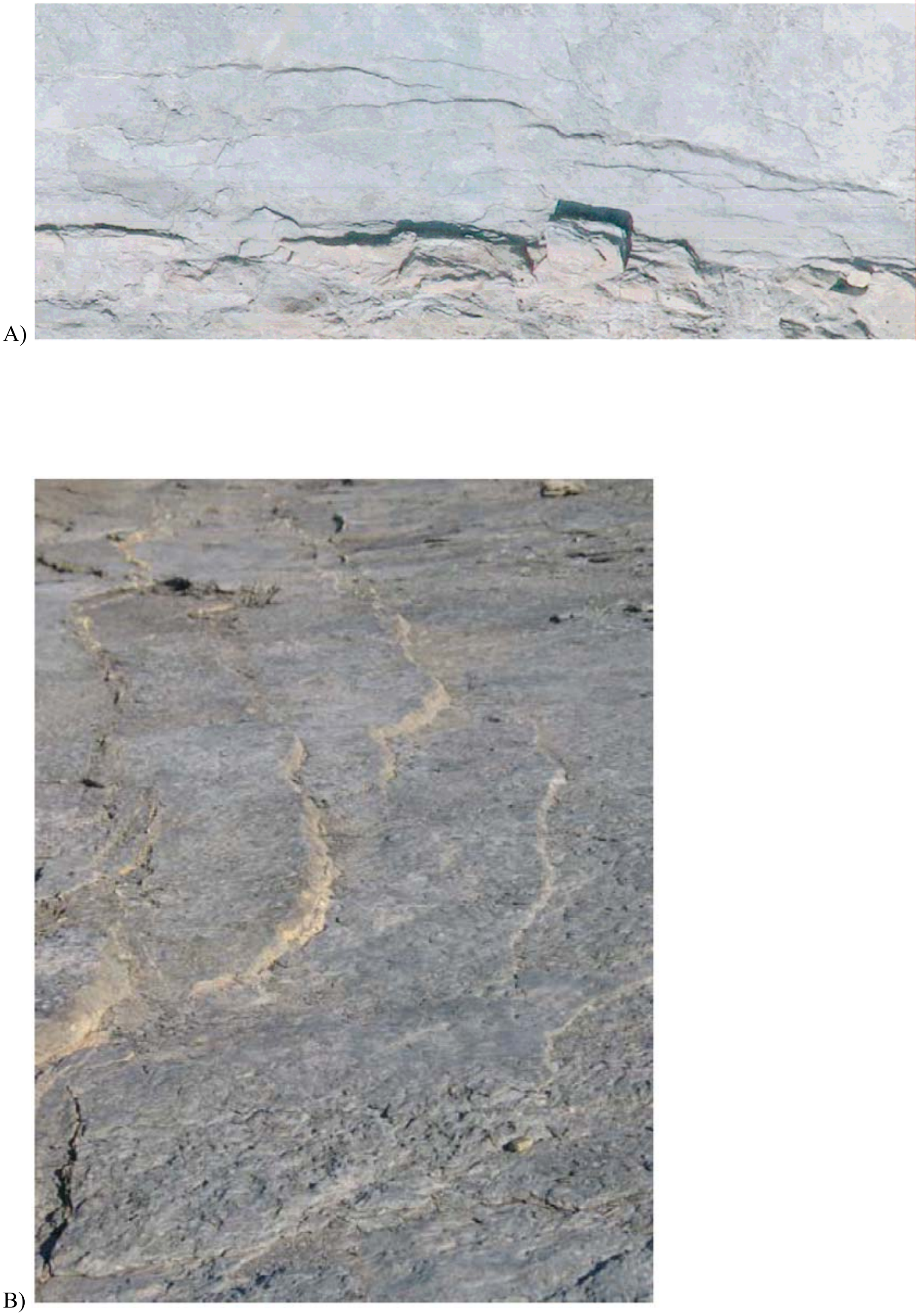

Figure 29 - Relay ramp structure running parallel to the eastern portion of Body 2 A) aerial view B) photo taken from the ground

As mentioned in Chapter 1.4, there are several areas inside the dolomite bodies where brecciation is observed. The most obvious of these occurrences are the tips of each body, however they can also be found in various locations throughout the bodies. Breccia clasts consist of fine-crystalline matrix dolomite surrounded by coarse crystalline dolomite (Fig. 30). The locations of all brecciated regions appear on the fracture map. Vugs also occur in many parts of the outcrop. They are commonly found near the brecciated zones at the tips of the bodies. All the vugs are lined with saddle dolomite and calcite. Many also contain quartz and bitumen (Fig. 31). Areas with vuggy porosity are also labeled on the fracture map.

Figure 30 – Cross-section of a brecciated block from inside dolomite body

Figure 31 - A large vug filled with saddle dolomite and calcite crystals, located at the eastern tip of body 1

Another notable structure which appears on the fracture map is the “tail”-like feature connected to the central portion of Body 2. This long, thin section of coarse-grained dolomite extends from the northern side of the jog and runs west, sub-parallel to the western half of the body. It continues for approximately 12 feet then thins to a point. Figure 32 shows an aerial view of the tail, while Figure 33 shows the feature in the wall of Trench 5. From the trench wall, one can see that the “tail” dips to the north away from the dolomite body. The significance of the structure is discussed in Chapter 5.4.

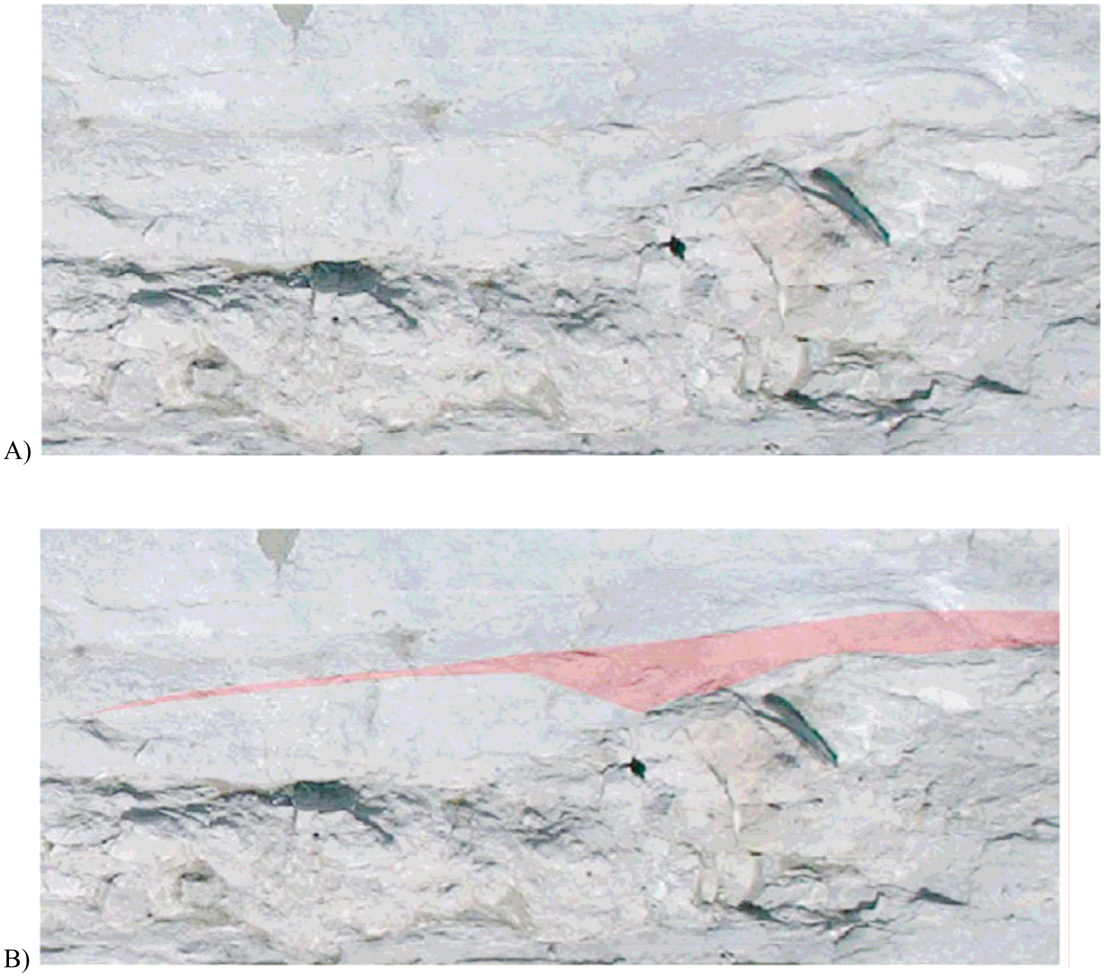

Figure 32 - Aerial photo of the tail-like structure
A) without highlight B) with structure highlighted in pink

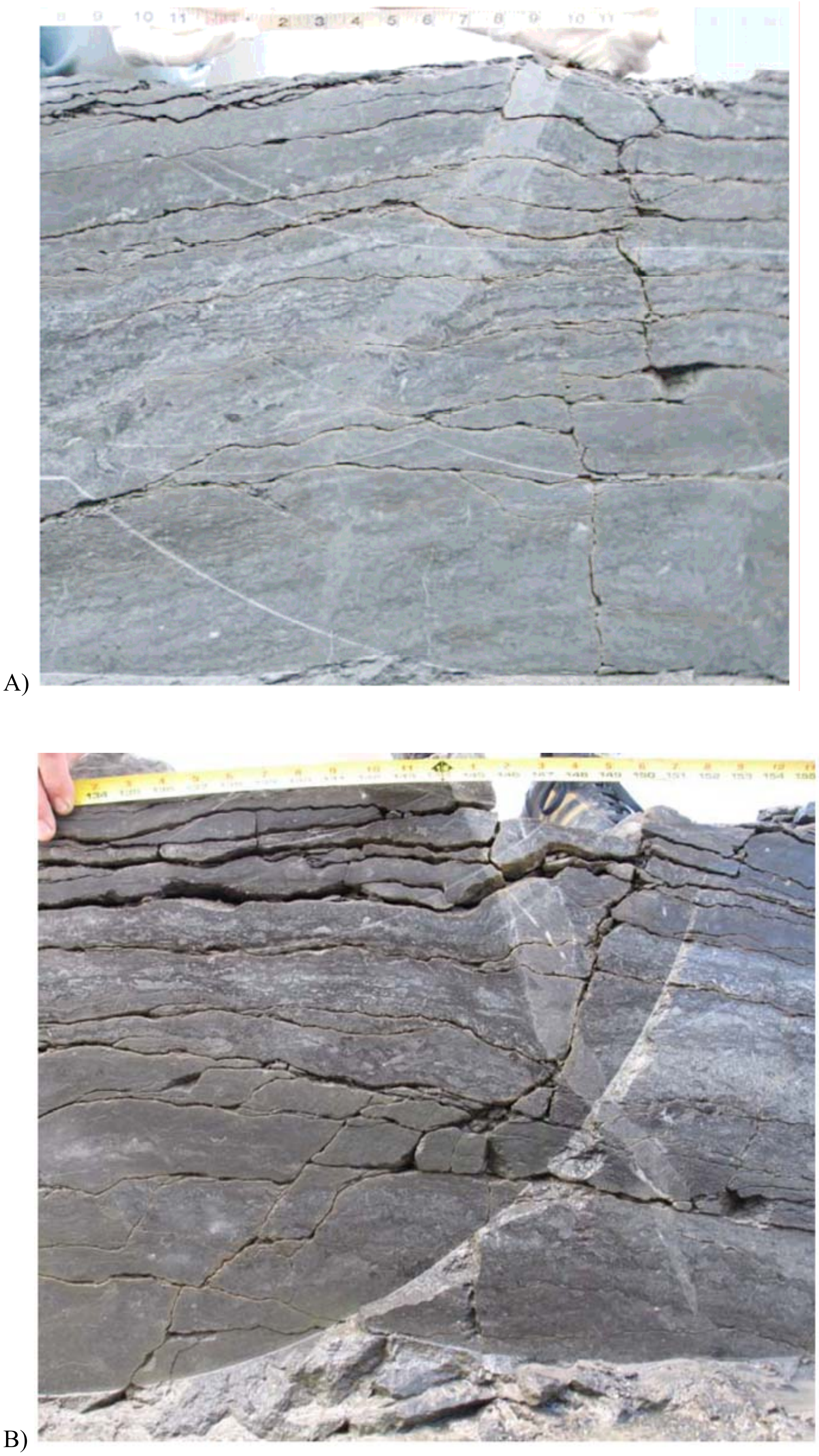

Figure 33 - Profile photos of tail-like structure taken from trench 5

A) looking east B) looking west

4.4. Trenches

The walls of the six trenches allow analysis of the bodies and surrounding fracture zone in profile view. Plates 3 through 6 show photo-mosaics made for trenches 3, 4, and 5. The walls of all trenches have not yet been photographed.

Variations in color help show the transition from limestone to dolomite. Contact between the limestone and dolomite is relatively sharp (Fig. 34). The texture of the dolomite also coarsens during this transition. Grains of the Tribes Hill Limestone range from 88 to 125µm, while matrix dolomite crystals from inside the bodies can measure up to 500µm in diameter.

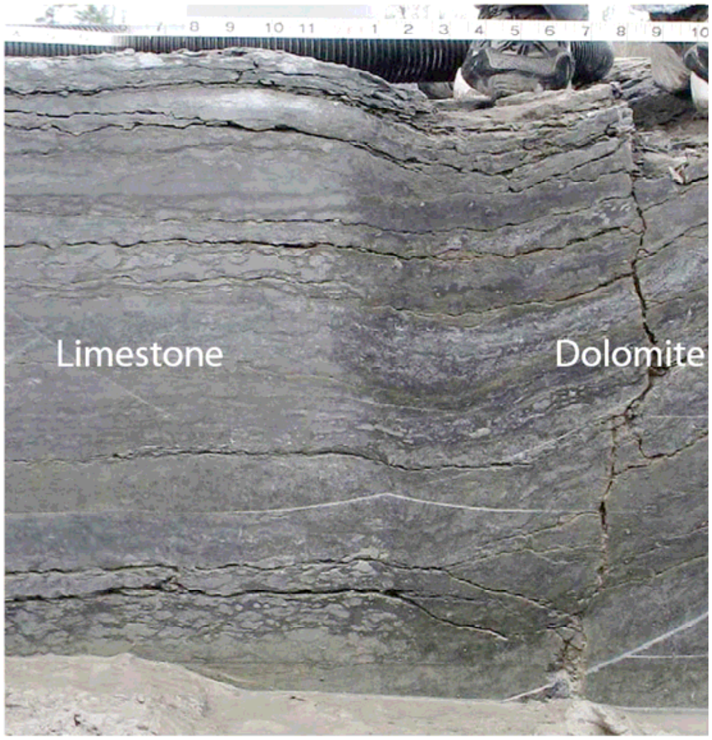

Figure 34 – Transition from limestone to dolomite in Trench 4

Like the GPR profile, the trench walls reveal that both bodies consist of a central syncline, or sag, which is flanked by anticlines on either side. A shaley layer approximately three inches thick appears in a number of the trench walls and serves as a good marker bed for correlation between trenches and for measurement of displacement across fractures/faults (Fig. 35). The offset of this bed can be as much as seven inches as seen in Figure 35. Unfortunately, nearly all original rock texture is lost on entering the dolomitized portion of the trench walls. This makes it difficult to follow an individual layer across the entire body. In each case the central sag consists of a breccia in which clasts have been moved and rotated relative to one another (Fig. 36).

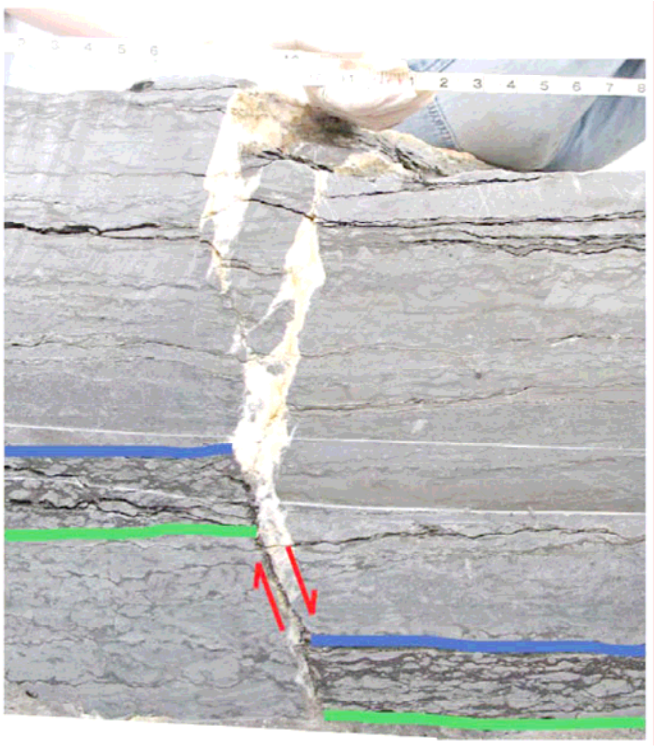

Figure 35 - Offset shaley bed in the eastern wall of Trench 5

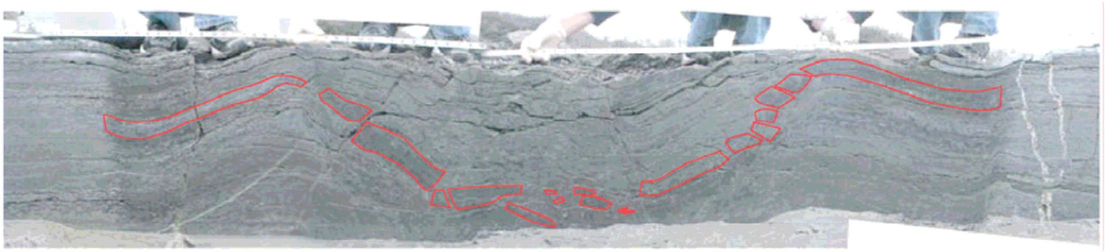

Figure 36 - Rotated bocks located within the central sag of body 2 (taken from western wall of Trench 4)

The trench walls also give excellent exposures of the mineralization along fractures and faults especially along each side of the bodies. One observation made by looking at the trenches, which could not be seen in map view, is the relationship between amount of mineralization and proximity to the dolomite bodies. The fractures in outer extremes of the fracture zone are fully mineralized with little or no porosity. Moving inward (from either side) toward the transition zone of limestone to dolomite, the fractures are commonly open or only partially healed. Many are lined with saddle dolomite crystals, but void space remains where mineralization has not completely occluded the fractures. Inside the zone of coarse dolomite all fractures are completely open and show no signs of mineralized filling.

Many of the faults display both shear and extensional motion. Segments that fail with a shear sense commonly dip toward the dolomite body, while segments with a larger extensional component dip away from the bodies (Fig. 37). In some cases, movement along faults caused the opening of rhomb-shaped segments. These features have a saddle dolomite lining and calcite fill. Figure 38 shows a rhomb exposed in Trench 6. Figure 39 shows a similar rhomb with slickensides indicating the same sense of motion.

Figure 37 - Fractures change dip direction when crossing shaley bed taken from eastern wall of Trench 4, body two lies to the left)

Figure 38 - Rhombohedral pull-apart with red arrow to indicate motion direction (taken from eastern wall of trench 6)

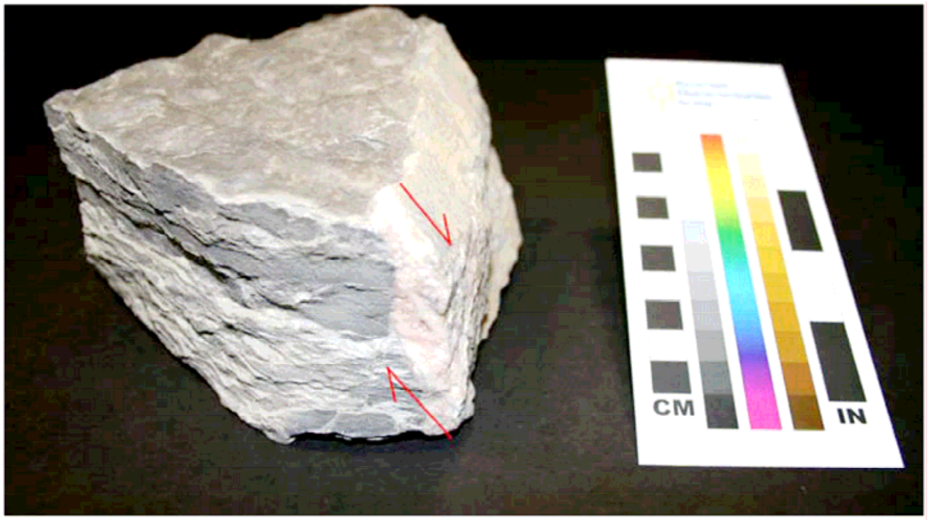

Figure 39 - Calcite/dolomite rhomb with slickensides taken from the quarry

4.5 Paragenetic Sequence

Thin sections made from the quarry samples were analyzed at the New York State Museum. These sections helped determine the relative timing of the diagenetic and epigenetic processes that have acted on the Tribes Hill since deposition. Figure 40 is a chart depicting this series of events. Figure 41 shows a thin section example for each event.

The earliest processes to affect the Tribes Hill, fragmentation, desiccation and lithification, are all common in the formation of limestone. Some dolomite replacement occurred before fracturing began and this should therefore not necessarily be considered hydrothermal. This initial dolomitization could have been caused by meteoric mixing. The first incidence of fracturing was followed by a second period of dolomite replacement and growth of saddle dolomite crystals. In this case, the dolomitization was directly related to the faulting and can be considered epigenetic in origin. These saddle crystals are zoned with alternating iron-rich and non iron-rich regions. Later, dedolomitization and dissolution of saddle dolomite occurred. Oil was then emplaced and later dehydrogenated to form bitumen. A second fracturing event caused another episode of hydrothermal fluid flow and precipitation of saddle dolomite, pyrite, and a late calcite spar. The precipitation of Herkimer Diamond type quartz crystals and a late calcite spare was the last stage in the diagenesis of the Tribes Hill outcrop. These quartz crystals commonly contain solid bitumen inclusions.

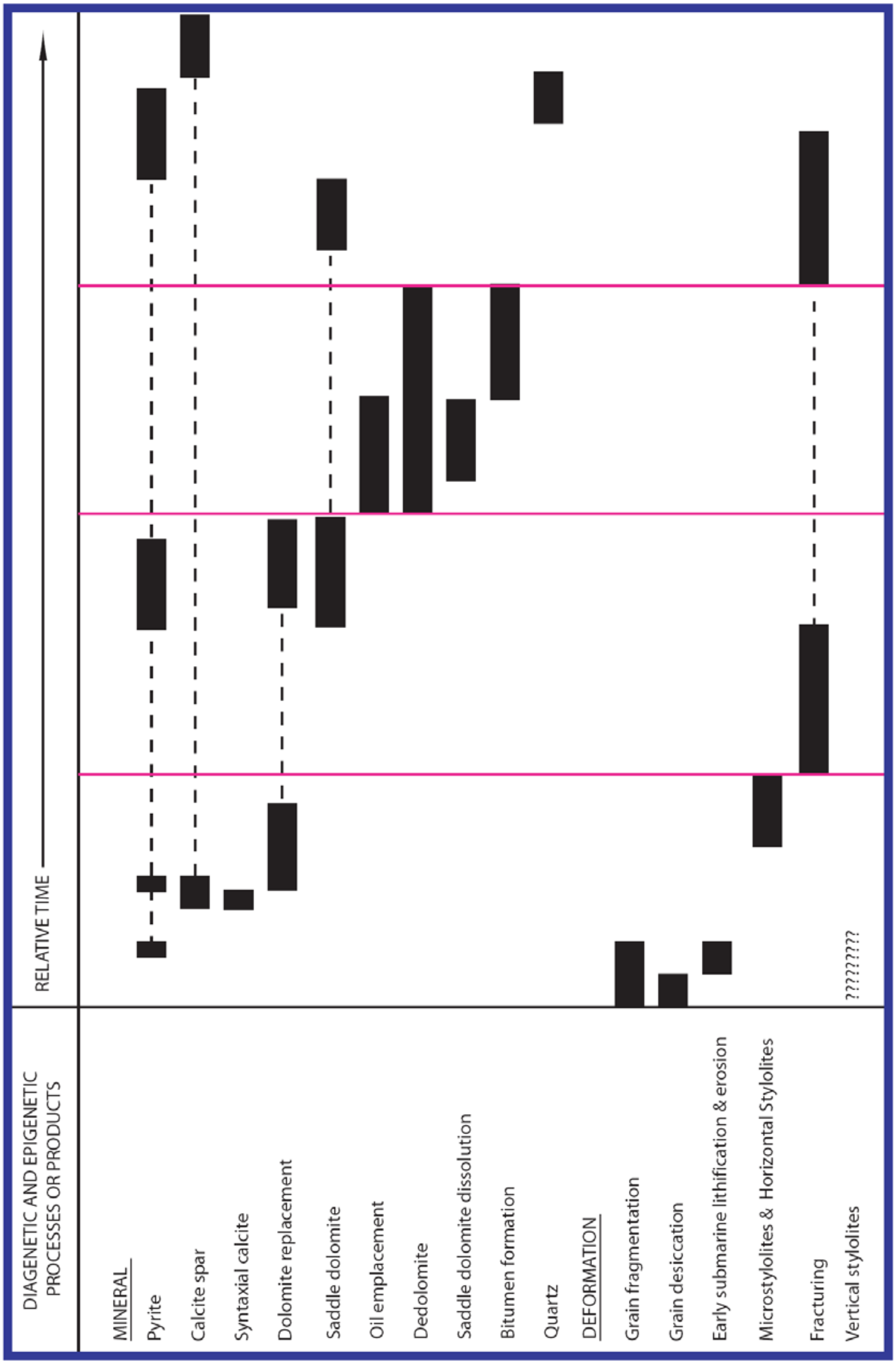

Figure 40 –Graph of paragenetic sequence in relative time

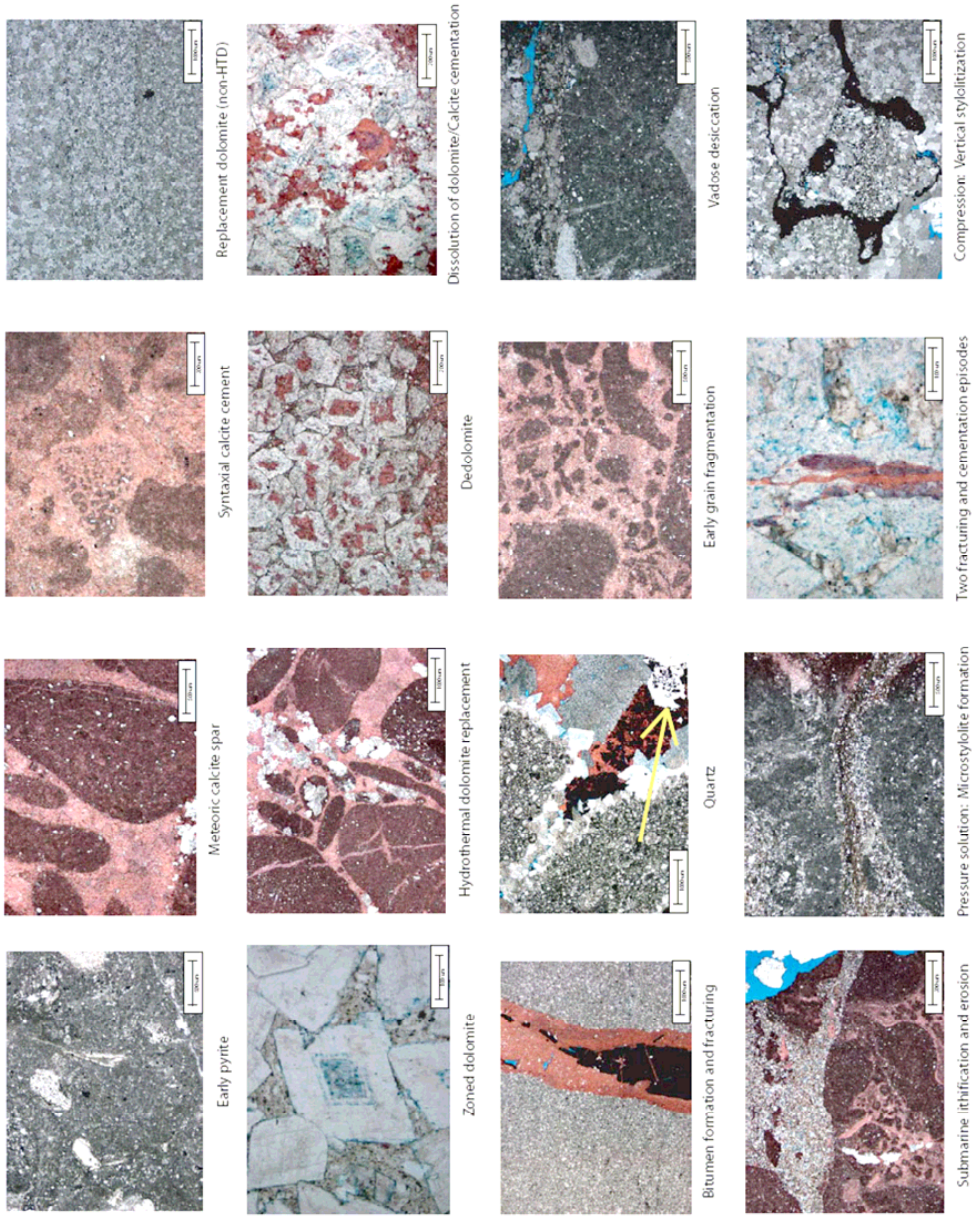

Figure 41 - Thin section images from quarry cores illustrating the types of diagenesis and epigenesis observed

4.6. Stable Isotopes

As described in Chapter 3.6, three sets of samples were analyzed for δ^{13}C and δ^{18}O: the initial surface samples, all plugs from the transect, and the core plugs from Holes 1 and 2. The results of these analyses are shown in Tables 4-1 through 4-3 and in Figure 42. Carbon isotope values for dolomite in the Tribes Hill range from -1.31 to -3.06‰ with an average of -2.01‰. Values for the surrounding limestone are slightly more negative with a range of -1.70 to -3.25‰ and an average of -2.19‰. The δ^{18}O values follow a similar pattern. In the dolomite, values range from -7.66 to -10.74‰ with an average of -8.86‰, while in the limestone ratios range from -8.52 to -11.40‰ and have an average of -9.49‰. As a general rule, the δ^{18}O values for a dolomite that formed from the same fluid as a limestone are generally 3‰ heavier than that limestone. Therefore, using the oxygen isotope values for the unaltered Tribes Hill limestone, we should be able to predict where dolomite that formed from the same fluid should plot. Figure 42 shows that the dolomites from the quarry do not plot in this “seawater dolomite” window. This indicates that they formed from a different fluid than the Tribes Hill Limestone.

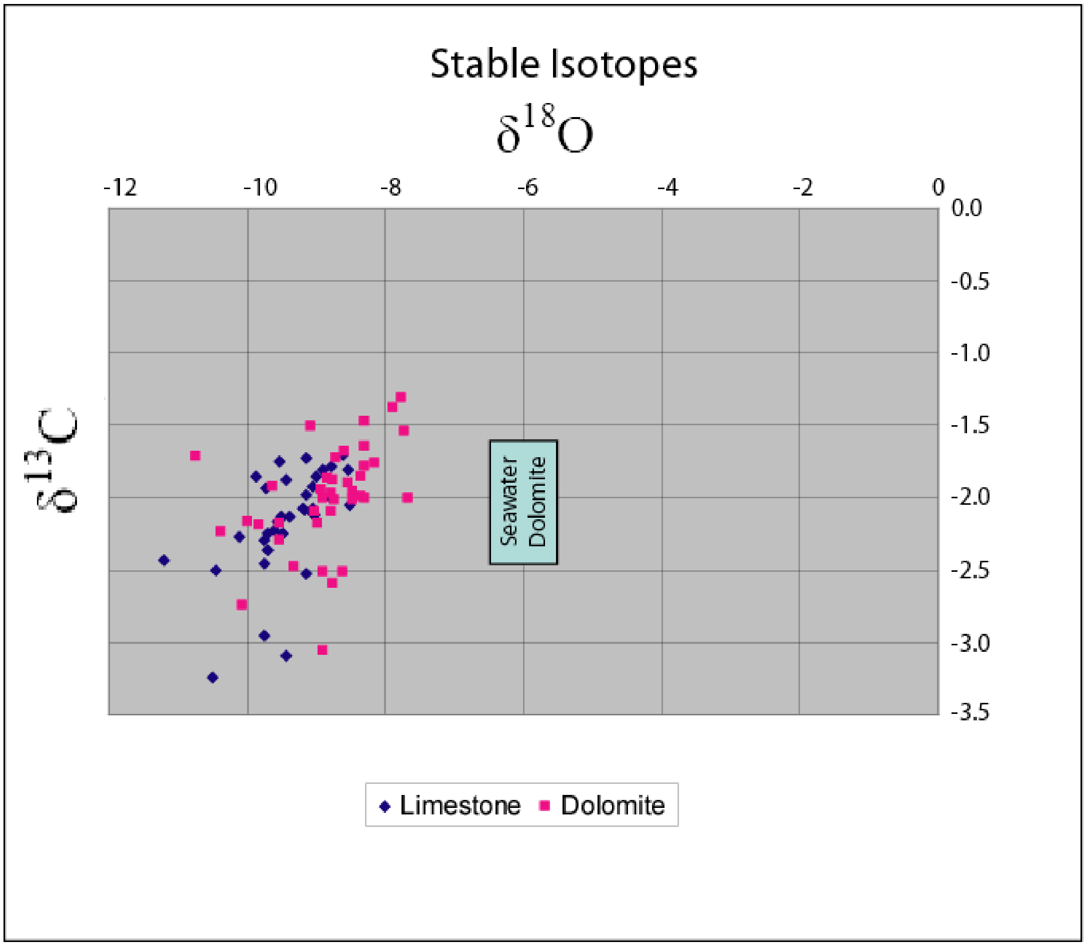

Figure 42 - Cross-plot of stable isotope ratios in comparison with the standard seawater dolomite window

Table 4-1 - Stable isotope results for transect plugs

ID #	Footage	Sampled	Comments	$\delta^{18}O$	$\delta^{13}C$
T1-1	1	transect plugs	outside fracture zone-limestone	-9.01	-1.86
T1-2	2	transect plugs	outside fracture zone-limestone	-9.20	-2.07
T1-3	3	transect plugs	outside fracture zone-limestone	-9.06	-2.07
T1-4	4	transect plugs	outside fracture zone-limestone	-8.79	-1.78
T1-5	5	transect plugs	outside fracture zone-limestone	-10.49	-3.25
T1-6	6	transect plugs	outside fracture zone-limestone	-9.86	-1.85
T1-7	7	transect plugs	outside fracture zone-limestone	-9.55	-2.17
T1-8	8	transect plugs	outside fracture zone-limestone	-9.76	-2.29
T1-9	9	transect plugs	outside fracture zone-limestone	-9.16	-2.09
T1-10	10	transect plugs	outside fracture zone-limestone	-9.14	-2.53
T1-11	11	transect plugs	outside fracture zone-limestone	-9.48	-2.25
T1-12	12	transect plugs	outside fracture zone-limestone	-9.15	-1.98
T1-13	13	transect plugs	outside fracture zone-limestone	-9.53	-2.16
T1-14	14	transect plugs	outside fracture zone-limestone	-9.76	-2.96
T1-15	15	transect plugs	outside fracture zone-limestone	-8.62	-1.70
T1-16	16	transect plugs	outside fracture zone-limestone	-9.69	-2.25
T1-17	17	transect plugs	outside fracture zone-limestone	-10.45	-2.50
T1-18	18	transect plugs	outside fracture zone-limestone	-9.38	-2.13
T1-19	19	transect plugs	outside fracture zone-limestone	-8.54	-1.81
T1-20	20	transect plugs	outside fracture zone-limestone	-10.11	-2.27
T1-21	21	transect plugs	outside fracture zone-limestone	-9.44	-3.10
T1-22	22	transect plugs	outside fracture zone-limestone	-9.61	-2.22
T1-23	23	transect plugs	outside fracture zone-limestone	-8.90	-1.81
T1-24	24	transect plugs	outside fracture zone-limestone	-8.81	-1.99
T1-25	25	transect plugs	first fracture - fades into dolomite	-11.40	-2.87
T1-25.5	25.5	transect plugs	inside fracture zone	-9.54	-2.18
T1-26	26	transect plugs	inside fracture zone	-10.00	-2.17
T1-26.5D	26.5	transect plugs	inside fracture zone	-9.31	-2.48
T1-26.5L	26.5	transect plugs	inside fracture zone	-8.82	-1.87
T1-27	27	transect plugs	inside fracture zone	-9.02	-2.10
T1-27.5	27.5	transect plugs	inside fracture zone	-9.53	-2.29
T1-28	28	transect plugs	inside fracture zone	-7.88	-1.38

T1-29.5	29.5	transect plugs	inside fracture zone	-8.73	-2.02
T1-30	30	transect plugs	inside fracture zone	-8.62	-2.51
T1-30.5	30.5	transect plugs	inside fracture zone	-8.72	-1.73
T1-31	31	transect plugs	inside fracture zone	-8.34	-1.86
T1-31.5	31.5	transect plugs	inside fracture zone	-8.92	-1.95
T1-32	32	transect plugs	inside fracture zone	-8.30	-1.64
T1-33	33	transect plugs	inside fracture zone	-8.30	-2.01
T1-33.5	33.5	transect plugs	inside fracture zone	-8.90	-3.06
T1-34	34	transect plugs	inside fracture zone	-8.91	-2.52
T1-34.5	34.5	transect plugs	inside fracture zone	-8.30	-1.47
T1-35	35	transect plugs	inside fracture zone	-8.75	-2.60
T1-35.5	35.5	transect plugs	inside fracture zone	-10.06	-2.75
T1-36	36	transect plugs	inside fracture zone	-9.83	-2.19
T1-36.5	36.5	transect plugs	last fracture - fades out of dolomite	-9.43	-2.12
T1-38	38	transect plugs	outside fracture zone-limestone	-9.52	-2.13
T1-39	39	transect plugs	outside fracture zone-limestone	-9.03	-2.12
T1-41	41	transect plugs	outside fracture zone-limestone	-9.05	-1.92

Table 4-2 - Stable isotope results for core plugs

ID #	Footage	Sampled	Comments	$\delta^{18}O$	$\delta^{13}C$
H1D3	3	plugs from core 1	limestone	-9.44	-1.88
H1D5	5	plugs from core 1	dolomite	-10.38	-2.24
H1D7	7	plugs from core 1	dolomite	-8.78	-2.10
H1D9	9	plugs from core 1	dolomite	-8.35	-1.99
H1D11	11	plugs from core 1	dolomite	-8.58	-1.68
H1D13	13	plugs from core 1	dolomite	-7.66	-2.01
H1D15	15	plugs from core 1	dolomite	-8.97	-2.18
H1D17	17	plugs from core 1	dolomite	-8.16	-1.76
H1D19	19	plugs from core 1	dolomite	-8.29	-1.79
H1D21	21	plugs from core 1	dolomite	-7.72	-1.54
H1D27	27	plugs from core 1	LF dolostone	-5.75	-1.45
H1D29	29	plugs from core 1	LF dolostone	-8.81	-2.12
H1D31	31	plugs from core 1	LF dolostone	-9.98	-1.31
H1D33	33	plugs from core 1	LF dolostone	-8.48	-2.26
H1D35	35	plugs from core 1	LF dolostone	-5.51	-1.08
H2D1.5	1.5	plugs from core 2	limestone	-10.20	-2.28
H2D3m	3	plugs from core 2	LS matrix	-9.72	-1.94
H2D5.7d	5.7	plugs from core 2	dolomite	-10.74	-1.71
H2D7.2m	7.2	plugs from core 2	matrix dolomite	-9.63	-1.92
H2D9	9	plugs from core 2	limestone	-9.14	-1.73
H2D11	11	plugs from core 2	limestone	-9.54	-1.75
H2D13	13	plugs from core 2	limestone	-11.21	-2.43
H2D19	19	plugs from core 2	dolomite	-7.76	-1.31
H2D23	23	plugs from core 2	dolomite	-8.76	-1.88
H2D25	25	plugs from core 2	LF dolostone	-7.31	-1.74
H2D27	27	plugs from core 2	LF dolostone	-8.13	-1.96
H2D29c	29	plugs from core 2	calcite	-6.83	-1.53
H2D29m	29	plugs from core 2	LF dolostone	-7.27	-1.52
H2D31c	31	plugs from core 2	calcite	-6.95	-1.13
H2D33	33	plugs from core 2	LF dolostone	-7.51	-1.86
H2D35	35	plugs from core 2	LF dolostone	-6.93	-2.14
H2D37	37	plugs from core 2	LF dolostone	-4.90	-1.07

Table 4-3 - Stable isotope results for surface samples

ID #	Sampled	Comments	$\delta^{18}O$	$\delta^{13}C$
PB1	against fault	matrix dolomite	-8.47	-2.02
PB2	against fault	matrix dolomite	-8.47	-1.93
PB3	against fault	matrix dolomite	-8.55	-1.90
PB4	against fault	matrix dolomite	-8.33	-1.76
PB5	6" from dolomite	limestone matrix	-9.04	-2.11
PB6	3' from fault	limestone matrix	-9.70	-2.37
PB7c	fault related	calcite	-8.48	-1.33
PB7d	fault related	matrix dolomite	-9.07	-1.51
PB8c	fault related	calcite	-11.41	-3.10
PB8d	fault related	matrix dolomite	-9.41	-2.24
PB9	fault related	limestone matrix	-8.52	-2.05
PB10	fault related	matrix dolomite	-8.79	-1.97
PB11c	fault related	calcite	-11.30	-3.03
PB11L	fault related	limestone matrix	-9.75	-2.46
PB13	fault related	calcite	-9.33	-1.97
PB14	dolomite from fault	matrix dolomite	-8.90	-2.01

Strontium isotope analyses were run on the surface samples only. This set includes seven samples of dolomite, four of the Tribes Hill limestone, and four of vein- filling calcite from the fracture zone. The results of these tests are reported in Table 4-4 and shown in Figure 43. The dolomite values ranged from 0.7095 to 0.7103 with an average of 0.7098 and a standard deviation of 4.21 x 10^{-4}. The 0.7090 value appears to be an outlier from the rest of the data as it is drastically different than any of the other samples. The limestone values are a bit lower those of the dolomite. They range from 0.7091 to 0.7094 with an average of 0.7093 and a standard deviation of 1.25 x 10^{-4}. The $^{87}Sr/^{86}Sr$ of the calcite samples are still lower, with the exception of one outlier. They have a range of 0.7091 to 0.7116 with an average of 0.7099 and a standard deviation of 1.28 x 10^{-3}. The inferences made and conclusions derived from this data are given in the discussion, Chapter 5.

Table 4-4 - Strontium isotope results for surface samples

ID #	Sampled	Comments	^{87}Sr / ^{86}Sr
PB1	against fault	matrix dolomite	0.7095362
PB2	against fault	matrix dolomite	0.7097077
PB3	against fault	matrix dolomite	0.7101632
PB5	6" from dolomite	limestone matrix	0.70909
PB6	3' from fault	limestone matrix	0.7093616
PB7c	fault related	calcite	0.7115766
PB7d	fault related	matrix dolomite	0.7103485
PB8c	fault related	calcite	0.708903
PB9	fault related	limestone matrix	0.7093411
PB10	fault related	matrix dolomite	0.7098332
PB11c	fault related	calcite	0.7090517
PB11L	fault related	limestone matrix	0.709223
PB13	fault related	calcite	0.7091137
PB14	dolomite from fault	matrix dolomite	0.7096135

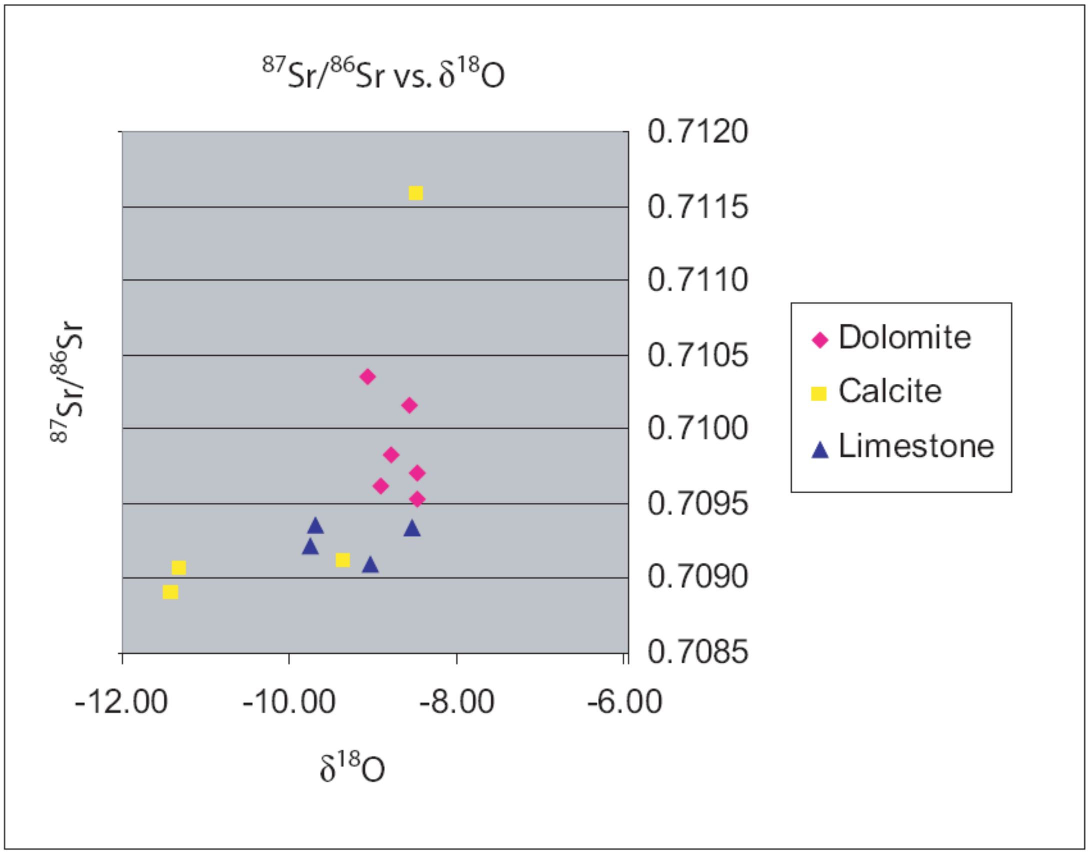

Figure 43 - Graph of strontium isotope values from surface samples collected in the quarry

4.7 Fluid Inclusions

As discussed in Chapter 3.7, fluid inclusion analyses were performed in two separate batches. One set, consisting of two samples, was sent to Fluid Inclusion Technologies Inc. (FIT), while a second set of ten was analyzed at the University at Albany.

The two samples sent to FIT were given the names PB200 and PB201. A summary of their results follows and FIT's full results are available in Appendix 2. Table 4-5 contains the data from their analyses. Sample PB200 was made up of a coarse matrix dolomite, an early matrix calcite, a very coarse saddle dolomite, and late calcite. Primary inclusions in the matrix dolomite give homogenization temperatures ranging from 120-130°C, and have indeterminate salinities. Secondary or pseudo-secondary inclusions in the early calcite give homogenization temperatures of 80-95°C with salinities of 26-28 wt.% NaCl equiv. Secondary or pseudo-secondary inclusions in the late calcite cement have homogenization temperatures of 65-75°C and salinities of 14.5-18.6 wt.% NaCl equiv. Sample PB201 consisted of mainly coarse zoned dolomite with some late calcite spar. Primary aqueous inclusions in the dolomite have homogenization temperatures of 105-132°C and secondary or pseudo-secondary inclusions have homogenization temperatures of 90-129°C. Salinities ranged from 26-30 wt.% NaCl (near halite saturation).

Table 4-5- Fluid inclusion results from samples sent to FIT

FIT Samples	Population	Type	Th °C	Tm °C	Sal (wt%)
PB 200	late calcite A	s / ps	65 - 75	-13.0 to -14.0	16.9 - 17.8
PB 200	late calcite B	s / ps	65 - 75	-13.5 to -14.5	17.3 - 18.2
PB 200	late calcite C	s / ps	65 - 75	-14.0 to -15.0	17.8 - 18.6
PB 200	late calcite D	s / ps	120 - 130	10.5 to -11.0	14.5 - 15.0
PB 200	matrix calcite E	s / ps	80 - 95	-30 to -35	26 - 28
PB 200	matrix dol F	pr / s	120 - 130	-	-
PB 200	matrix dol G	pr / s	120 - 130	-	-
PB 201	dol core A	pr / ps	95 - 105	-30 to -40	26 - 30
PB 201	dol mid A	pr / s	100 - 110	-30 to -40	26 - 30
PB 201	dol mid A	pr / s	90 - 100	-30 to -40	26 - 30
PB 201	dol rim A	pr / s	90 - 95	-30 to -40	26 - 30
PB 201	dol rim B	pr / s	95 - 105	-30 to -40	26 - 30
PB 201	dol rim C	pr	110 - 120	-30 to -40	26 - 30
PB 201	dol mid D	pr / s	110 - 120	-30 to -40	26 - 30
PB 201	dol mid D	pr / s	120 - 125	-30 to -40	26 - 30
PB 201	dol rim E	pr	132	-30 to -40	26 - 30
PB 201	dol core F	pr / s	129	-30 to -40	26 - 30
PB 201	dol outer core G	pr	105 - 115	-40.0	30.0
PB 201	dol rim H	pr	120 - 130	-30 to -35	26 - 28
PB 201	dol rim I	pr	125 - 130	-30 to -35	26 - 28

The second set of inclusions, analyzed at the University at Albany, support and supplement the data from FIT. All the inclusions analyzed were determined to be primary or pseudo-secondary based on the criteria set forth by Goldstein and Reynolds (1994). Inclusions which are confined to growth zones were labeled primary, while inclusions with seemingly random distribution, no association with secondary features, and no clear association with growth zonation were labeled pseudo-secondary. Unfortunately, all 41 of the inclusions found were extremely small, less than 3µm in diameter, and were not frozen since the ice would be too difficult to observe. Therefore, no melt temperatures or subsequent salinities were obtained from these analyses. Vapor bubbles were clearly visible in every inclusion and homogenization temperatures were measured to the nearest 1.0°C. These homogenization temperatures are reported in Table 4-6 and plotted graphically in Figure 44. The inclusions found in saddle dolomite crystals yielded the highest homogenization temperatures, ranging from 132 - 154°C with an average of 139°C. Matrix dolomite inclusions were slightly cooler with a range of 107 - 135°C and an average of 121°C. The calcite inclusions were also cooler than the saddle crystals. They ranged from 104 - 132°C with an average of 117°C. Interpretations of thse data are discussed in Chapter 5.2.

Table 4-6 - Fluid inclusion results from samples analyzed at SUNY Albany

Sample ID	Source	Type	Th °C
SB1-1 (surface body 1)	matrix dolomite	pr / ps	120
SB1-2 (surface body 1)	matrix dolomite	pr / ps	135
SB1-3 (surface body 1)	matrix dolomite	primary	119
SB2-1 (surface body 2)	matrix dolomite	pr / ps	111
SB2-2 (surface body 2)	matrix dolomite	primary	124
SB2-3 (surface body 2)	matrix dolomite	pr / ps	112
SB2-4 (surface body 2)	matrix dolomite	pr / ps	109
FF1-1 (fracture fill 1)	calcite	pr / ps	129
FF1-2 (fracture fill 1)	calcite	pr / ps	119
FF1-3 (fracture fill 1)	calcite	pr / ps	132
FF2-1 (fracture fill 2)	calcite	pr / ps	106
FF2-2 (fracture fill 2)	calcite	pr / ps	122
FF2-3 (fracture fill 2)	calcite	pr / ps	108
FF2-4 (fracture fill 2)	calcite	pr / ps	104
FF2-5 (fracture fill 2)	calcite	pr / ps	113
FF3-1 (fracture fill 3)	calcite	pr / ps	119
P1-1 (plug 1)	matrix dolomite	pr / ps	120
P1-2 (plug 1)	matrix dolomite	pr / ps	113
P1-3 (plug 1)	matrix dolomite	pr / ps	126
P1-4 (plug 1)	matrix dolomite	pr / ps	119
P2-1 (plug 2)	matrix dolomite	pr / ps	123
P2-2 (plug 2)	matrix dolomite	pr / ps	118
P2-3 (plug 2)	matrix dolomite	pr / ps	113
P2-4 (plug 2)	matrix dolomite	pr / ps	107
P3-1 (plug 3)	matrix dolomite	pr / ps	128
P3-2 (plug 3)	matrix dolomite	pr / ps	139
P3-3 (plug 3)	matrix dolomite	pr / ps	132
P3-4 (plug 3)	matrix dolomite	pr / ps	127
P3-5 (plug 3)	matrix dolomite	pr / ps	133
VF1-1 (vug fill 1)	saddle dolomite	primary	141
VF1-2 (vug fill 1)	saddle dolomite	primary	137
VF1-3 (vug fill 1)	saddle dolomite	primary	137
VF1-4 (vug fill 1)	saddle dolomite	primary	140
VF2-1 (vug fill 1)	saddle dolomite	pr / ps	136
VF2-2 (vug fill 2)	saddle dolomite	pr / ps	132
VF2-3 (vug fill 2)	saddle dolomite	pr / ps	132
VF2-4 (vug fill 2)	saddle dolomite	pr / ps	134
VF2-5 (vug fill 2)	saddle dolomite	pr / ps	142
VF2-6 (vug fill 2)	saddle dolomite	pr / ps	148
VF2-7 (vug fill 2)	saddle dolomite	pr / ps	154

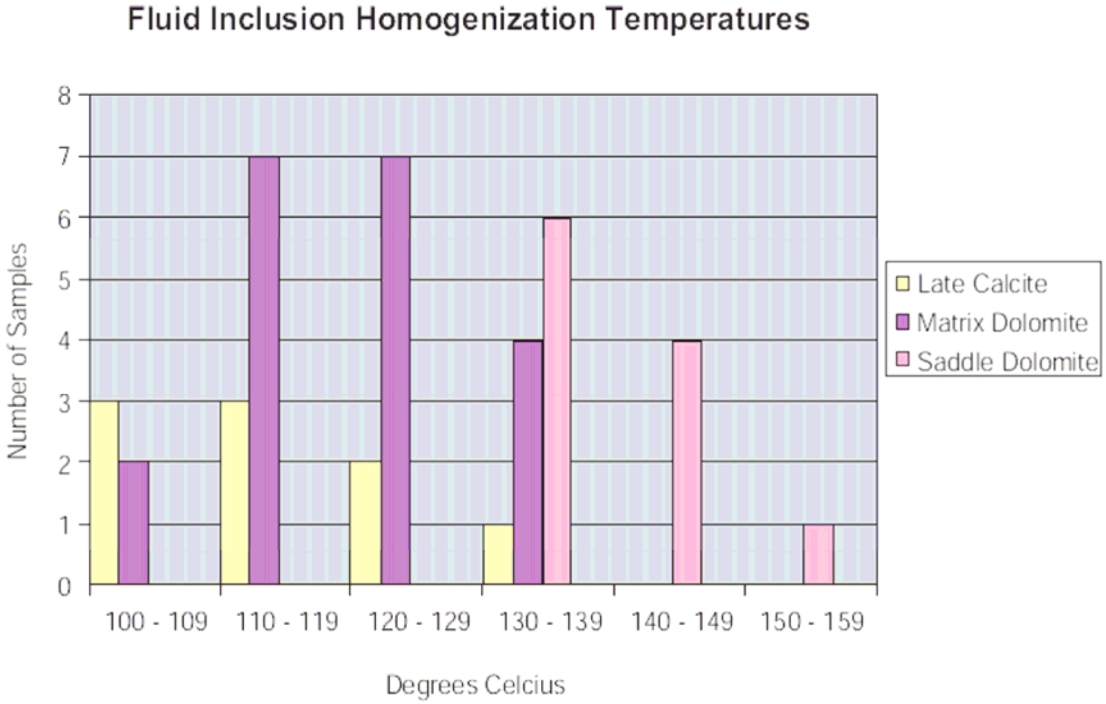

Figure 44 - Graph of homogenization temperatures from fluid inclusions analyzed at SUNY Albany

Section 5
DISCUSSION

5.1 Hydrothermal Alteration in Palatine Bridge

Although there is no single characteristic of the Palatine Bridge outcrop that can unequivocally prove its origin to be hydrothermal, the compilation of data from geochemical, structural, and pertrographical analyses make a strong argument for dolomitization by means of relatively hot fluids that have traveled upward from depth through faults and fractures.

The most obvious indications of fault control on dolomitization in the quarry are field relations and geometry of the rock types in the outcrop. Other near surface processes of dolomitization should all produce a widespread, laterally extensive dolomite. The quarry dolomite only occurs around mineralized faults and fractures and is absent away from the faults. Fluid flow along fault planes is also evident in the cores. Figure 45 is an image of core taken from Hole 2 at a depth of 31 feet. Calcite mineralization along the fracture gives good evidence for the passage of fluids and precipitation of minerals along fracture openings in the Little Falls and upward into the Tribes Hill. The dolomitized breccias present at the tips and within the dolomite bodies suggests fault control on brecciation as well as dolomitization. This texture has been interpreted as a fault breccia and is related to the lengthwise propagation of the bodies as they developed.

Despite its clear association with faulting, there are other processes of dolomitization that cannot be completely discounted by the geometry of the outcrop alone. For example, localized dolomite formations have also been interpreted to form in karst environments (Loucks and McMechan, 1998). These structures may also contain breccias, however they are related to cave collapse rather than faulting. Although the quarry breccias do appear to be karst related, field relations alone are not enough to wholly eliminate this process as a possible origin of the breccias in the outcrop. Geochemical and fluid inclusion analyses help do this.

Figure 45 - Calcite mineralization in a fracture from Hole 2 core at 31 ft.

Homogenization temperatures (T_H) measured in primary aqueous inclusions give the minimum temperature of the parent fluid from which a given crystal was precipitated. Therefore, by comparing the homogenization temperatures of a hydrothermal formation to the maximum burial temperature of the unaltered host rock, one may demonstrate that the fluids were hotter than the host rock had ever been. Such is the case for many hydrothermal dolomite gas fields (Allan and Wiggins, 1993; Smith, 2006). Although finding homogenization temperatures greater than the maximum burial temperature for a unit is an excellent way to prove hydrothermal alteration, it should be noted that homogenization temperatures lower than the maximum burial temperature do not conclusively prove that a structure is not hydrothermal in origin. A unit may be altered at a shallow depth, when the fluids traveling upward along fault planes are hotter than the surrounding rock. Then subsequent burial may expose the unit to temperatures greater than that of the earlier hydrothermal fluid. In such a case, homogenization temperatures from the unit would not be hotter than the unit's maximum burial temperature, yet it would have undergone hydrothermal alteration.

Comparison of the quarry homogenization temperatures and NY burial temperature data do not conclusively prove that the dolomite formed by hydrothermal fluid flow. Conodont alteration studies performed in upstate New York yield CAI values of 3.5 in Ordovician aged rocks of the Mohawk Valley (Weary et al., 2001). Using the equations established by Hulver (1997) this translates to a burial temperature between 142°C and 206°C. Therefore, the homogenization temperatures from the quarry inclusions (107 - 154°C) may fall above or below the actual maximum burial temperature for the Tribes Hill.

By plotting the $^{87}Sr/^{86}Sr$ values for the quarry samples in reference to that of seawater (Fig. 46) it is clear that the unaltered Tribes Hill limestone samples lie directly on the seawater curve for the early Ordovician, the time of their deposition. The dolomite samples, however, plot well above the seawater curve, indicating that they did not precipitate from the same marine fluids. In fact, the dolomites plot above all values for the seawater curve interpretation. This enrichment of the dolomite in radiogenic strontium can be attributed to interaction between the parent fluid and basement rock or immature sandstone (Allan and Wiggins, 1993). Therefore, these fluids must have circulated through the basement or overlying silici-clastics prior to precipitating dolomite.

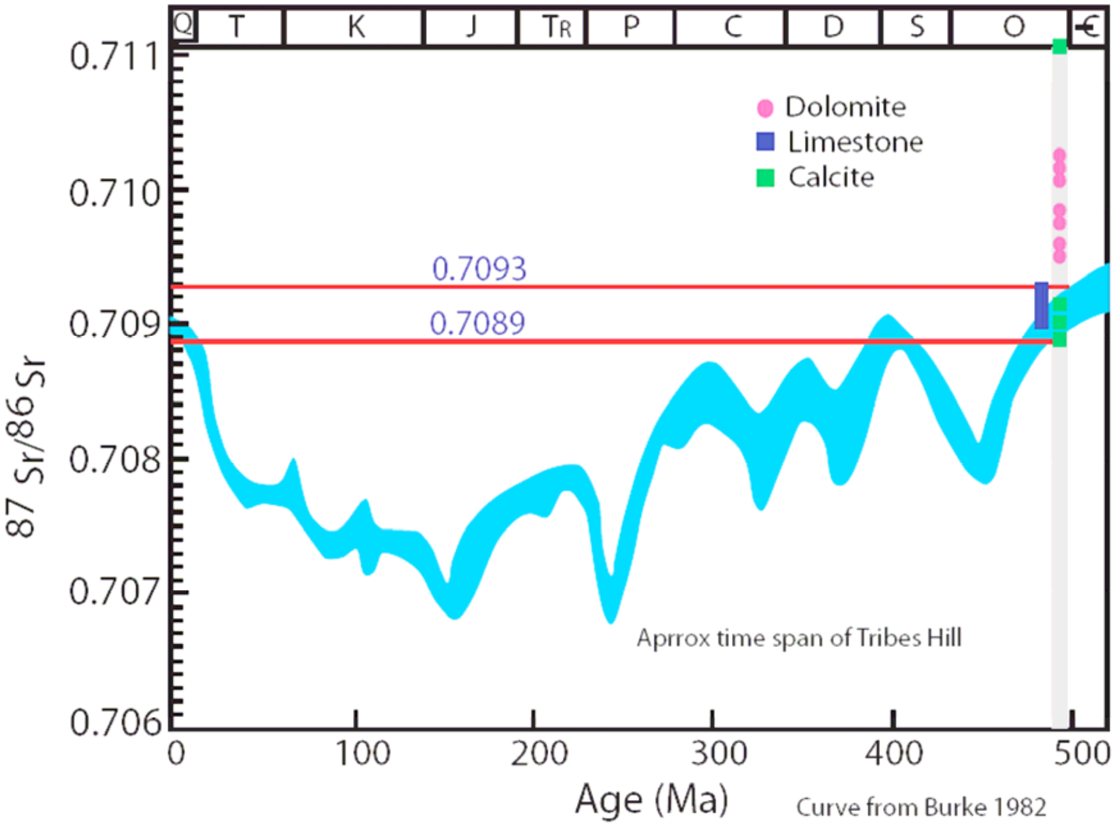

Figure 46 - Strontium isotope ratios from quarry samples plotted in comparison with that of prehistoric seawater

As noted in Chapter 4.6, the oxygen isotope values for the quarry dolomites are about two per mil lighter than one would expect if they had precipitated from the same fluid as the Tribes Hill limestone. However, the temperature of the parent fluid must be considered when working out its original composition. Figure 47 shows a temperature vs. δ^{18}O cross plot from Friedman and O'Neil (1977). Data from the quarry samples plot in the range of +2 to +4‰ meaning that the fluid from which they precipitated was in that range. Unevolved Late Ordovician seawater has been calculated to have been approximately -6 to -10‰ (Smith, 2006).

Where salinities could be measured, the fluid inclusions had 26-30 wt% NaCl quiv. These values are much higher than seawater salinity, in fact they border on halite saturation (31-32 wt% NaCl equiv.). When combined with the strontium and stable isotope data it becomes clear that dolomitization of the quarry outcrop took place under the influence of fluids which were geochemically disparate from normal ocean water.

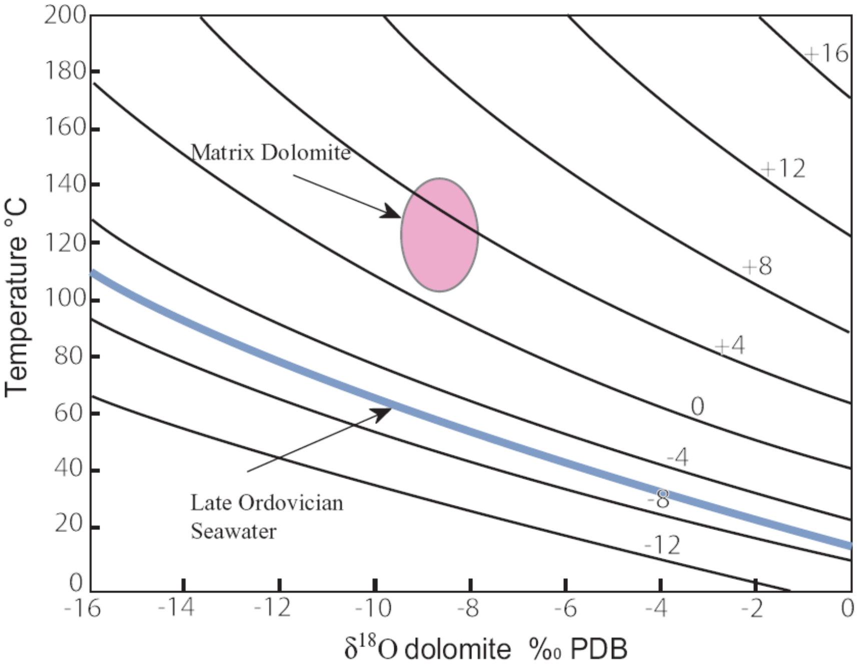

Figure 47 – Homogenization temperature vs. δ^{18}O cross plot (graph from Friedman and O'Neil, 1977)

5.2 Timing of Faulting and Fluid Flow

Because the formation of hydrothermal dolomite is reliant on the release of pressurized fluids trapped at depth, faulting and fracturing are necessary components of the process (Davies and Smith, 2006). It is important to note that formation of the dolomite bodies is unlikely to have occurred in a single event, but rather throughout a sequence of fluid flow episodes. It is equally important to note that mineralization is most likely to occur while faults are active, not after.

Geochemical analyses of dolomite crystals from around the world have shown that the crystals are typically zoned, like those found in the Palatine Bridge Quarry (Fig. 48) (Braithwaite and Rizzi, 1997; Auajjar and Boulegue, 2002). The chemical composition of the fluid may have changed during crystallization while fluid flow itself remained continuous. More likely, the crystal grew episodically with a series of short fluid flow events each with a slightly different chemical composition. Episodic fluid flow may be caused by the cyclic increase in pressure before a fracturing event and decrease in pressure immediately following the event. The growth of crystals along open fractures may block fluid flow by occluding the pore/fracture network. In this case fluid flow will only be cease until pressures increase enough to reactivate the fault or create a new one. Sibson (1994) discusses the cyclic time-scale of accumulation and release of stress in a hydrothermal system. He states that the build-up of shear stress during the inter-seismic period can last tens to many thousands of years. However, during a rupture, the drop in shear stress and subsequent fluid flow may last only a few seconds. This is followed by a period of "post-seismic adjustment" which may last for days to years.

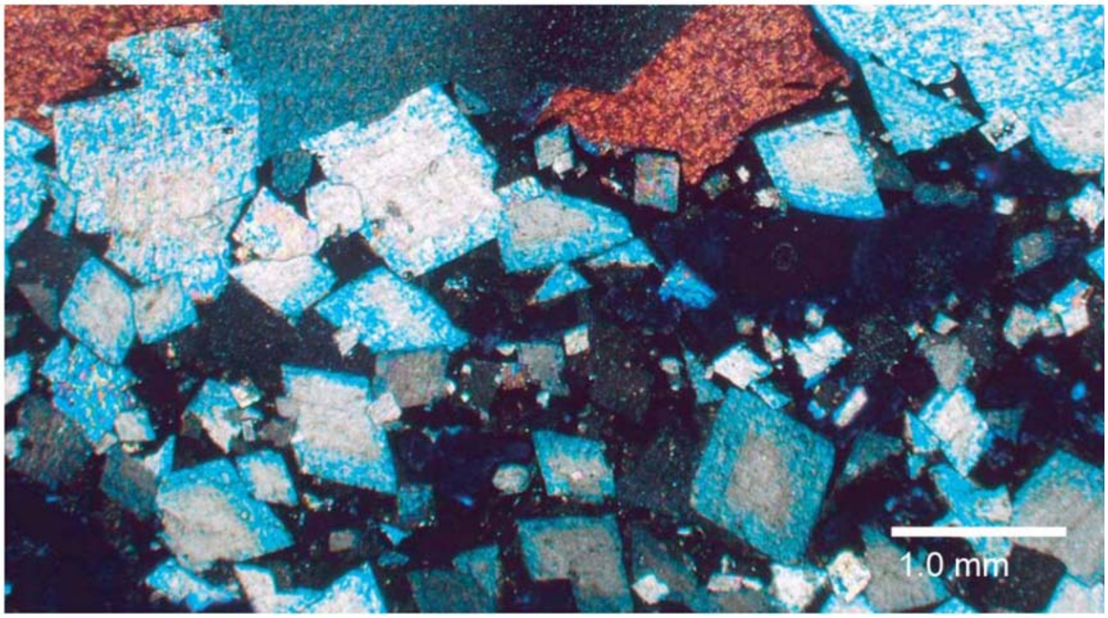

Figure 48 - Zoned saddle dolomite crystals

Taking this concept into consideration, the timing of formation of the Palatine Bridge Quarry outcrop is likely complicated and not restricted to a single event. As discussed in Chapter 2.3, most of the faulting in the Cambrian and Ordovician units of the Mohawk Valley occurred during the Late Ordovician Taconic Orogeny (Bradley and Kidd, 1991). This collision may not have caused the initial faulting in the basement beneath the quarry, but it could have reactivated older faults and made a large contribution to the overall deformation. During this period of time the Tribes Hill formation was shallowly buried beneath the Black River, Trenton, and newly deposited Utica Shale to an estimated depth of only 500-1500 feet. Such a shallow depth could not account for the high T_H reported in the fluid inclusion analyses. Without an alternative source of heat, the fluids must have originated from a depth at which the geothermal gradient (as high as 67ºC/mile during the late Paleozoic) can account for these higher temperatures. The T_H's in our samples (104-154°C) correspond to a burial depth of at least 3-5 km (>10,000 ft). This places the fluids well below the Little Falls formation and into the Precambrian basement. Reactivation of pre-existing basement faults during the onset of the Taconic Orogeny would have allowed these fluids to travel upward into the Tribes Hill. This theory is also supported by the elevated strontium content from the geochemical analyses which suggest that these fluids were in prolonged contact with basement rocks.

The core descriptions also support the interpretation that the Tribes Hill formation experienced faulting relatively early in its burial history. The soft sediment deformation observed in the cores verify that the unit was not fully lithified during the onset of tectonic activity. However, the extensive brecciation throughout the dolomite bodies is an indication that, at some point during its alteration, the rock was at least partially lithified. This contrast in evidence implies that dolomitization was episodic, occurring while the unit was soft, then again when hard. A separate collision is not necessary to explain this occurrence as the Taconic Orogeny took place over 40 million years which is more than enough time for the Tribes Hill to lithify. Paragenetic sequencing in thin sections show reactivation of bitumen filled fractures with an influx of late-stage calcite and quartz. It is possible that this event occurred during a later orogeny as there is no direct association between these minerals and the breccia. The system may have become reactivated during the Devonian Acadian Orogeny or the Carboniferous to Permian Alleghanian Orogeny, but there is little if any evidence for this.

5.3 Orientation and Structure of Faulting

Displacement in the study area is predominantly extensional, as seen in the normal faults of the fracture zone and central sag of the dolomite bodies. However, the origin of the stresses necessary to account for this deformation is likely much more complicated. The main problem with a purely extensional model is that 100% extension can not account for features such as the anticlines that flank the entire length of the dolomite bodies. Transtensional faulting is necessary to account for the characteristics observed.

Faults in the Mohawk Valley generally have two orientations: North-Northeast and Northwest (Bradley and Kidd, 1991; Jacobi and Mitchell, 2002). With a strike of 305° (W-NW) the dolomite bodies of the quarry display a trend most closely related to the NW faults described by Jacobi and Mitchell (2002). Although these faults were active during the Taconic Orogeny, some believe they have an older history. Rifting associated with the opening of the Iapetus Ocean during the Eocambrian parallels the NE-striking fault system and is thought by some to be related to the faulting. Consequently, transfer zones between the Iapetan rift segments may correspond to the NW-striking fault system and possibly the Palatine Bridge Quarry outcrop. The effects of the Iapetan rifting are not well documented and may not have extended as far west as the Palatine Bridge site. However, there are multiple sites in close proximity to the quarry in which horizontal slickensides have been found. In the neighboring town of Little Falls, horizontal slicks have been found in the Precambrian basement with a trend similar to that of the quarry bodies.

Sandbox modeling of strike-slip pull-apart basins has revealed that lateral motion is not always recorded in slip along basin faults. In many cases, some of the faults surrounding a transtensional system may only show vertical offset, while lateral displacement occurs at greater depth (Dooley and McClay, 1997). Strike-slip motion along a releasing bend can create a relatively open space into which overlying units sink. As this deformation propagates upward, a negative flower structure consisting of normal fault displacement will form (Fig. 49). This system may also involve a component of reverse faulting along the edges of the basin as indicated in Figure 49. The flanking anticlines observed in the quarry may be a surface expression of this phenomenon. The cross-body scissor fault discussed in Chapter 4.3 also gives good evidence for a transtensional origin of the quarry fault and fracture system. Sandbox modeling of pull-aparts depict cross-basin scissor faults that change dip direction as they cross the "basin" (Fig. 49) (Dooley and McClay, 1997). The same research also describes the formation of relay ramp structures like the one seen in the quarry. Therefore, although the most common indications of strike-slip motion (horizontal slickensides or laterally offset markers) are absent from the outcrop, the characteristics which are present fit into a transtensional regime very well.

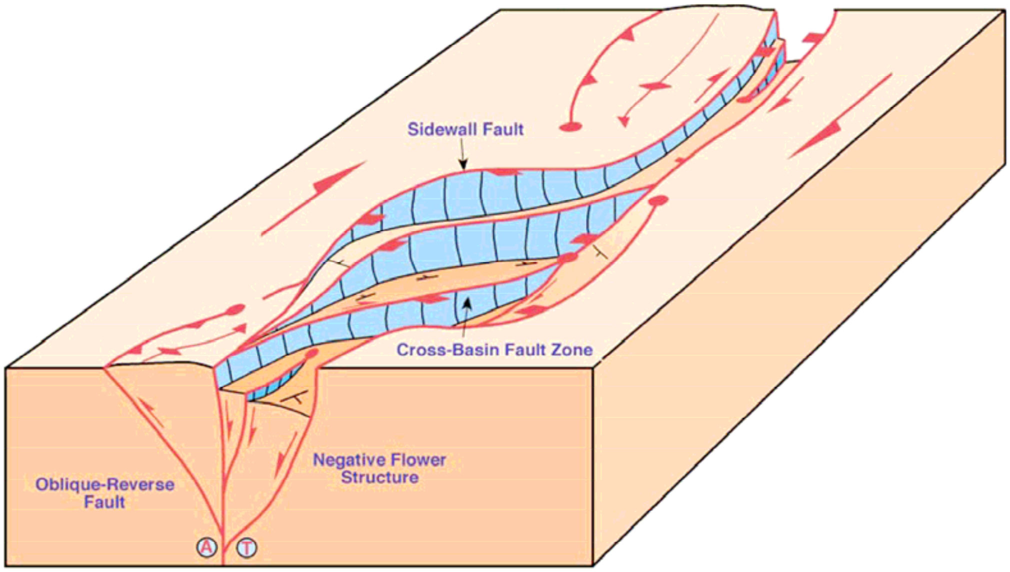

Figure 49 – Strike-slip pull-apart basin structure (Dooley and McClay, 1997)

Many of the structures in the quarry appear to reflect the conclusions of Sibson (1994, 2000) in his research of geodynamics and fluid involvement in faulting. He states that the interconnection of faults and fractures is directly related to the mechanical properties of alternating layers in a unit. Layers with a relatively high tensile strength such as sandstones or limestones typically undergo hydraulic extension fracturing perpendicular to $\sigma 3$, whereas layers with a lower tensile strength such as shales experience brittle shear failure. "Thus, in a typical sequence of alternating sandstones/limestones and shales, differences in tensile strength relative to the differential stress may result in the formation of a natural fault/fracture mesh" (Fig. 50b) (Sibson, 1994). The relict mesh structure is often preserved through cementation by mineralization of silica, carbonate, and bitumen (all present at the quarry). Many of the faults and fractures in the quarry display a similar pattern of shear failure across shaley beds while limestone layers contain extension fractures (Fig. 50a). Sibson states that the passage of large fluid volumes through these fault/fracture meshes leads to brecciation. As noted in Chapters 4.3 and 4.4, breccias are common in many sections of the outcrop. Figure 51 shows an idealized sketch of an extensional chimney, one type of fault/fracture mesh described by Sibson. Note that the cumulative offset along the shear zones creates a sag feature much like that seen in the quarry.

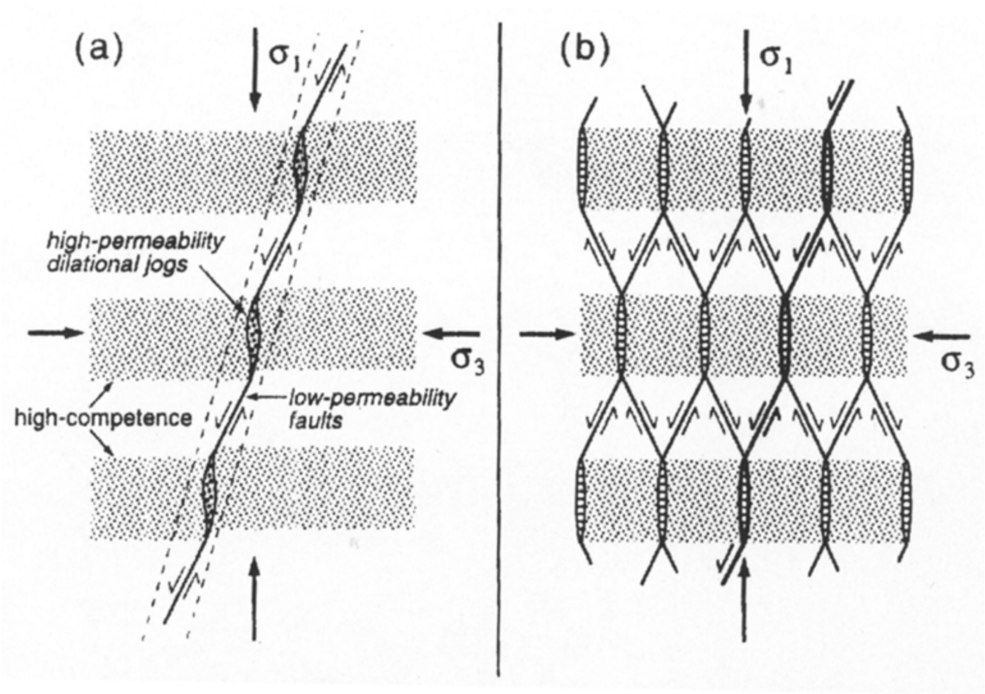

Figure 50 - a) Illustration showing the effect of alternating layers of competence on the formation of faults and fractures. b) Illustration of an idealistic fault/fracture mesh (Sibson, 1994)

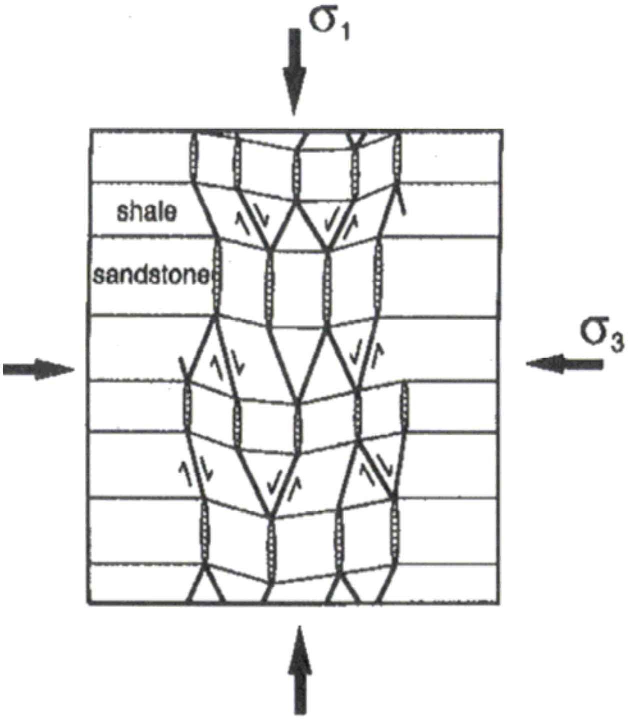

Figure 51 - Extensional chimney created by interconnected fault/fracture mesh
(from Sibson 1994)

Harding (1974) discusses the significance of strike-slip faulting and its relationship to the en-echelon patterns of oil fields such as Albion-Scipio, MI and Newport-Inglewood, CA. He notes that the dolomitization of Albion-Scipio must have been fault related due to its unusually straight, ribbonlike distribution of porous zones that crosscut depositional facies and create sags in the overlaying units. He goes on to state that synthetic shear faults associated with strike-slip motion best explain the en-echelon pattern of these bodies. However, pure strike-slip would not create openings sufficient for fluid flow transport. Instead, Harding states, "an oblique divergent component would have emphasized the extensional effects of the mild deformation and would have tended to pen the synthetic fractures, facilitating dolomitization."

Several structures in the quarry also match structural geometries described by Childs et al. (1995; 1996) in fault overlap zones within developing segmented fault systems. Fault overlap zones, as described by these workers, are mostly temporary features. Unless growth of a fault ceases, overlap zones will eventually be breached forming transfer zones where bends in the fault occur (Fig. 52). It is also important to note that overlap zones are spatially variable in that at one place a pair of fault segments may exist as separate overlapping faults, but join along strike or at a stratigraphically higher or lower depth (Fig. 53c). In the quarry of this study, the jog in middle of Body 2 may be a breach between what were once two separate fractures. The tail-like feature described in Chapter 4.3 might be a remnant tip of the eastern portion of Body 2 before it joined with the western portion, and be a breached overlap as described by Childs and others. It is possible that Bodies 1 and 2 are connected at greater depth. Although the dolomitic parts of the bodies do not overlap at the surface, the calcite veins running from their tips do. We also know, from the analysis of Core 4, that the limestone bridge between these bodies is only four feet thick, beneath which dolomite occurs. This implies that Bodies 1 and 2 do meet at depth. This core alone is not sufficient evidence for a complete structural interpretation, but future seismic work may help explain the way these bodies interact in the subsurface.

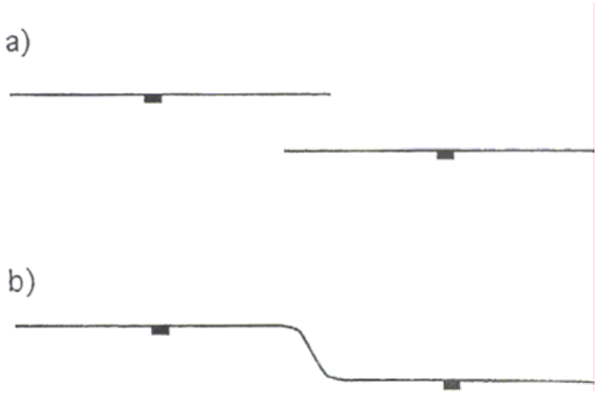

Figure 52 - a) fault overlap zone b) overlap breached creating a sharp bend in a fault
(Childs et al., 1995)

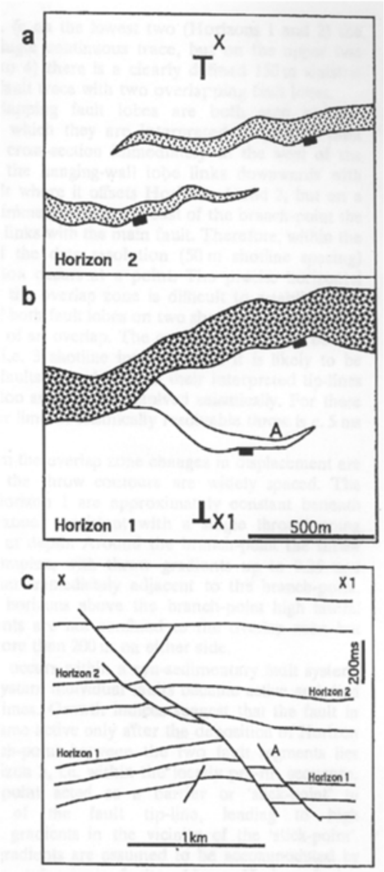

Figure 53 - a) illustration of fault overlap zone (horizon 2) b) illustration of breached overlap with remnant tail (horizon 1) c) profile view of fault interaction (Childs et al., 1995)

5.4 Comparison to Producing Fields

As potential oil and gas reservoirs, occurrences of hydrothermal dolomite have attracted increasing attention with each successful field discovered. Among the most productive of these fields are the Ladyfern Field of British Columbia, the Albion-Scipio fields in south-central Michigan, the Rochester field in southern Ontario, and the Trenton-Black River fields of south-central New York. Each of these fields shares a number of geometrical and geological characteristics with the Palatine Bridge Quarry outcrop.

The Ladyfern Reservoir, discovered in 2000, was Canada's largest onshore gas discovery in 20 years (Boreen and Davies, 2002). By the end of March 2002, the field consisted of 40 wells producing a total of 777 million ft^3 of gas per day. Like the quarry outcrop, the Ladyfern reservoir is a fault controlled hydrothermal dolomite alteration. According to Boreen and Davies, "episodic burial reactivation of faults has resulted in extensive fracturing and created active conduits for hydrothermal fluids which have variably leached, dolomitized and cemented the rock. In areas of maximum extension near fault intersections, intense dissolution, brecciation and hydrothermal dolomitization has resulted in seismically-resolvable collapse synclines." In many ways, this description mirrors that of the Palatine Bridge dolomite structure. The same type of collapse synclines have been described and can be seen in the GPR data presented in Chapter 4.1. The leached rock texture and brecciation are also characteristics common to these two fault-localized dolomite occurrences.

The Rochester Field is located in southern Ontario, Canada, near Lake Erie just east of Detroit. It is one of the area's six major oil and gas pools, all of which produce from hydrothermally altered portions of the Trenton-Black River. As of 2005, the Rochester Field had a cumulative oil production of 1.5 million bbl and a cumulative gas production of 1.45 bcf (Carter et al., 2005). The reservoir is associated with basement-related en-echelon synthetic shear faults which compartmentalize the dolomite bodies (Ogiesoba, 2005). Figure 54 shows a horizontal slice of a 3-D seismic survey shot over the Rochester field. Note the geometric similarities between it and the quarry outcrop. Both are linear features that step in an en-echelon pattern. Figure 55 shows 2 cartoon cross sections of the field. They depict the same type of localized body and central sag as the trench walls and GPR data from the quarry.

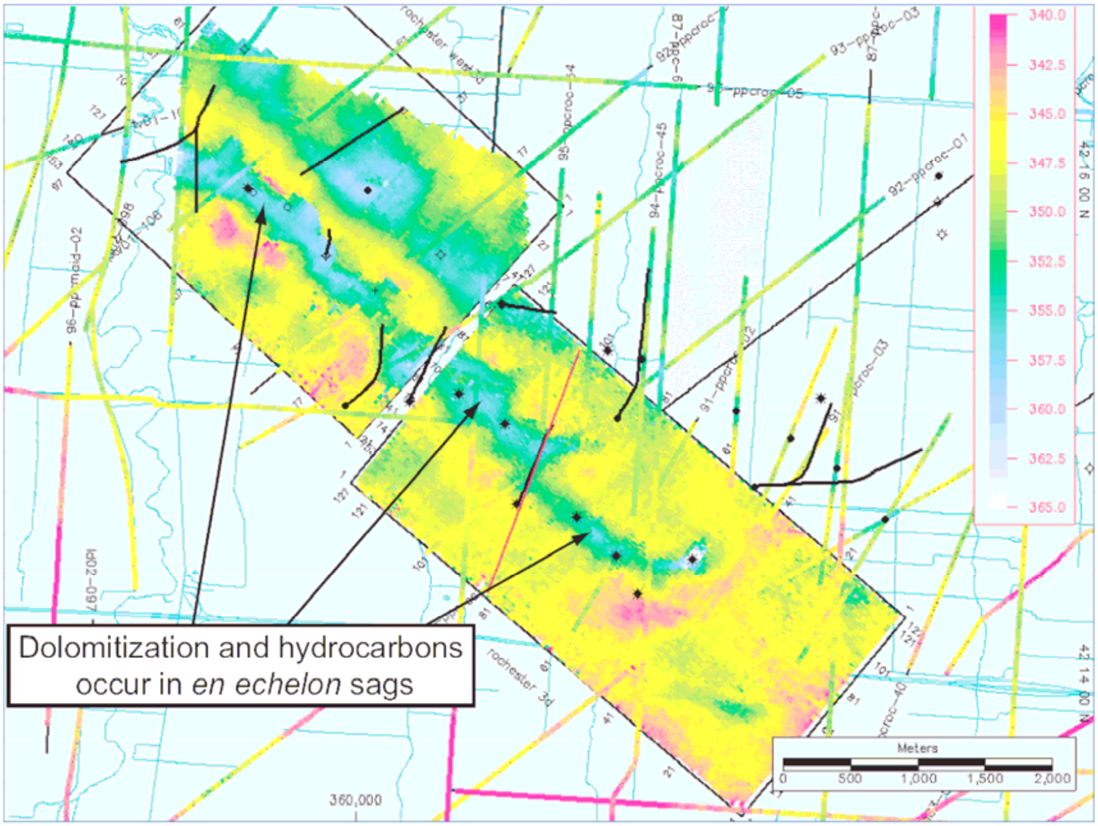

Figure 54 - Horizontal slice taken from 3-D seismic survey of the Rochester field, Ontario

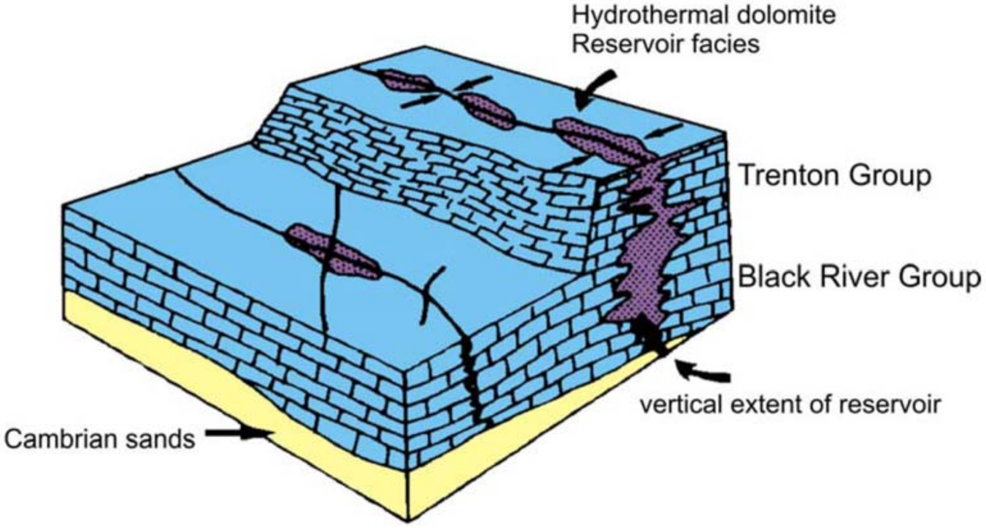

a)

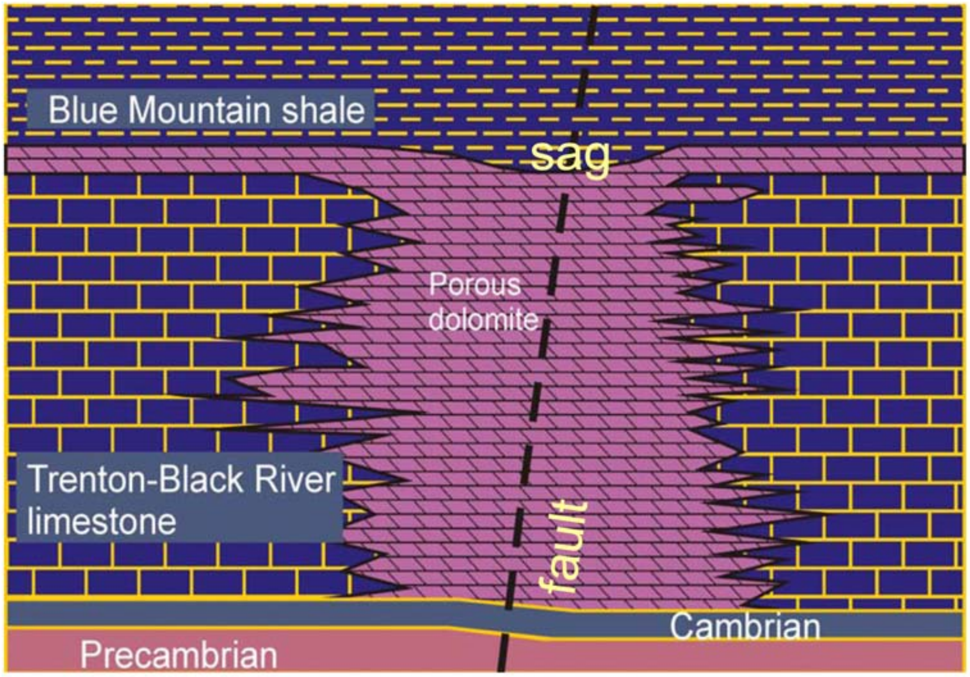

b)

Figure 55 - cartoon cross-sections of dolomitization in the Rochester field (Carter et al., 2005)

The Albion-Scipio Fields of south-central Michigan cover approximately 14,500 acres and also target hydrothermally dolomitized regions of the Trenton-Black River Formations. At the time of their discovery in 1957 these fields were estimated to contain over 290 million barrels of oil with a range of 10,000 to 25,000 barrels per surface acre (Hurley and Budros, 1990). They are considered “unusual” because, like Ladyfern, the hydrocarbon-bearing structures are synclinal sag-like features rather than the typical anticline trap. This sag is characteristic of most hydrothermal dolomite reservoirs and the Palatine Bridge outcrop. Perhaps the most interesting element of the Albion-Scipio Fields is that not only do they resemble the quarry bodies in cross-section, but in plan view as well. The Albion-Scipio Fields occur as long, linear en-echelon segments (Fig. 56). Note the Pulaski Break between these fields bears a striking resemblance to the bridge between Bodies 1 and 2 at the quarry. And although their orientation differs, the bend in the Scipio field looks much like the jog in Body 2 at the quarry. In fact, when reflected, or flipped, vertically and placed next to the Rochester and Albion-Scipio outlines, all three structures display the same general geometry (Fig. 57). Other similarities between the Michigan fields and New York study area include vuggy porosity, brecciation, and occurrences of saddle dolomite, calcite, and pyrite.

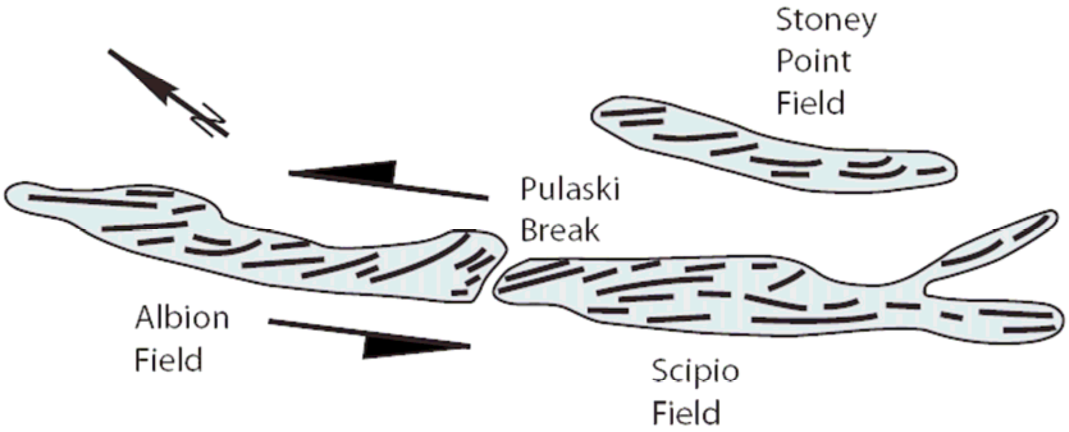

Figure 56 - Illustration of Albion - Scipio fields with interpreted faults (digitized from Hurley and Budros, 1990)

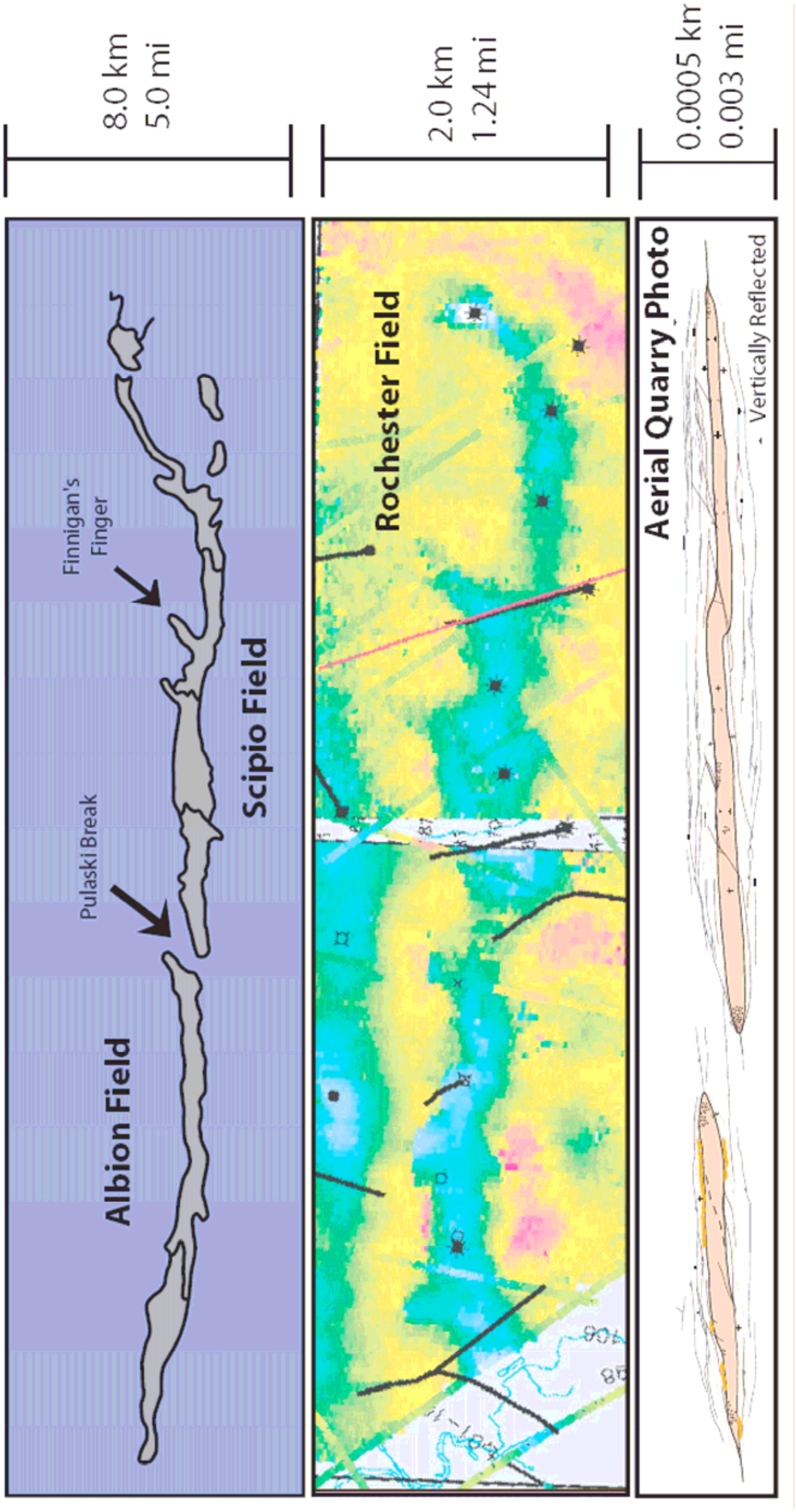

Figure 57 - Comparison of Albion - Scipio field and Rochester field to vertically reflected quarry fracture map

Like the Albion-Scipio Fields of Michigan and the Rochester Field of Ontario, a large portion of the hydrocarbon production in New York targets the Trenton - Black River dolomite occurrences. Fields such as Quackenbush Hill and Wilson Hollow produce natural gas from hydrothermally dolomitized sections of these formations. These fields contain wells that have produced over 40 million ft^3 of gas a day. In map view, these fields appear as elongate fault-bounded structural lows (Fig. 58) (Smith, 2006). Geochemical analysis of dolomitic cores taken from these fields yield δ^{18}O values between -9 and -12.5‰ (Smith, 2006). The cores also show elevated strontium content and vuggy porosity with saddle dolomite like the quarry cores and outcrop. Fluid inclusions in the dolomite from the New York fields have homogenization temperatures ranging from 100 to 160 ºC and very high salinities (13 – 17 wt% NaCl equiv.). Quarry values for all these analyses lie within the same ranges.

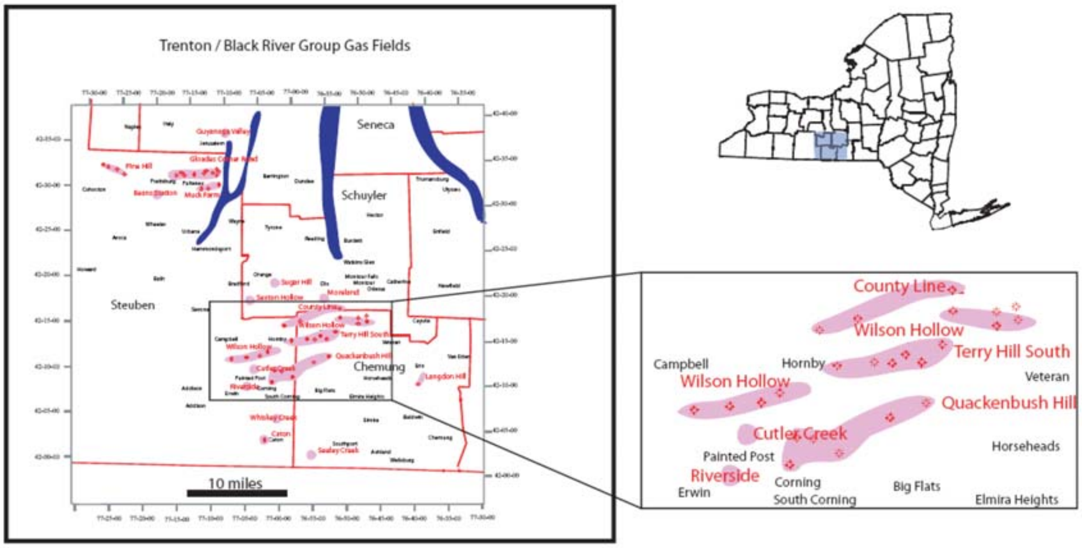

Fig. 58 – Trenton-Black River hydrothermal dolomite fields of south - central New York as of 2003

Section 6

CONCLUSIONS

Homogenization temperatures of fluid inclusions in the dolomite are not definitively higher than the maximum ambient burial temperature of the Tribes Hill in NY. Therefore, the outcrop cannot be demonstrated by this evidence to be unequivocally hydrothermal in origin. However, all other characteristics of the quarry point to fault-related fluid flow and precipitation of crystals at temperatures that must have been higher than the shallowly buried Tribes Hill during the Taconic Orogeny. Both GPR and core analysis show that the outcrop is directly associated with faults and fractures while the size and geometry of the bodies eliminate many other possible methods of dolomitization. Enrichment in radiogenic strontium content indicates that the parent fluid interacted with the Precambrian basement before precipitation of dolomite. This could only mean that the fluids came from a greater depth and would consequently have been hotter than the rock they intruded. By a simple process of elimination, hydrothermal alteration of the Tribes Hill is the only way these dolomite bodies could have formed.

The timing of this alteration is complicated by the issue of reactivated faults and episodic fluid flow. Fault activity during the Taconic Orogeny (Mid-Late Ordovician) when the Tribes Hill was only shallowly buried would explain the soft sediment deformation seen in the cores. An upper limit on the timing of faulting is constrained by the termination of this regional set of faults in the Trenton and Utica formations. However, the coexistence of soft sediment deformation and brecciation implies that the faulting was episodic and occurred while the sediment was soft then again later after it had lithified.

As an analog for hydrothermal dolomite reservoirs, the Palatine Bridge outcrop appears to mirror every aspect of producing fields with the single exception of size. Like its larger counterparts, the quarry outcrop occurs as long, linear, highly localized dolomite bodies. These bodies step in an en-echelon pattern that is believed to be associated with riedel shears in a strike-slip fault system. Similar interpretations have been made for many of the producing dolomite fields. In profile both the quarry bodies and producing fields appear as depressions, or sags, that are commonly flanked by anticlines. Where data is available, the geochemical signature of the quarry dolomite is nearly identical to that of the reservoirs. Relatively negative $\delta^{18}O$ values, elevated $^{87}Sr/^{86}Sr$ ratios, high salinities, and fluid inclusion homogenization temperatures ranging between 100 and 160ºC are all common between the outcrop and the Trenton-Black River hydrothermal dolomite fields of south-central NY (Smith, 2006). This study has proven the value of the Palatine Bridge site as an outcrop analog, so that it may be used in further studies to aid in the exploration for future hydrothermal dolomite oil and gas reservoirs.

Section 7

REFERENCES

Allan, J.R., Wiggins, W.D., 1993, Dolomite reservoirs: geochemical techniques for evaluating origin and distribution: AAPG Continuing Education Course Note Series, 36, p. 169.

Auajjar, J., Boulegue, J., 2002, Dolomites in the Tazekka Pb-An district, eastern Morocco: polyphase origin from hydrothermal fluids: Terra Nova, v.14, n.3, p. 175 - 182.

Bird, J.M., Dewey, J.F., 970, Lithosphere plate – continental margin tectonics and the evolution of the Appalachian orogen: Geological Society of America Bulletin 81, p. 1031–1059.

Boreen, T., Davies, G., 2002, Hydrothermal Dolomite and Leached Limestones in TCF Gas Play: the Laydfern Slave Point Reservoir, NEBC: abstract from 2004 Dolomite Conference, The Spectrum: Mechanisms, Models, Reservoir Development. CSPG Seminar and Core Conference, Calgary, Alberta (CD format)

Bradley, D., Kusky, T., 1986, Geologic evidence for rate of plate convergence during the Taconic arc-continent collision (USA): Journal of Geology 94, no.5, p. 667 - 681

Bradley, D., Kidd, W.F.S., 1991, Flexural extension of the upper continental crust in Collisional foredeeps: Geological Society of America Bulletin 103, no.11, p. 1416-1438.

Braithwaite, C.J.R., Rizzi, G., 1997, The geometry and petrogenesis of hydrothermal Dolomites at Navan, Ireland: Sedimentology 44, no.3, p. 421 - 440.

Burke, W.H., 1982, Variation of seawater Sr^{87}-S^{r86} throughout Phanerozoic time: US Geological Survey Bulletin 1529E, p. 16

Carter, T., McFarland, S., Trevail, R., Gorman, R., Walsh, P., 2005, Trenton-Black River Hydrothermal Dolomite Reservoirs in Ontario: Geology, Reserves and Potential Resources: 2005 AAPG Annual Convention.

Childs, C., Watterson, J., Walsh, J.J., 1995, Fault overlap zones within developing normal fault systems: Journal of the Geological Society, London, v.152, p. 535 - 549.

Childs, C., Nicol, A., Walsh, J.J., Watterson, J., 1996, Growth of vertically segmented normal faults: Journal of Structural Geology, v.18, n.12, p. 1389 - 1397.

Dooley, T., K.R., McClay, 1997, Analog modeling of strike-slip pull-apart basins: AAPG Bulletin, v.81, p. 804-826.

Davies, G., Smith, L., 2006, Hydrothermal Structurally controlled hydrothermal dolomite reservoir facies: An overview: 2006 AAPG Bulletin 90, no.11, p. 1641 – 1690.

Fisher, D.W., 1954, Lower Ordovician (Canadian) stratigraphy of the Mohawk Valley, New York: Geological Society of America Bulletin 65, p. 71 - 96.

Friedman, I., O'Neil, J.R., 1977, Compilation of stable isotope fractionation factors of geochemical interest: U.S.Geol.Survey Professional.Paper.

Goldstein, R.H., Reynolds, J. T., 1994, Systematic of fluid inclusions in diagenetic minerals: SEPM short course 31. 199p.

Harding, T. P., 1974, Petroleum Traps Associated with Wrench Faults: AAPG Bulletin, v.58, p. 1290 - 1304.

Hulver, M. L., 1997, Post-orogenic evolution of the Appalachian basin mountain system and its foreland: Ph.D. thesis, University of Chicago, Chicago, Illinois, p. 917.

Hurley, N.F., Budros, R., 1990, Albion-Scipio and Stoney Point Fields - USA, Michigan Basin: Treatise of Petroleum Geology Atlas of Oil and Gas Fields, The American Association of Petroleum Geologists, Tulsa, OK, p.1 - 38.

Jacobi, R., 1981, Peripheral bulge - a causal mechanism for the Lower/Middle Ordovician unconformity along the western margin of the northern Appalachains: Earth and Planetary Science Letters 56, p.245 - 251.

Jacobi, R., Fountain, J., 2005, The character and reactivation history of the southern extension of the seismically active Clarendon-Linden Fault system, western New York State: Tectonophysics 353, no.1-4, p.215 - 262.

Jacobi, R., Mitchell, C., 2002, Basement faults and seismicity in the Appalachian Basin of New York State: Tectonophysics 353, n.1-4, p.75 - 113.

Joy, M.P., Mitchell C.E., Adhya S., 2000, Evidence of a tectonically driven sequence succession in the Middle Ordovician Taconic foredeep: Geology 28, no.8, p. 727 - 730.

Landing, E., Westrop S.R., Knox L.A., 1996, Conodonts, stratigraphy, and relative sea-level changes of the Tribes Hill Formation (Lower Ordovician, east-central New York): Journal of Paleontology 70, no.4, p. 656 - 680.

Loucks, R., McMechan, G., 1998, Ground penetrating radar imaging of a collapsed paleocave system in Ellenburger dolomite, central Texas: Journal of Applied Geophysics, v. 39, p.1 - 10.

Ogiesoba, O.C., 2005, Fault-Controlled Porosity Within a Trenton-Black River Hydrothermal Dolomite Reservoir: abstract from AAPG Annual Convention Technical Program.

Peacock, D.C.P., Knipe, R. J., Sanderson, D.J., 2000, Journal of Structural Geology 22, no.3, p. 291-305.

Sibson, R.H., 1994, Crustal stress, faulting and fluid flow: Geological Society Special Publication, no.78, p. 69 - 84.

Sibson, R.H., 2000, Fluid involvement in normal faulting: Journal of Geodynamics 29, p. 469 - 499.

Smith, L., 2006, Origin and Reservoir Characteristics of Upper Ordovician Trenton-Black River Hydrothermal Dolomite Reservoirs in New York, USA: AAPG Bulletin 90, no.11, p. 1691 - 1718.

Swart, P. K., Kendall, C. G., Cantrell, D. L., Westphal, H., Handford, C. R., 2005, Origin of dolomite in Arab-D reservoir from the Ghawar field, Saudi Arabia: Journal of Sedimentary Research 75, no.3, p. 476 – 491.

Warren, J., 2000, Dolomite: Occurrence, evolution and economically important associations: Earth Science Reviews 52, no.1-3, p. 1 – 81.

Weary, D.J., Ryder, R.T., Nyahay, R.E., 2001, Thermal Maturity Patterns in New York State Using CAI and %Ro: Northeastern Geology and Environmental Sciences 23, no.4, p. 356 - 376.

White, D.E., 1957, Thermal waters of volcanic origin: Geological Society of America Bulletin, V.68, p. 1637 - 1658.

Zenger, D.H., 1981, Stratigraphy and Petrology of the Little Falls Dolomite (Upper Cambrian), East-Central New York, New York State Museum Map and Chart Series 34, 138p.

Section 8
APPENDICES

8.1 - Hole 1

Little Falls Formation

38.8-24.1 ft.

Little Falls-Tribes Hill Transitional Beds

24.1-22.9 ft.
Brownish gray and medium gray, silty dolomite. Bedded mudstone. Rare to sparse microstylolites. Rare horizontal burrows. Large bitumen- and pyritized bitumen-filled fracture. Small, dolomite-filled fracture. Sparse pyrite outside fracture. Fractures exhibit little displacement. Patchy, intercrystalline porosity is restricted to individual beds. Rare porosity in horizontal burrow partially cemented with dolospar. Upper surface of the unit is undulatory.

Tribes Hill Formation

Unit 1: 22.9-22.5 ft.
Medium light gray, slightly argillacous, silty dolomite. Crinkly laminated mudstone. Rare moldic or vuggy porosity.

Unit 2: 22.5-22.4 ft.
Medium dark gray dolomite and dusky yellowish brown, pyritic dolomite. Intraclastic packstone (?). Abundant bitumen. Large intraclasts often preserved as pyrite. Rare glauconite in the pyrite deficient dolomite.

Unit 3: 22.4-21.2 ft.
Brownish gray, silty argillacous dolomite. In situ breccia (pseudobreccia) composed of numerous mudstone clasts. Pressure solution appears to have removed matrix. Common microstylolites. Rare shelter voids. Common pyrite. Rare vuggy or moldic porosity.

Unit 4: 21.2-19.6 ft.

Brownish gray and olive gray, silty dolomite. Bedded to lenticular mudstone. Sharp transition to olive gray dolomite at the 20.1 ft., apparently is a flat pebble conglomerate. Sparse pyrite. Fracture from 20.1-20.4 ft. propped open with pyrite. Rare intercrystalline porosity.

Unit 5: 19.6-17.8 ft.
Brownish gray to olive gray, slightly argillaceous to argillaceous, silty dolomite. The top of this interval is a well-defined, undulatory surface, apparently a dolomitized intraclastic grainstone. Original textures, which have largely been obliterated by intense dolomitization, are not immediately apparent. Bedding appears to be largely horizontal. Scattered clasts and horizontal burrows locally are identifiable. Local concentrations of microstylolites provide evidence of “ribbon rock” and nodular textures. Rare to sparse intercrystalline and vuggy porosity.

Unit 6: 17.8-11.7ft.
Brownish gray silty, argillaceous dolomite. Bedding horizontal, although original textures obscure due to intense dolomitization. Rare microstylolite swarms. Well-developed intercrystalline and vuggy porosity.

Unit 7: 11.7-0.0 ft.
Brownish gray, olive gray and olive black silty, argillaceous dolomite. Fracture zone between 7.2-10.0 ft. Brecciated, deformed strata. Bedding is vertical to slightly inclined. Fabrics appear streaked, probably ductiley deformed. Numerous breccia clasts lack well-defined margins. Silt and clays are abundant. Porous fabrics, although very rare, has well-developed intercrystalline and vuggy porosity.

8.2 - Hole 2

Little Falls Formation

54.0-24.6 ft.

Little Falls-Tribes Hill Transitional Beds

24.6-23.6 ft.
Brownish gray slightly argillaceous and silty dolomite. Bedded mudstone. Some beds, which are lenticular, contorted and not continuous, were probably affected by soft sediment deformation. Rare high angle, bitumen-filled fracture near base continues into the Little Falls Formation. Sparse to rare burrows, especially immediately above base. Rare microstylolites. Rare pyrite. Upper contact is an undulatory surface.

Tribes Hill Formation

Unit 1: 23.6-23.2 ft.
Medium light gray and medium gray slightly argillaceous, silty dolomite. Crinkly laminated mudstone. Conspicuous dark gray interbed near middle. Numerous gravel sized intraclasts. Trace echinoderms. Some laminae are fragmented in situ at base. Rare to sparse vuggy porosity in the upper third of the unit.

Unit 2: 23.2-23.0 ft.
Brownish gray dolomite. Intraclastic packstone with thin mudstone drape. Intraclasts not distinct. Diffuse glauconite above mudstone drape. Sparse intergranular porosity associated with the intraclast-rich portions.

Unit 3: 23.0-21.6 ft.
Light brownish gray and brownish gray silty dolomite: In situ breccia (pseudobreccia), which is somewhat obscured by dolomitization. Interbedded, light, early cemented mudstone bed and dark, organic-stained, silty muds. Bioturbation also disrupts bedding. Rare cemented shelter voids. Sparse fracture porosity associated with early fractures of mudstone chips. Sparse vuggy porosity in the beds which were not cemented syndepositionally. Rare moldic and vuggy pores in dolomitized mud chips.

Unit 4: 21.6-20.2 ft.
Medium dark gray and medium gray dolomite silty dolomite. Mudstone interbedded with thin cross-laminated grainstones. Laminated beds and lenticular beds near top. Rare calcite-cemented fractures. Rare small intraclasts. Rare wispy microstylolites. Rare clays. Rare pyrite. Silt more common in cross laminated

beds. Intercrystalline porosity restricted cross-laminated beds. Flat pebble conglomerate with cemented shelter voids at top of interval.

Unit 5a: 20.2-17.8 ft.
Brownish gray, olive gray and medium dark gray dolomite and argillaceous, silty dolomite. “Ribbon rock” which is somewhat obscured by dolomitization. Common microstylolites. Mudstone? Rare pyrite. Well-developed, intercrystalline porosity (approximately 10-15%).

Unit 5b: 17.8- 16.6 ft.
Brownish gray, argillaceous, silty dolomite and white saddle dolospar cement. A conspicuous hydrothermally fractured/brecciated zone cemented with saddle dolomite. Later coarse, calcite spar is rare. Common vuggy, intergranular (between breccia clasts) and intercrystalline porosity. Pores, several centimeters in diameter, are associated with the intergranular voids.

Unit 5c: 16.6-16.0 ft.
Brownish gray, olive gray and medium dark gray dolomite and argillaceous, silty dolomite. “Ribbon rock” , which is somewhat obscured by dolomitization. Similar in most respects to Unit 5a, except less intercrystalline and vuggy porosity.

Unit 6: 16.0-12.6 ft.
Brownish gray and medium dark gray sandy (very fine), slightly calcitic dolomite grading quickly upward to silty, dolomitic limestone at top. Perhaps a less distinct “ribbon rock”. Calcitic portion appear to be wackestone to muddy packstone. Trilobites, echinoderms and intraclasts, peloids and echinoderms are most common carbonate grains. Brachiopods and bivalve mollusks are rare. Rare echinoderms. Rare saddle dolomite (at base). Replacement dolomitization (medium crystalline-replacement) is patchy and not obviously fabric selective. Sparse to common pyrite. Wispy microstylolites appear to concentrate silt. Some beds or intraclasts have fine, calcite-filled syndepositional fractures. Rare to sparse calcite-cemented horizontal burrows, especially conspicuous near top of interval.

Unit 7: 12.6-0.0
Olive gray, light brownish gray, medium light gray and medium dark gray dolomitic limestone. “Ribbon rock”. Wackestone and the rare packstone and grainstone. Thin, non-skeletal grainstones may have eroded tops. Limestone interbeds generally less than 5 centimeters. Limestone of the nodular intervals generally mudstone. Intervening matrix-rich beds often no more than dense microstylolite swarms, which locally may be argillaceous. Several packstone beds composed of large intraclasts. Grainy interbeds dominated by non-skeletals (intraclasts, rare peloids) and rarer skeletals (trilobites). Algal fragments (Ortonella?) are locally present. Intraclasts may have blackened rim. Some intraclasts have thin, syndepositional calcite-filled

fractures. Rare stylolites. Replacement dolomite is locally abundant. Rare horizontal burrows often filled with fine dolomite replacement. Rare to sparse pyrite. Fractures at 3.0-3.1 ft. and 5.3-6.3 ft. filled with saddle dolomite. Later calcite spar fills fracture at 5.3-6.3 ft.. Fracture and breccia at 7.1-7.5 ft. cemented with saddle dolomite and later calcite spar. All fractures and breccia show little displacement. Sparse, large intercrystalline pores (up to 2 millimeters) associated with saddle dolospar.

8.3 - Hole 3

Little Falls Formation

55.0-24.6 ft.

Little Falls-Tribes Hill Transitional Beds

24.6 -23.7 ft.
Light brownish gray and brownish gray silty dolomite. Bedded and laminated mudstone. Rare horizontal and vertical burrows. Bitumen- and dolospar-filled fracture (24.3-24.6 ft.). Sparse, low amplitude stylolites. Rare pyrite. Rare fracture porosity and trace moldic porosity.

Tribes Hill Formation

Unit 1: 23.7-23.3 ft.
Light brownish gray argillaceous, silty dolomite. Crinkly, laminated mudstone. Several thin argillaceous rich beds with dolomitized intraclasts and skeletals. Rare pyrite. Rare burrows.

Unit 2: 23.3-23.0 ft.
Light brownish gray dolomite. Intraclastic packstone (?). Intraclasts angular. Rare pyrite. Rare glauconite. Perhaps a thin hard ground and algal mat stabilizing top. Sparse to common moldic and vuggy porosity.

Unit 3: 23.0-21.7 ft.
Light brownish gray and brownish gray and silty, argillaceous dolomite. In situ breccia (pseudobreccia) composed of numerous mudstone clasts, some undisturbed beds and imbricated flat pebble conglomerate at very top. Saddle dolospar partially occludes larger pores. Rare pyrite. Well-developed vuggy, moldic and intercrystalline porosity especially near base of unit. Largest pore approximately 3 millimeters.

Unit 4: 21.7-20.5 ft.
Medium gray and brownish gray, silty dolomite. Bedded to lenticular mudstone with conspicuous laminated portions. Upper surface irregular. Flat pebble conglomerate near top of unit. Irregular surface at 21.3 ft.. Rare bitumen- and dolospar-filled vugs. Rare microstylolitic seams and stylolites. Large, open fracture, which is partly occluded by pyrite and dolospar, extends from top of unit to 21.2 ft.. Rare vuggy porosity associated with the flat pebble conglomerate.

Unit 5: 20.5-17.9 ft.

Olive gray, silty, slightly argillaceous dolomite. “Ribbon rock” and nodular fabric of interbedded dolomite and silty, argillaceous dolomitic, microstylolitic seams. Depositional texture obliterated by dolomitization. Numerous microstylolites. Scattered intraclasts. Rare horizontal burrows near base of unit. Rare pyrite. Excellent intercrystalline and vuggy porosity. Largest pore approximately 1 millimeter.

Unit 6: 17.9-17.2 ft.

Olive gray, slightly silty dolomite. Primary depositional texture not immediately apparent. Probably an intraclastic packstone. Many voids cemented with saddle dolospar. Very good intercrystalline and vuggy porosity. Largest pore approximately 2 millimeters.

Unit 7: 17.2-7.1 ft.

Light brownish gray, brownish gray and medium dark gray silty, argillaceous dolomite. Primary depositional texture not apparent although probably a “ribbon rock” with an especially dense concentration of microstylolites at top of unit. Sparse pyrite. Excellent intercrystalline and vuggy porosity. Largest pore 1 millimeter.

Unit 8: 7.1-0.0 ft.

Brownish gray, silty, argillaceous dolomite. Dolomitization and diagenesis has obscured primary depositional fabric. Some micro zebra fabrics. Numerous breccia clasts throughout the interval. Rare, small (<1 millimeter) calcite-filled fractures. Rare intercrystalline porosity.

8.4 - Hole 4

Little Falls Formation

55.0-24.9 ft.

Little Falls-Tribes Hill Transitional Beds

24.9-24.3 ft.
Light brownish gray, silty dolomite. Rare organic-filled fractures. Thinly bedded mudstone. Some beds are contorted . Rare burrows. Rare microstylolites. Rare pyrite near top of unit. Undulatory upper surface.

Tribes Hill Formation

Unit 1: 24.3-24.0 ft.
Light brownish gray to brownish gray, silty, argillaceous, dolomite. Crinkly laminated mudstone and thinly bedded mudstone. Rare burrows. Numerous, thin, silty, argillacous laminae. Laminae fragmented in situ at base. Sparse microstylolites that concentrate silt and clay. Rare pyrite. Irregular, undulatory upper surface.

Unit 2: 24.0-23.9 ft.
Light brownish gray and medium dark gray dolomite. Probable intraclast packstone to grainstone. Rounded very coarse sand and gravel sized intraclasts. Pyrite abundant at base of unit. Rare glauconite. Sparse vuggy and moldic porosity.

Unit 3: 23.9-22.7 ft.
Brownish gray and olive gray silty, argillaceous, dolomite. In situ breccia (pseudobreccia) composed of angular clasts. Rare pyrite. Numerous stylolitized grain contacts, which are near top of unit, indicate vertical as well as horizontal pressure solution. Rare intercrystalline and fracture porosity.

Unit 4: 22.7-21.0 ft.
Brownish gray, light brownish gray and olive gray silty dolomite. Bedded mudstone. Conspicuous, porous, flat pebble conglomerate at the top. Pressure solution has created numerous vertical stylolites and obscured the character of the bedding. Common pyrite disseminated in the matrix and concentrated along stylolites, probably as pyritized bitumen in the latter. Saddle dolomite cement partially fills large voids in the flat pebble conglomerate at the top. Porosity associated with stylolites and best developed in the flat pebble conglomerate at the top of the unit. Largest pore 1 millimeter.

Unit 5: 21.0-14.4 ft.

Olive gray and brownish gray slightly argillacous, silty dolomite. Deformation and dolomitization have largely obliterated the depositional fabric, although lack of microstylolite swarms indicate the unit largely consists of bedded carbonates. Beds are brecciated and often inclined. Microstylolites traces are rare. Sparse large voids partially cemented with saddle dolospar and later, rare calcite spar. Intercrystalline, vuggy and, perhaps, moldic porosity generally well developed. Largest pores approximately 1 millimeter.

Unit 6: 14.4-10.2 ft.

Olive gray, silty, argillaceous dolomite. Deformation, brecciation and dolomitization have largely obliterated the depositional fabric, although abundance of microstylolite swarms indicate the unit largely consists of “ribbon rock” and nodular carbonates. Beds are brecciated or inclined. Microstylolites traces are common. Some microstylolites, beds and breccia clasts appear stretched or smeared, probably ductilely deformed. Saddle dolospar and later calcite spar fill or partially fill larger pores. Fracture trace between 11.1-12.0 ft.. Porosity commonly developed as vuggy and intercrystalline voids. Largest pores up to 1 millimeter.

Unit 7: 10.2-8.1 ft.

Brownish gray and olive gray, silty, argillaceous dolomite. Bedded carbonate, presumably deposited as limestone. Little or no disruption of beds. Rare microstylolites. Prominent surfaces at 8.3 and 8.5 ft.. Intraclasts at the very top. Rare to sparse vugs and intercrystalline pores.

Unit 8: 8.0-3.1 ft.

Brownish gray and olive gray, very silty, very argillaceous dolomite. Dolomitization obscures the depositional texture of this unit. Apparently little disruption of beds by faulting. The basal portion of the unit (6.9-8.1 ft.) appears disturbed, but disruption most probably related to deposition. Often the fabric displays a linearity, perhaps a microzebra fabric reflecting an alignment of the dolomite crystals. There is some inclined zebra fabric immediately below the sharp, irregular contact with the overlying limestone. Vuggy and intercrystalline porosity is rare to sparse and not uniformly developed throughout the unit.

Unit 10: 3.1-0.0 ft.

Olive gray, silty, argillaceous, slightly dolomitic limestone. “Ribbon rock” and nodular fabric of interbedded limestone and silty, argillaceous microstylolitic seams. Limestone beds up to 5 centimeters. Limestone interbeds generally are mudstone and wackestones with several thick intraclast packstone beds. Many intraclasts are mudstone and have a blackened rims. Intraclasts, peloids and echinoderms are the most common carbonate grains. Some stylolitized contacts between beds and intraclasts near the base of the unit. More dolomitic near basal contact with underlying dolomitized beds.

8.5 - Hole 5

Little Falls Formation

73.0-24.2 ft.

Little Falls-Tribes Hill Transitional Beds

24.2-23.2 ft.
Light brownish gray and brownish gray silty dolomite. Bedded and laminated mudstone. Bitumen-defined laminae at the very top. Several irregular surfaces, clotted fabrics and wavy bedding. Horizontal burrows immediately below two irregular surfaces.

Little Falls Formation

Unit 1: 23.2-22.8 ft.
Light brownish gray argillaceous, silty dolomite. Crinkly laminated mudstone.

Unit 2: 22.8-22.7 ft.
Light brownish gray dolomite. Intraclastic packstone (?). Sparse pyrite. Rare glauconite at the upper surface. Sparse vuggy porosity.

Unit 3: 22.7-21.0 ft.
Light brownish gray, brownish gray and medium gray silty, argillacous dolomite. In situ breccia (pseudobreccia) composed of numerous mudstone clasts and some undisturbed beds. Common pyrite, especially in more porous portion. Saddle dolospar and calcite spar partially occlude larger pores. Common vuggy, moldic and intercrystalline porosity. Largest pore approximately 2 millimeters.

Unit 4: 21.0-19.6 ft.
Medium gray to brownish gray and olive gray, silty dolomite. Bedded to lenticular mudstone with conspicuous laminated units. Porous, flat pebble conglomerate with rare shelter voids at very top. Irregular surface at 20.9 ft. Common moldic porosity (after mud clasts) in the flat pebble conglomerate.

Unit 5: 19.6-17.3 ft.
Olive gray silty, argillaceous dolomite. Primary depositional texture not apparent. Scattered intraclasts. Local deformation of beds. Sparse microstylolites. Sparse to common intercrystalline and vuggy porosity.

Largest pore 5 millimeters, although pores 0.25 millimeters or smaller are more characteristic of the interval.

Unit 6: 17.3-13.3 ft.

Brownish gray and olive gray silty, slightly argillaceous dolomite. Primary depositional texture not apparent. Unit capped by microstylolites swarm. Top 0.4 ft. with abundant intraclasts. Small void at 15.2 ft. filled with quartz silt and clay. Rare to sparse microstylolites. Rare to sparse pyrite. Excellent vuggy and intercrystalline porosity. Largest pore 0.5 millimeters.

Unit 7: 13.3-11.5 ft.

Brownish gray and olive gray silty argillaceous dolomite. Primary depositional texture not apparent. Largely (11.9-13.3 ft.) a brecciated unit with fault trace at the top. Pressure solution contacts between clasts. Apparently compressional deformation and oblique orientation of clasts at the base. No brecciation at the top, although beds undulate. No apparent porosity adjacent to fault. Rare vuggy porosity in brecciated portion. Largest pore 1 millimeter.

Unit 8: 11.5-3.4 ft.

Brownish gray and olive gray silty, argillaceous dolomite, rarely slightly calcitic. Although, deformation and diagenesis have obscured primary depositional fabric, it appears to be a “ribbon rock”. Beds locally brecciated and often inclined. Beds often appear smeared or distorted by ductile deformation. Sparse pyrite. Common microstylolites. Rare calcite-filled fractures. Rare voids filled with saddle dolomite and calcite spar, are adjacent to the fault. Intercrystalline and vuggy porosity best developed proximal to fault trace.

Unit 9: 3.4-0.0 ft.

Olive gray, silty, argillaceous dolomite. Diagenesis have obscured primary depositional fabric. Minor deformation, but texture is, overall, homogenous. Rare clasts. No apparent porosity.

8.6 - Hole 6

Little Falls Formation

45.0-25.1 ft.

Little Falls-Tribes Hill Transitional Beds

25.1-24.3 ft.
Brownish gray, slightly argillaceous and slightly silty dolomite to dolomitic limestone at top. Thinly bedded mudstone. Some beds are lenticular, contorted and not continuous, probably reflecting early, soft sediment deformation. Rare burrows. Rare microstylolites. Rare pyrite.

Tribes Hill Formation

Unit 1: 24.3-23.7 ft.
Brownish gray, silty, argillaceous, slightly dolomitic limestone. Basal 0.2 ft. more clastic rich and dolomitic. Crinkly laminated mudstone, thinly bedded mudstone and rare packstone. Rare burrows. Numerous, thin silty, argillacous laminae. Rare lenticular lenses of gravel size intraclasts. Laminae fragmented in situ at base. Numerous, microstylolites which concentrate silt and clay. Rare pyrite.

Unit 2: 23.7-23.4 ft.
Olive gray, dolomitic limestone. Intraclast packstone to grainstone. Rounded very coarse sand and gravel sized well-rounded micritic intraclasts. Many intraclasts appear to have small post-depositional fractures. Intergranular (matrix) pores filled and replaced by dolomite and glauconite.

Unit 3: 23.4-21.9 ft.
Olive black silty, argillaceous, dolomitic limestone. In situ breccia (pseudobreccia). Many laminated mudstone chips later tectonically fractured. Sparse cemented shelter voids associated with mudstone chips. Sparse compactional fracturing. Extensive bioturbation disrupts mudstone beds. Rare glauconite. Clay and silt generally as thin microstylolites. Rare pyrite.

Unit 4: 21.9-20.1 ft.

Olive black silty dolomite, with a sharp transition to an olive gray, silty dolomitic limestone (at 20.5 ft.). Bedded to lenticular bedded mudstone and, perhaps, fine peloidal grainstone at base. Sparse microstylolites. Fine cross-laminations near base. Sparse pyrite. Rare mudstone flat pebble conglomerate and cemented shelter voids at top. Rare pyrite.

Unit 5: 20.1-17.3 ft.

Olive black to olive gray silty, argillaceous, slightly dolomitic limestone. “Ribbon rock” and nodular fabric of interbedded limestone and silty, argillacous dolomitic microstylolitic seams. Mudstone and rare packstone and grainstone. Capped by a planar surface (hardground?), on an intraclastic grainstone. Limestone generally less than 5 centimeters. Carbonate grains include peloids, intraclasts and echinoderms. Rare pyrite. Rare to sparse horizontal and vertical burrows, some geopetally filled with calcite spar. Rare echinoderm and trilobite fragments.

Unit 6: 16.5-17.3 ft.

Brownish gray and medium dark gray to olive gray, silty dolomitic limestone. Locally very silty and very dolomitic. Intraclastic-peloidal packstone and rare wackestone. Numerous hardgrounds. Rare stylolites and microstylolites. Rare to sparse pyrite. No visible porosity.

Unit 7: 17.3-12.9 ft.

Olive gray silty, argillaceous dolomitic limestone to calcitic dolomite. Perhaps a less distinct “ribbon rock” with fewer, conspicuous microstylolitic seams and thicker limestone interbeds. Locally nodular. Mudstone with rare, thin grainstone and packstone interbeds. Carbonate grains include peloids, gastropods, intraclasts, echinoderms, brachiopods and trilobites. Rare pyrite. Sparse, thin, discontinuous microstylolites except for abundance of microstylolites in mudstone near base and top of unit.

Unit 8: 12.9-0.0 ft.

Olive gray, silty, clayey slightly dolomitic limestone. “Ribbon rock” and nodular fabric of interbedded limestone and silty, clayey dolomitic microstylolitic seams. Limestone beds rarely greater than 10-15 millimeters. Limestone interbeds generally are wackestones and packstone. Many intraclasts are mudstone. Algal fragments (Ortonella?) are a conspicuous and common component. Trilobites, echinoderms, ostracods brachiopods, intraclasts, peloids are the most common carbonate grains. Some “intraclasts” may be the steinkerns of gastropods. Rare calcite-filled fractures.

8.7 - FIT's Fluid Inclusion Results

PB200: This sample consists of relatively coarse, possibly recrystallized matrix dolomite with very coarse saddle spar and late calcite spar. No visible liquid petroleum inclusions are identified. Possible non-fluorescent gas inclusions are observed in saddle spar, but these are small and difficult to image. These inclusions may have pyrobitumen coatings. None responded to micro-thermometric tests. Pyrobitumen may be present, and appears to post-date dolomite, but predate calcite.

Primary aqueous inclusions in early matrix dolomite have homogenization temperatures of 120-130°C and indeterminate salinities. Secondary or pseudo-secondary inclusions in early matrix calcite have homogenization temperatures of 80-95°C and salinities of 26-28 weight percent salt (estimated from the $NaCl$-$CaCl_2$-H_2O system). No aqueous inclusions could be found in late saddle dolomite, and possible gas inclusions did not respond to heat/cooling tests, as mentioned. Secondary or pseudo-secondary inclusions in late calcite cement have consistent homogenization temperatures of 65 - 75°C and salinities of 14.5-18.6 weight percent NaCl equivalent.

PB201: This sample consists of relatively coarse zoned dolomite with minor, possibly partially dissolved, late calcspar. No visible liquid petroleum inclusions are identified. Abundant pyrobitumen is noted.

Primary aqueous inclusions in dolomite have homogenization temperatures of 105-132°C with a possible weak trend of higher temperature from core (105-120°C) to rim (120-132°C). Secondary or pseudo-secondary aqueous inclusions in dolomite have homogenization temperatures of 90-129°C. Salinities are uniformly very high at 26-30 weight percent salt (estimated from the $NaCl$-$CaCl_2$-H_2O system). No aqueous inclusions could be measured from late calcite.

Plate 1 - Aerial photo mosaic of the quarry outcrop

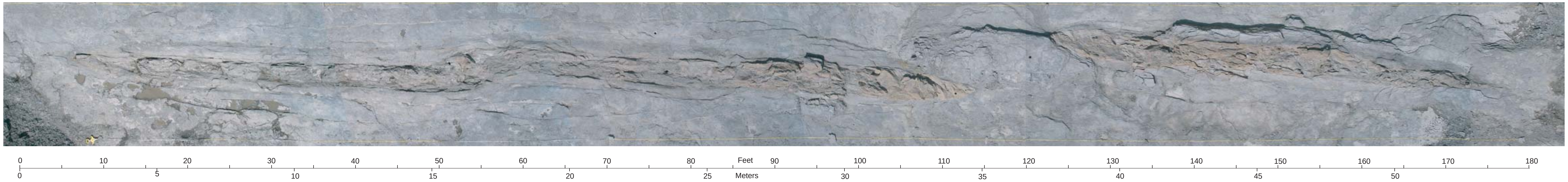

Plate 2 - Fracture map of the quarry outcrop

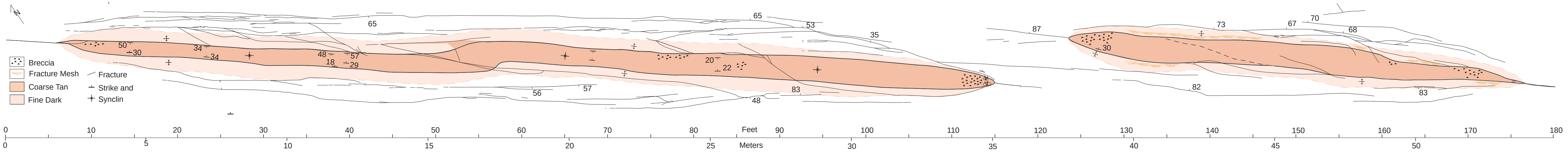

Trench 3 - Eastern Wall

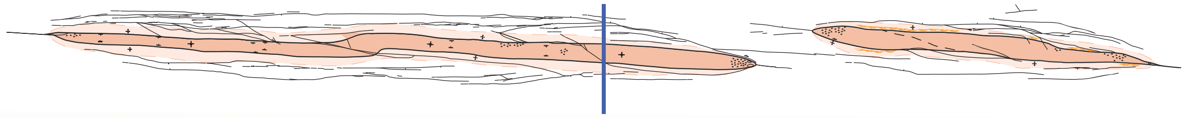

By Brian Slater

Trench 4 - Eastern Wall

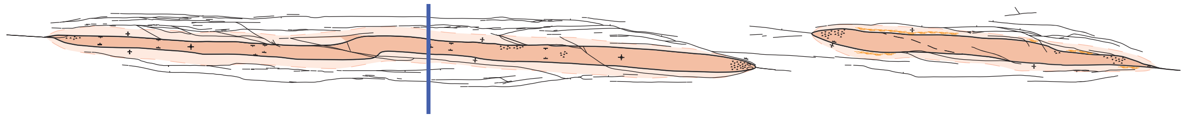

By Brian Slater

Trench 4 - Western Wall

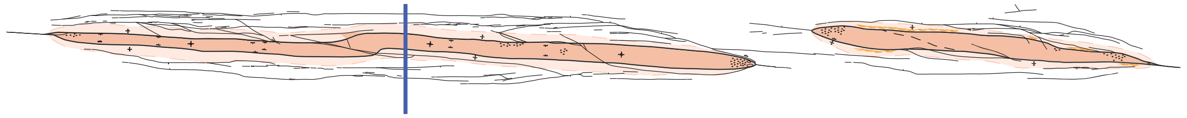

By Brian Slater

Trench 5 - Eastern Wall

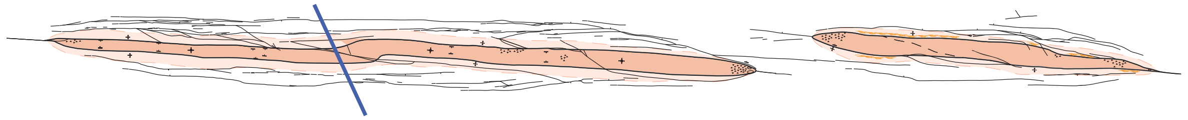

By Brian Slater